

การสังเคราะห์เพปไทด์นิวคลีอิกแอซิดคอนจูเกตที่สามารถผ่านเข้าสู่เซลล์ได้



นางสาวเบญจวรรณ บุญแก้ว

วิทยานิพนธ์นี้เป็นส่วนหนึ่งของการศึกษาตามหลักสูตรปริญญาวิทยาศาสตรมหาบัณฑิต
สาขาวิชาเคมี ภาควิชาเคมี

คณะวิทยาศาสตร์ จุฬาลงกรณ์มหาวิทยาลัย

ปีการศึกษา 2551

ลิขสิทธิ์ของจุฬาลงกรณ์มหาวิทยาลัย

SYNTHESIS OF POTENTIAL CELL-PENETRATING PEPTIDE
NUCLEIC ACID CONJUGATES



Miss Benjawan Boonkaew

A Thesis Submitted in Partial Fulfillment of the Requirements
for the Degree of Master of Science Program in Chemistry

Department of Chemistry

Faculty of Science

Chulalongkorn University


Academic Year 2008

Copyright of Chulalongkorn University

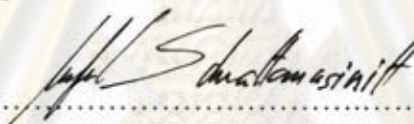
511059

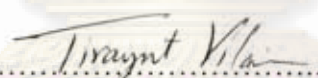
Thesis Title SYNTHESIS OF POTENTIAL CELL-PENETRATING PEPTIDE
NUCLEIC ACID CONJUGATES
By Miss Benjawan Boonkaew
Field of Study Chemistry
Advisor Associate Professor Tirayut Vilaivan, D. Phil.

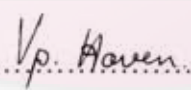
Accepted by the Faculty of Science, Chulalongkorn University in Partial
Fulfillment of the Requirements for the Master's Degree

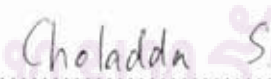
..... Dean of the Faculty of Science
(Professor Supot Hannongbua, Dr.rer.nat.)

THESIS COMMITTEE

.....Chairman
(Associate Professor Mongkol Sukwattanasinitt, Ph.D.)

.....Advisor
(Associate Professor Tirayut Vilaivan, D.Phil.)

.....Examiner
(Assistant Professor Voravee P. Hoven, Ph.D.)

.....External Examiner
(Choladda Srisuwannaket, Ph.D.)

คุณย์วิทย์ศรีพิทยากร
จุฬาลงกรณ์มหาวิทยาลัย

เบญจวรรณ บุญแก้ว : การสังเคราะห์เปปไทด์นิวคลีอิกแอซิดคอนจูเกตที่สามารถผ่านเข้าสู่เซลล์ได้. (SYNTHESIS OF POTENTIAL CELL-PENETRATING PEPTIDE NUCLEIC ACID CONJUGATES) : อ.ที่ปรึกษาวิทยานิพนธ์หลัก : รศ.ดร.ธีรยุทธ วิไลวัลย์; 86 หน้า.

งานวิจัยนี้สนใจที่จะใช้โพลีแคตไอออนิกเพปไทด์ $(KFF)_3K$ R_{10} และ phosphonium cation (P^+) เป็นตัวพาพีเอ็นเอเข้าสู่เซลล์ของ *E. coli* ATCC 25922 พีเอ็นเอคอนจูเกตสามชนิดคือ Flu-O-T₃-O-(KFF)₃K-NH₂ Flu-O-T₃-O-R₁₀-NH₂ และ Flu-O-T₃-O-Lys-(P⁺)-NH₂ ได้ถูกสังเคราะห์ขึ้นแบบ sequential coupling โดยวิธีสังเคราะห์บนวัฏภาคของแข็งและได้ใช้เทคนิคฟลูออเรสเซนส์ศึกษาการพาพีเอ็นเอคอนจูเกตเข้าสู่เซลล์ ผลการศึกษาพบว่า $(KFF)_3K$ เป็นตัวพาพีเอ็นเอคอนจูเกตที่ดีกว่า R₁₀ และ phosphonium cation นอกจากนี้ การเจริญเติบโตของเซลล์แสดงว่า Flu-O-T₃-O-(KFF)₃K-NH₂ และ Flu-O-T₃-O-Lys-(P⁺)-NH₂ ไม่เป็นอันตรายต่อเซลล์ ส่วน R₁₀ มีความเป็นพิษต่อเซลล์เนื่องจากมีผลทำให้การเจริญเติบโตของเซลล์ช้าลง

การศึกษาคงความยาวของพีเอ็นเอที่มีผลต่อการผ่านเข้าสู่เซลล์โดยใช้พีเอ็นเอที่มีสายยาวขึ้นคือ Flu-O-T₉-O-(KFF)₃K-NH₂ แสดงให้เห็นว่าแม้จำนวนเบสของพีเอ็นเอจะเพิ่มขึ้น Flu-O-T₉-O-(KFF)₃K-NH₂ สามารถผ่านเข้าสู่เซลล์ได้ดีเช่นเดียวกับ Flu-O-T₃-O-(KFF)₃K-NH₂

นอกจากนี้ยังได้สังเคราะห์พีเอ็นเอคอนจูเกต H-(KFF)₃K-O-T₉-Lys(Flu)-NH₂ เพื่อศึกษาความสำคัญของตำแหน่งที่ต่อ $(KFF)_3K$ บนพีเอ็นเอคอนจูเกตที่มีต่อการนำส่งพีเอ็นเอเข้าสู่เซลล์แต่ผลการทดลองยังไม่สามารถสรุปได้ชัดเจนซึ่งอาจเกิดจากการตกตะกอนหรือความไม่เสถียรของพีเอ็นเอที่มี $(KFF)_3K$ ต่ออยู่ด้านปลายเอ็น $\{H-(KFF)_3K-T_9-Lys(Flu)-NH_2\}$ ในสถานะทดลอง

การศึกษาคงเสถียรของพีเอ็นเอต่อ Proteolytic enzyme ใช้ Ac-T₉-Lys-NH₂ เป็นพีเอ็นเอต้นแบบร่วมกับ proteinase K ผลการศึกษาพบว่าเปปไทด์ที่เป็นตัวควบคุม ACTH 4-10 ถูกย่อยสลายอย่างสมบูรณ์ที่สภาวะ 0.15 units/mL ของ proteinase K ที่ 37°C ในขณะที่พีเอ็นเอ นั้นสามารถทนทานต่อสภาวะ 15 units/mL proteinase K ที่ 37°C ได้มากกว่า 18.5 ชั่วโมง

จุฬาลงกรณ์มหาวิทยาลัย

ภาควิชา.....เคมี.....ลายมือชื่อนิสิต.....
 สาขาวิชา.....เคมี.....ลายมือชื่อ อ.ที่ปรึกษาวิทยานิพนธ์หลัก.....
 ปีการศึกษา.....2551.....

4973826023 : MAJOR CHEMISTRY

KEY WORD : PEPTIDE NUCLEIC ACID (PNA)/CELLULAR UPTAKE

BENJAWAN BOONKAEW : SYNTHESIS OF POTENTIAL CELL-PENETRAING PEPTIDE NUCLEIC ACID CONJUGATES. THESIS ADVISOR : ASSOC. PROF. TIRAYUT VILAIVAN, D.Phil., 86 pp.

In this work, polycationic peptides and a lipophilic phosphonium, namely (KFF)₃K, R₁₀, and phosphonium cation (P⁺) has been evaluated for their cellular deliver of PNA to *E. coli* ATCC 25922 cells. Three model PNA conjugates, Flu-O-T₃-O-(KFF)₃K-NH₂, Flu-O-T₃-O-R₁₀-NH₂ and Flu-O-T₃-Lys(P⁺)-NH₂ have been successfully prepared by sequential coupling using standard solid phase synthesis. Fluorescence techniques were used to determine the cell penetration of the PNA conjugates into the cells. It was demonstrated that (KFF)₃K was a better carrier than R₁₀ and photphonium cation. In addition, the cell growth rates showed that Flu-O-T₃-O-(KFF)₃K-NH₂ and Flu-O-T₃-Lys(P⁺)-NH₂ had no cytotoxicity. By contrast, Flu-T₃-R₁₀ conjugate should be considered as somewhat toxic because a reduced rate of cell growth was observed.

The PNA length requirement has also determined using a longer PNA conjugate namely Flu-O-T₉-O-(KFF)₃K-NH₂. The results demonstrated that despite the increased length of the PNA part, the uptaking ability of Flu-O-T₉-O-(KFF)₃K-NH₂ was better than Flu-O-T₃-O-(KFF)₃K-NH₂.

To determine the importance of the position of attachment of (KFF)₃K, H-(KFF)₃K-O-T₉-Lys(Flu)-NH₂ were also prepared. No conclusion can be made with H-(KFF)₃K-O-T₉-Lys(Flu)-NH₂ possibly due to precipitation or degradation under the assay conditions.

The stability of a model PNA: Ac-T₉-Lys-NH₂ towards a model proteolytic enzyme: proteinase K has been evaluated. The control: ACTH 4-10 was completely digested under condition 0.15 units/mL of proteinase K at 37°C whereas the PNA remained stable over 18.5 h at 15 units/mL protenase K at 37°C.

Department:.....Chemistry.....Student's Signature.....Benjawan Boonkaew
Field of Study:.....Chemistry.....Advisor's Signature.....Tirayut Vilaivan
Academic Year:.....2008.....

ACKNOWLEDGEMENTS

I would like to thank Associate Professor Dr. Tirayut Vilaivan, my thesis advisor, for providing knowledge, suggestions and assistance throughout this research. I'm also grateful to thesis examiners: Associate Professor Dr. Mongkol Sukwattanasinitt, Assistant Professor Dr. Voravee P. Hoven and Dr. Choladda Srisuwannaket for all valuable comments and suggestions regarding to the improvement of thesis.

I also would like to thank The Development and Promotion of Science and Technology Talent Project (DPST) for the financial support; Thailand-Japan Technology Transfer Project (TJTTP), Organic Synthesis Research Unit and Department of Chemistry, Chulalongkorn University for the use of facilities, equipment, glassware and chemicals

The experiments relating to cellular studies carried out at Department of Microbiology, Faculty of Pharmacy, Mahidol University, Bangkok, under supervision of Assistant Professor Dr. Mullika T. Chomnawang and Miss Piyatip Khuntayaporn. I would like to thank for their kindness, helpful guidance and friendship while working at Mahidol.

I wish to thank Dr. Chaturong Suparpprom, Miss Cheeraporn Ananthanawat, Miss Boonjira Boontha, Miss Roejarek Kanjanawarut, Miss Wanna Bannarukkul and Miss Pratchayaporn Korkeaw for their advice and suggestions, teaching how to use instruments, synthesis of some intermediates and starting materials for PNA synthesis. I also wish to thank Mrs. Chotima Vilaivan, Miss Woraluk Mansawat and all TV & WB group members for their helpfulness and great friendship.

I wish to expand my sincere thankfulness to my close friends, Mr. Nakorn Niumnon for giving me helps when I need. Mr. Valomyalin Tipmanee, Mr. Ekawit Pongpet, Mr. Theeraphan Sungthong and Mr. Andreas Hohenleutner for correcting some parts of my thesis and searching for literatures. I also thank all who give moral support during writing my thesis.

Finally, I would like to pay abeissance to my parent and all of my family members who give me spirit to do research during the past three years.

CONTENTS

	page
Abstract (Thai).....	iv
Abstract (English).....	v
Acknowledgements.....	vi
Contents.....	vii
List of Tables.....	x
List of Figures.....	xiii
List of Abbreviations.....	xxii
CHAPTER I: INTRODUCTION.....	1
1.1 Peptide nucleic acid (PNA).....	1
1.2 Hybridization of PNA and DNA/RNA.....	1
1.3 Structure modifications of PNA	3
1.4 PNA as antisense agents... ..	5
1.4.1 Applications of PNA as antisense agents... ..	7
1.4.2 Limitations of PNA as antisense agents.....	7
1.5 Cellular uptake strategies.....	8
1.6 Review of literatures concerning cationic carriers	8
1.6.1 Applications of (KFF) ₃ K as a carrier.....	8
1.6.2 Applications of Arginine rich peptides as carriers.....	10
1.6.3 Application of Tat and other CPPs as carriers.....	13
1.6.4 Application of Phosphonium cations as carriers.....	14
1.7 Objectives of this work	15
CHAPTER II: EXPERIMENTAL SECTION.....	16
2.1 General Procedures.....	16
2.1.1 Measurements.....	16

	Page
2.1.2 Materials and methods.....	17
2.2 Synthesis of monomers.....	18
2.2.1 Synthesis of activated peptide monomers	18
2.2.2 Synthesis of <i>trans</i> -(1 <i>S</i> ,2 <i>S</i>)-2-aminocyclopentanecarboxylic acid (ACPC) spacer.....	21
2.3 Synthesis of PNA conjugates.....	24
2.3.1 Preparation of the reaction pipette and apparatus for solid phase peptide synthesis.....	24
2.3.2 Procedures for solid phase synthesis of PNA conjugates....	24
2.4 Selected examples of PNAs, peptides or their conjugates.....	30
2.5 T_m experiments of PNA·DNA hybrids.....	40
2.6 Cell uptake ability studies.....	40
2.6.1 Measurements.....	41
2.6.2 General procedures.....	41
2.6.3 Evaluation of uptake abilities.....	42
2.7 Determination of PNA stabilities toward proteases.....	43
2.7.1 Measurements.....	43
2.7.2 General procedures.....	44
2.7.3 Evaluation of Ac-TTTTTTTTT-Lys-NH ₂ (Ac-T ₉ -K: P17) stabilities toward proteinase K.....	44
CHAPTER III: RESULTS AND DISCUSSION.....	45
3.1 Synthesis of activated peptide monomers.....	45
3.1.1 Synthesis of activated phenylalanine monomer.....	45
3.1.2 Synthesis of activated cysteine monomer.....	46
3.2 Synthesis of activated PNA monomers.....	46
3.3 Synthesis of ACPC spacer	47
3.4 Synthesis of PNA conjugates by solid phase peptide synthesis.....	49
3.5 Study of the hybridization properties of PNA conjugates by UV-melting technique	55
3.6 Uptake ability studies.....	57
3.6.1 Theory and Experimental Design.....	57

	page
3.6.2 Cationic peptides (KFF and R ₁₀) as carriers.....	58
3.6.3 Phosphonium as a carrier.....	60
3.7 Uptake studies with longer PNA (9 mer).....	62
3.7.1 Comparison of uptake abilities of Flu-O-TTT-O-(KFF) ₃ K-NH ₂ (P4) and Flu-O- TTTTTTTTTT-O-(KFF) ₃ K-NH ₂ (P9).	62
3.8 Comparison of two different lysis methods (I and II).....	63
3.9 Position requirement of peptide (KFF) ₃ K as a carrier of PNA.....	64
3.10 Evaluation of Cytotoxicities.....	66
3.11 Determination of stabilities of PNA toward cellular enzymes.....	68
3.11.1 Theory and experiment design.....	68
3.11.2 Stabilities of PNA toward proteinase K.....	68
CHAPTER IV: CONCLUSION.....	76
REFERENCES.....	78
APPENDICES	87
VITAE.....	116



 ศูนย์วิจัยทรัพยากร
 จุฬาลงกรณ์มหาวิทยาลัย

LIST OF TABLES

	Page
Table 1.1 Summary of modified PNA properties	4
Table 1.2 PNAs and antisense control of <i>S. aureus</i> gene expression and growth.....	10
Table 2.1 The PNAs, peptides and their conjugates.....	29
Table 2.2 Synthesis of H-KFFKFFKFFKC-NH ₂ (KFF-C: P1).....	30
Table 2.3 Synthesis of Fmoc-KFFKFFKFFK-NH ₂ (Fmoc-KFF: P2).....	31
Table 2.4 Synthesis of Fmoc-RRRRRRRRRR-NH ₂ (Fmoc-R ₁₀ : P3).....	32
Table 2.5 Synthesis of Flu-O-TTT-O-KFFKFFKFFK-NH ₂ (Flu-T ₃ -KFF: P4).....	33
Table 2.6 Synthesis of Flu-O-TTT-O-RRRRRRRRRR-NH ₂ (Flu-T ₃ -R ₁₀ : P5).....	34
Table 2.7 Synthesis of H-KFFKFFKFFK-O-TTT-Lys(Flu)-NH ₂ (KFF-T ₃ -Flu: P8).....	35
Table 2.8 Synthesis of Flu-O-TCATGAGGCCT-O-KFFKFFKFFK-NH ₂ (Flu-anti-KFF: 12).....	36
Table 2.9 Synthesis of Bz-O-TCATGAGGCCT-O-KFFKFFKFFK-NH ₂ (Bz-anti-KFF: 13).....	37
Table 2.10 Synthesis of Flu-O-TCATGAGGCCT-Lys(P ⁺)-NH ₂ (Flu-anti-Phos: P14).....	38
Table 2.11 Synthesis of Flu-O-TCATGAGGCCT-Lys-NH ₂ (Flu-anti-K: P15).....	39
Table 3.1 Percent coupling efficiency of PNAs, peptides and their conjugates	53
Table 3.2 <i>t_R</i> and mass spectral data of the PNAs peptides and their conjugates used in this study.....	54
Table 3.3 <i>T_m</i> values of hybrids between PNAs/PNA conjugates and their complementary DNA targets.....	56
Table A-1 Data from UV analysis of Flu-O-TTTTTTTTTT-O-KFFKFFKFFK-NH ₂ (P9) & dA ₉ at 20.0-90.0 °C.....	103

	Page
Table B-1 Fluorescence intensities of the solutions obtained from cell culture at 0 h, cell culture at 4 h, supernatant, and lysis (method I) of 0.1× dilution of the <i>E. coli</i> ATCC 25922 cells after treatment with PNA conjugates (5 μM, 37 °C for 4 h).....	109
Table B-2 Fluorescence intensities of the solutions obtained from cell culture at 0 h, cell culture at 8 h, supernatant, and lysis (method I) of 0.1× dilution of the <i>E. coli</i> ATCC 25922 cells after treatment with PNA conjugates (5 μM, 37 °C for 8 h).....	110
Table B-3 Fluorescence intensities of the solutions obtained from cell culture at 0 h, cell culture at 4 h, supernatant, and lysis (method I) of 0.01× dilution of the <i>E. coli</i> ATCC 25922 cells after treatment with PNA conjugates (5 μM, 37 °C for 4 h)	110
Table B-4 Fluorescence intensities of the solutions obtained from cell culture at 0 h, cell culture at 8 h, supernatant, and lysis (method I) of 0.01× dilution of the <i>E.coli</i> ATCC 25922 cells after treatment with PNA conjugates (5 μM, 37 °C for 8 h).....	111
Table B-5 Fluorescence intensities of the solutions obtained from cell culture at 0 h, cell culture at 4 h, supernatant, and lysis (method II) of 0.01× dilution of the <i>E. coli</i> ATCC 25922 cells after treatment with PNA conjugates (5 μM, 37 °C for 4 h).....	112
Table B-6 Fluorescence intensities of the solutions obtained from cell culture at 0 h, cell culture at 2 h, supernatant, and lysis (method II) of 0.1× dilution of the <i>E. coli</i> ATCC 25922 cells after treatment with PNA conjugates (5 μM, 37 °C for 2 h).....	113
Table B-7 Fluorescence intensities of the solutions obtained from cell culture at 0 h, cell culture at 2 h, cell culture at 4 h, supernatant, and lysis (method II) of 0.1× dilution of the <i>E. coli</i> ATCC 25922 cells after treatment with PNA conjugates (5 μM, 37 °C for 4 h).....	113
Table B-8 Optical densities at 590 nm of cell growth at 0 h, 4 h and 8 h of 0.1× dilution of the <i>E. coli</i> ATCC 25922 cells after treatment with PNA conjugates (5 μM, 37 °C for 8 h).....	114

	Page
Table B-9 Optical densities at 590 nm of cell growth at 0 h, 4 h and 8 h of 0.01× dilution of the <i>E. coli</i> ATCC 25922 cells after treatment with PNA conjugates (5 μM, 37 °C for 8 h).....	114
Table B-10 Optical densities at 590 nm of cell growth at 0 h, 4 h and 8 h of 0.1× dilution of the <i>E. coli</i> ATCC 25922 cells after treatment with PNA conjugates (5 μM, 37 °C for 4 h).....	115



ศูนย์วิทยทรัพยากร
จุฬาลงกรณ์มหาวิทยาลัย

LIST OF FIGURES

	Page
Figure 1.1	Structures of DNA and <i>aeg</i> PNA.....1
Figure 1.2	Hydrogen bonding between base pairs according to Watson- Click base paring rules.....2
Figure 1.3	Structure of a PNA·DNA hybrid.....2
Figure 1.4	Structure modifications of PNA..3
Figure 1.5	Structures of Nielsen's PNA and Vilaivan's PNA5
Figure 1.6	Structure of a DNA-pyrrolidinyl PNA hybrid5
Figure 1.7	Antisense inhibition concept. (A) normal cell (B) cell treated with an antisense oligonucleotide agent6
Figure 1.8	Blocking nucleic targets by antisense oligonucleotides (A) Inhibition of gene expression by preventing ribosomal binding (B) Inhibition of gene expression by preventing translocation of the ribosome (C) Alteration of splicing. (D) Inhibition of ribonucleoprotein.....6
Figure 1.9	PNA-Peptide-DETA conjugates.....9
Figure 1.10	Inhibition of <i>phoB</i> expression in <i>S. aureus</i> . Relative enzyme activities are shown for cultures lacking PNA, containing anti- <i>phoB</i> PNAs (Sua130-Sua132), and containing control PNAs (Sua129, SP58, and 1900). The values indicate the level of alkaline phosphatase activity relative to cultures lacking PNA. Values are representative of the results from three independent experiments. The error bars indicate the SEM.....10
Figure 1.11	Antisense activity and toxicity of oligo-arginine-PNA conjugates, Arg(6), Arg(7), Arg(8), and Arg(9)-1 (and pTat-1) were tested head-to-head in the PLuc 705 HeLa cells in the indicated concentration (A) Cell viability was determined in parallel cultured by indirected ATP determinations. (B) Control cultures were given sterilized water in volumes equal to the volumes of conjugate solutions added to obtain the test concentrations. Luciferase activities and cell viability were

	Page
	normalized to the control cultures.....11
Figure 1.12	HeLa cell uptake of 1 μ M fluorescein-labeled peptide after 1 h quantified by flow cytometer. Plot illustrates the mean cellular fluorescence \pm the standard error of three experiments.....12
Figure 1.13	Unmodified PNA: T ₁₀ -Lys and GPNA: (T _g) ₁₀12
Figure 1.14	Fluorescence microscope images of HCT116 cells following incubation with unmodified PNA (A: Fl-T ₁₀ -Lys), TAT domain (B: Fl-Tyr-Gly-Arg-Lys-Lys-Arg-Arg-Gln-Arg-Arg-Arg), and GPNA (C: Fl-(T _g) ₁₀), respectively. Cells were incubated with each respective oligomer at 37 °C for 10 min at 1 μ M, following by a thorough wash (5 \times) with PBS and fixing with 4% paraformaldehyde. Cells were then imaged with confocal fluorescence microscope.....13
Figure 1.15	Synthesis of Phosphonium-PNA conjugates and their uptake into mitochondria.....14
Figure 1.16	Structures of the cyclic PNA fluorescent-labelled-cysteine-TBTP conjugates.....15
Figure 2.1	Colonies of <i>E. coli</i> ATCC 25922.....42
Figure 3.1	Synthesis of (<i>N</i> -Fluoren-9-ylmethoxycarbonyl)-L-phenylalanine-pentafluorophenyl ester (1).....45
Figure 3.2	Synthesis of (<i>N</i> -Fluoren-9-ylmethoxycarbonyl)-L-cysteine-pentafluorophenyl ester (2).....46
Figure 3.3	PNA monomers.....47
Figure 3.4	Synthesis of ACPC spacer.....47
Figure 3.5	¹ H-NMR spectrum of ethyl (1 <i>S</i> ,2 <i>S</i>)-2-[(1' <i>S</i>)-phenylethyl]-amino-cyclopentane carboxylate hydrochloride (3).....48
Figure 3.6	¹ H-NMR spectrum of (1 <i>S</i> ,2 <i>S</i>)-2-(<i>N</i> -Fluoren-9-ylmethoxycarbonyl)-aminocyclopentane carboxylic acid (6).....49
Figure 3.7	HPLC chromatogram of crude product of Flu-TTT-RRRRRRRRRR-NH ₂ (Flu-T ₃ -R ₁₀ : P5)51

	Page
Figure 3.8	MALDI-TOF mass spectrum of purified Flu-TTT-RRRRRRRRRR-NH ₂ (Flu-T ₃ -R ₁₀ : P5) showed $M \cdot H^+_{obs} = 3228.3$; $M \cdot H^+_{calcd} = 3225.6$51
Figure 3.9	Synthesis of PNA-peptide conjugated using convergent fashion by thiol-maleimide interaction.....52
Figure 3.10	T_m curves of Flu-anti-K (P15), Flu-anti-Phos (P14) and Bz-anti-KFF (P16) with d(AGGCCTCATGA) (perfect match DNA). Experimental conditions: PNA:DNA = 1:1, [PNA] = 1.0 μ M, 10 mM sodium phosphate buffer, pH 7.0, heating rate 1.0 $^{\circ}$ C/min.....56
Figure 3.11	First-derivative T_m plots of Flu-anti-K (P15), Flu-anti-Phos (P14) and Bz-anti-KFF (P16) with d(AGGCCTCATGA) (perfect match DNA). Experimental conditions: PNA:DNA = 1:1, [PNA] = 1.0 μ M, 10 mM sodium phosphate buffer, pH 7.0, heating rate 1.0 $^{\circ}$ C/min.....57
Figure 3.12	Fluorescence intensities of the solutions obtained from lysis of the <i>E. coli</i> ATCC 25922 cells after treatment with PNA conjugates (5 μ M, 37 $^{\circ}$ C, 4 h) Flu-T ₃ -KFF (P4), Flu-T ₃ -R ₁₀ (P5), Flu-T ₃ -K (P7) and none (water).....59
Figure 3.13	Fluorescence microscope images of <i>E. coli</i> ATCC 25922 cells (A) treated with 5 μ M of Flu-T ₃ -K (P7) at 37 $^{\circ}$ C for 4 h (control) (B) treated with 5 μ M of Flu-T ₃ -KFF (P4) at 37 $^{\circ}$ C for 4 h.....60
Figure 3.14	Percentages of fluorescence intensities of the solutions obtained from cell culture at 0 h, 4 h, 8 h, supernatant and lysis of the 0.1 \times dilution cells after treatment with 5 μ M of Flu-T ₃ -KFF (P4), Flu-T ₃ -Phos (P6) and the control: Flu-T ₃ -K (P7) at 37 $^{\circ}$ C for 4 h.....61
Figure 3.15	Percentages of fluorescence intensities of the solutions obtained from cell culture at 0 h, 4 h, supernatant and lysis of the 0.01 \times dilution cells after treatment with 5 μ M of Flu-T ₃ -KFF (P4) and Flu-T ₉ -KFF (P9) at 37 $^{\circ}$ C for 4 h.....62

	Page
Figure 3.16	Percentages of fluorescence intensities of the solutions obtained from lysis by method I and method II of the 0.01× dilution cells after treatment with 5 μM of Flu-T ₃ -KFF (P4) at 37 °C for 4 h.....63
Figure 3.17	Percentages of fluorescence intensities of the solutions obtained from lysis of the 0.01× dilution cells after treatment with 5 μM of Flu-T ₉ -KFF (P9), KFF-T ₉ -Flu (P10) and the control: Flu-T ₉ -K (P11) at 37 °C for64
Figure 3.18	Percentages of fluorescence intensities of the solutions obtained from lysis of the 0.1× dilution cells after treatment with 5 μM of Flu-T ₉ -KFF (P9), KFF-T ₉ -Flu (P10) and the control: Flu-T ₉ -K (P11) at 37 °C for 4 h.....65
Figure 3.19	Cytotoxic effects of PNA conjugates. <i>E. coli</i> ATCC 25922 at 0.01× dilution cells were treated with Flu-T ₃ -KFF (P4), Flu-T ₃ -R ₁₀ (P5), Flu-T ₃ -K (P7), and none (water), for 4 and 8 h, and then the absorbance at 590 nm was measured.....66
Figure 3.20	Cytotoxic effects of PNA conjugates. <i>E. coli</i> ATCC 25922 at 0.1× dilution cells were treated with Flu-T ₃ -KFF (P4), Flu-T ₃ -K (P7), none (water) and Flu-T ₃ -Phos (P6) for 4 and 8 h, and then the absorbance at 590 nm was measured.....67
Figure 3.21	Cytotoxic effects of PNA conjugates. <i>E. coli</i> ATCC 25922 0.1× dilution cells were treated with Flu-T ₉ -KFF (P9), KFF-T ₉ -Flu (P10), Flu-T ₉ -K (P11) and none (water), for 2 and 4 h, and then the absorbance at 590 nm was measured.....67
Figure 3.22	HPLC chromatogram (215 nm) of a mixture containing ACTH 4-10 (100 μM, <i>t_R</i> = 40.4 min) and P17 (30 μM, <i>t_R</i> = 45.6 min).....69
Figure 3.23	UV absorption patterns of HPLC peaks from the analysis of ACTH 4-10 (100 μM) and P17 (30 μM) mixture shown in Figure 3.2269
Figure 3.24	HPLC chromatogram (215 nm) of the PNA-peptide mixture without proteinase K treatment. Conditions: P17 30 μM and ACTH 4-10 100 μM in 100 mM Tris-HCl pH 7.5 at 37° C for

	Page
	20 h.....70
Figure 3.25	HPLC chromatogram (215 nm) of the PNA-peptide mixture with proteinase K treatment. Conditions: P17 30 μ M, ACTH 4-10 100 μ M and proteinase K at final conc. = 0.0005 mg/mL (0.015 units/mL) in 100 mM Tris-HCl pH 7.5 at 37° C for 20 min.....71
Figure 3.26	UV absorption patterns of HPLC peaks from the analysis of ACTH 4-10 (100 μ M) and P17 (30 μ M) mixture after proteinase K treatment as shown in Figure 3.2571
Figure 3.27	HPLC chromatogram (215 nm) of the PNA-peptide mixture with proteinase K treatment. Conditions: P17 30 μ M, ACTH 4-10 100 μ M and proteinase K at final conc. = 0.005 mg/mL (0.15 units/mL) in 100 mM Tris-HCl pH 7.5 at 37° C for 5 min.....72
Figure 3.28	HPLC chromatogram (215 nm) of the PNA-peptide mixture with proteinase K treatment. Conditions: P17 30 μ M, ACTH 4-10 100 μ M and proteinase K at final conc. = 0.5 mg/mL (15 units/mL) in 100 mM Tris-HCl pH 7.5 at 37° C for (a) 5 min, (b) 1 h, (c) 3.5 h and (d) 18.5 h.....73
Figure 3.29	UV absorption patterns of HPLC peaks from the analysis of ACTH 4-10 (100 μ M) and P17 (30 μ M) mixture after proteinase K treatment for 1 h as shown in Figure 3.28 (b)74
Figure 3.30	UV absorption patterns of HPLC peaks from the analysis of ACTH 4-10 (100 μ M) and P17 (30 μ M) mixture after proteinase K treatment for 18.5 h as shown in Figure 3.28 (d)75
Figure A-1	1 H NMR spectrum of (<i>N</i> -Fluoren-9-ylmethoxycarbonyl)-L-phenylalanine-pentafluorophenyl ester (1).....88
Figure A-2	1 H NMR spectrum of (<i>N</i> -Fluoren-9-ylmethoxycarbonyl)- <i>S</i> -trityl-L-cysteine pentafluoro-phenyl ester (2).....88
Figure A-3	1 H NMR spectrum of Ethyl (1 <i>S</i> ,2 <i>S</i>)-2-amino-cyclopentane-carboxylate hydrochloride (5).....89

	Page
Figure B-1	HPLC chromatogram of Flu-O-TTT-RRRRRRRRRR-NH ₂ (Flu-T ₃ -R ₁₀ : P5): 260 nm Conditions for reverse-phase HPLC: C-18 column 3 μm particle size 4.6 × 50 mm; gradient system of 0.01% TFA in MeOH/water 20:80 to 80:20 in 60 min; hold time 5 min.....90
Figure B-2	HPLC chromatogram of H-KFFKFFKFFK-O-TTT-Lys(Flu)-NH ₂ (KFF-T ₃ -Flu: P8): 260 nm. Conditions for reverse-phase HPLC: C-18 column 3 μm particle size 4.6 × 50 mm; gradient system of 0.01% TFA in MeOH/water 20:80 to 80:20 in 60 min; hold time 5 min.....91
Figure B-3	HPLC chromatogram of H-KFFKFFKFFK-O-TTT-Lys(Flu)-NH ₂ (KFF-T ₃ -Flu: P8): 440 nm. Conditions for reverse-phase HPLC: C-18 column 3 μm particle size 4.6 × 50 mm; gradient system of 0.01% TFA in MeOH/water 20:80 to 80:20 in 60 min; hold time 5 min.....91
Figure B-4	HPLC chromatogram of Flu-O-TTTTTTTTT-O-KFFKFFKFFK-NH ₂ (Flu-T ₉ -KFF: P9): 260 nm. Conditions for reverse-phase HPLC: C-18 column 3 μm particle size 4.6 × 50 mm; gradient system of 0.01% TFA in MeOH/water 20:80 to 80:20 in 60 min; hold time 5 min.....92
Figure B-5	HPLC chromatogram of Flu-O-TTTTTTTTT-O-KFFKFFKFFK-NH ₂ (Flu-T ₉ -KFF: P9): 440 nm. Conditions for reverse-phase HPLC: C-18 column 3 μm particle size 4.6 × 50 mm; gradient system of 0.01% TFA in MeOH/water 20:80 to 80:20 in 60 min; hold time 5 min.....92
Figure B-6	HPLC chromatogram of H-KFFKFFKFFK-O-TTTTTTTTT-Lys(Flu)-NH ₂ (KFF-T ₉ -Flu: P10): 260 nm. Conditions for reverse-phase HPLC: C-18 column 3 μm particle size 4.6 × 50 mm; gradient system of 0.01% TFA in MeOH/water 20:80 to 80:20 in 60 min; hold time 5 min.....93

	Page
Figure B-7	HPLC chromatogram of H-KFFKFFKFFK-O-TTTTTTTTTT-Lys(Flu)-NH ₂ (KFF-T ₉ -Flu: P10): 440 nm. Conditions for reverse-phase HPLC: C-18 column 3 μm particle size 4.6 × 50 mm; gradient system of 0.01% TFA in MeOH/water 20:80 to 80:20 in 60 min; hold time 5 min.....93
Figure B-8	HPLC chromatogram of Flu-O-TTTTTTTTTT-Lys-NH ₂ (Flu-T ₉ -K: P11): 260 nm. Conditions for reverse-phase HPLC: C-18 column 3 μm particle size 4.6 × 50 mm; gradient system of 0.01% TFA in MeOH/water 20:80 to 80:20 in 60 min; hold time 5 min.....94
Figure B-9	HPLC chromatogram of Flu-O-TTTTTTTTTT-Lys-NH ₂ (Flu-T ₉ -K: P11): 440 nm. Conditions for reverse-phase HPLC: C-18 column 3 μm particle size 4.6 × 50 mm; gradient system of 0.01% TFA in MeOH/water 20:80 to 80:20 in 60 min; hold time 5 min.....94
Figure B-10	HPLC chromatogram of Flu-O-TCATGAGGCCT-O-KFFKFFKFFK-NH ₂ (Flu-anti-KFF: P12): 260 nm. Conditions for reverse-phase HPLC: C-18 column 3 μm particle size 4.6 × 50 mm; gradient system of 0.01% TFA in MeOH/water 20:80 to 80:20 in 60 min; hold time 5 min.....95
Figure B-11	HPLC chromatogram of Bz-O-TCATGAGGCCT-O-KFFKFFKFFK-NH ₂ (Bz-anti-KFF: P13): 260 nm. Conditions for reverse-phase HPLC: C-18 column 3 μm particle size 4.6 × 50 mm; gradient system of 0.01% TFA in MeOH/water 20:80 to 80:20 in 60 min; hold time 5 min.....95
Figure B-12	HPLC chromatogram of Bz-O-KFFKFFKFFK-O-TCATGAGGCCT-NH ₂ (Bz-KFF-anti: P16): 260 nm. Conditions for reverse-phase HPLC: C-18 column 3 μm particle size 4.6 × 50 mm; gradient system of 0.01% TFA in MeOH/water 20:80 to 80:20 in 60min; hold time 5 min.....96

	Page
Figure B-13	HPLC chromatogram of Ac-TTTTTTTTTT-Lys-NH ₂ (Ac-T ₉ -K: P17): 260 nm. Conditions for reverse-phase HPLC: C-18 column 3 μm particle size 4.6 × 50 mm; gradient system of 0.01% TFA in MeOH/water 20:80 to 80:20 in 60 min; hold time 5 min.....96
Figure B-14	HPLC chromatogram (215 nm) of the PNA-peptide mixture without proteinase K treatment. Conditions: P17 30 μM and ACTH 4-10 100 μM in 100 mM Tris-HCl pH 7.5 at 37° C for 1 h. Condition for reverse-phase HPLC: C-18 column 3 μm particle size 4.6 × 50 mm; gradient system of 0.01% TFA in MeOH/water 10:90 to 90:10 in 60 min; hold time 5 min.....97
Figure C-1	MALDI-TOF mass spectrum of H-KFFKFFKFFKC-NH ₂ (KFF-C: P1) M·H ⁺ _{calcd} (monomer) = 1515.8, M·H ⁺ _{calcd} (dimer) = 3031.698.....98
Figure C-2	MALDI-TOF mass spectrum of Fmoc-KFFKFFKFFK-NH ₂ (Fmoc-KFF: P2) M·H ⁺ _{calcd} = 1635.9.....98
Figure C-3	MALDI-TOF mass spectrum of Fmoc-RRRRRRRRRR-NH ₂ (Fmoc-R ₁₀ : P3) M·H ⁺ _{calcd} = 1802.199.....99
Figure C-4	MALDI-TOF mass spectrum of Flu-O-TTT-KFFKFFKFFK-NH ₂ (Flu-T ₃ -KFF: P4) M·H ⁺ _{calcd} = 3059.4.....99
Figure C-5	MALDI-TOF mass spectrum of Flu-O-TTT-Lys(P ⁺)-NH ₂ (Flu-T ₃ -Phos: P6) M·H ⁺ _{calcd} = 1992.4.....100
Figure C-6	MALDI-TOF mass spectrum of Flu-O-TTT-Lys-NH ₂ (Flu-T ₃ -K: P7) M·H ⁺ _{calcd} = 1646.7.....100
Figure C-7	MALDI-TOF mass spectrum of Flu-O-TCATGAGGCCT-O-KFFKFFKFFK-NH ₂ (Flu-anti-KFF: P12) M·H ⁺ _{calcd} = 5763.7.....101
Figure C-8	MALDI-TOF mass spectrum of Bz-O-TCATGAGGCCT-O-KFFKFFKFFK-NH ₂ (Bz-anti-KFF: P13) M·H ⁺ _{calcd} = 5509.7.....101
Figure C-9	MALDI-TOF mass spectrum of Flu-O-TCATGAGGCCT-Lys(P ⁺)-NH ₂ (Flu-anti-Phos: 14) M·H ⁺ _{calcd} = 4555.5.....102
Figure C-10	MALDI-TOF mass spectrum of Flu-O-TCATGAGGCCT-Lys-NH ₂ (Flu-anti-K: P15) M·H ⁺ _{calcd} = 4207.6.....102

- Figure D-1** T_m curves of Flu-O-T₉-Lys-NH₂ (Flu-T₉-K: **P11**), Flu-O-T₉-O-(KFF)₃K-NH₂ (Flu-T₉-KFF: **P9**), H-(KFF)₃K-T₉-Lys(Flu)-NH₂ (KFF-T₉-Flu: **P10**) with d(AAAAAAAAAA) (perfect match): Conditions PNA:DNA = 1:1, [PNA] = 1.0 μM, 10 mM sodium phosphate buffer, pH 7.0, heating rate 1.0 °C/min.....106
- Figure D-2** First-derivative normalized UV- T_m plots of Flu-O-T₉-Lys-NH₂ (Flu-T₉-K: **P11**), Flu-O-T₉-O-(KFF)₃K-NH₂ (Flu-T₉-KFF: **P9**), H-(KFF)₃K-T₉-Lys(Flu)-NH₂ (KFF-T₉-Flu: **P10**) with d(AAAAAAAAAA) (perfect match): Conditions PNA:DNA = 1:1, [PNA] = 1.0 μM, 10 mM sodium phosphate buffer, pH 7.0, heating rate 1.0 °C/min.....107
- Figure D-3** T_m curves of Ac-TTTTTTTT-Lys-NH₂ (Ac-T₉-K: **P17**) with d(AAAAAAAAAA) (perfect match) Conditions PNA:DNA = 1:1, [PNA] = 1.0 μM, 10 mM sodium phosphate buffer, pH 7.0, heating rate 1.0 °C/min.....107
- Figure D-4** First-derivative normalized UV- T_m plots of Ac-TTTTTTTT-Lys-NH₂ (Ac-T₉-K: **P17**) and d(AAAAAAAAAA) (perfect match): Conditions PNA:DNA = 1:1, [PNA] = 1.0 μM 10 mM sodium phosphate buffer, pH 7.0, heating rate 1.0 °C/min.....108

ศูนย์วิทยทรัพยากร
จุฬาลงกรณ์มหาวิทยาลัย

LIST OF ABBREVIATIONS

δ	chemical shift
μL	microliter
μm	micrometer
μM	micromolar
μmol	micromole
$^{\circ}\text{C}$	degree celcius
$[\alpha]_{\text{D}}$	specific rotation
A	adenine
A_{xxx}	absorbance at xxx nm
Abs	absorbance
A^{Bz}	N^4 -benzoyladenine
Ac	acetyl
AcCl	acetyl chrolide
Ac_2O	acetic anhydride
AcOH	acetic acid
ACPC	2-aminocyclopentane-carboxylic acid
<i>acpP</i>	acyl carrier protein position
<i>aeg</i>	2-aminoethyl- glycine
<i>aep</i>	aminoethylprolyl
<i>aepip</i>	aminoethypipecolyl
<i>ap</i>	aminoprolyl
<i>aepone</i>	aminoethylpyrrolodinone
ACTH	Adrenocorticorpic hormone
ATP	adenosine triphosphate
Arg	arginine
ATCC	American type culture collection
<i>bep</i>	backbone extended pyrrolidine
BG	background
Boc	<i>tert</i> -butoxycarbonyl
Bz	benzoyl
C	cytosine

calcd	calculated
C ^{Bz}	<i>N</i> ⁴ -benzoylcytosine
CCA	α -cyano-4-hydroxy cinnamic acid
CPP	cell-penetrating peptide
CDCl ₃	deuterated chloroform
CFU	colony-forming unit
<i>ch</i>	cyclohexyl
conc.	Concentration
<i>cp</i>	cyclopentyl
Cys	cystein
d	doublet
Dans	dansyl
DBU	1,8-diazabicyclo[5.4.0] undec-7-ene
DETA	diethylenetriamine
DIEA	<i>N,N'</i> -dimethylaminopyridine
DMF	<i>N,N'</i> -dimethylformamide
DNA	deoxyribonucleic acid
D ₂ O	deuterium oxide
<i>E. coli</i>	<i>Escherichia coli</i>
EDC·HCl	<i>N</i> -(3-dimethylaminopropyl)- <i>N'</i> -ethyl-carbodiimide hydrochloride
EDTA	ethylenediaminetetraacetic acid
egl	ethylene glycol
equiv	equivalent (s)
EtOAc	ethyl acetate
F	phenylalanine
Fmoc	9-fluorenylmethoxycarbonyl
FmocOSu	9-fluorenylmethylsuccinimidyl carbonate
Flu	fluorescein
g	gram
G	guanine
G ^{Ibu}	<i>N</i> ² -isobutyrylgaunine
Gln	glutamine
Glu	glutamate

Gly	Glycine
GPNA	guanidine-based peptide nucleic acid
h	hour
HATU	<i>O</i> -(7-azabenzotriazol-1-yl)- <i>N,N,N',N'</i> -tetramethyluronium hexafluorophosphate
HeLa	Henrietta Lacks
His	histidine
HIV	human immunodeficiency virus
HOAt	1-hydroxy-7-azabenzotriazole
HPLC	high performance liquid chromatography
HTLV	human T-lymphotropic virus
Ibu	isobutyryl
int	initial
K	lysine
kV	kilovolt
LB	Lysogeny broth; Luria broth or Luria-Bertani broth
Lys	lysine
m	multiplet
MALDI-TOF	matrix-assisted laser desorption ionization-time of flight
MeCN	acetonitrile
MeOH	methanol
MERRF	myoclonic epilepsy with ragged red fibers
Met	methionine
mg	milligram
MHz	megahertz
min	minute
mL	milliliter
mM	millimolar
mmol	millimole
mtDNA	mitochondrial DNA
mp	melting point
mRNA	messenger ribonucleic acid
MS	mass spectrometry
Mtr	4-methoxy-2,3, 6-trimethyl-benzenesulphonyl

Mtt	4-methyltrityl
nm	nanometer
NMR	nuclear magnetic resonance
Obs	observe
OD _{xxx}	optical density at xxx nm
P ⁺	phosphonium cation
PBS	phosphate buffered saline
Pfp	pentafluorophenyl
PfpOH	pentafluorophenol
PfpOTfa	pentafluorophenyl trifluoroacetic acid
Ph	phenyl
Phe	phenylalanine
PNA	peptide nucleic acid or polyamide nucleic acid
POM	pyrrolidine-amide oligonucleotide mimic
PPII	polyproline II helix
ppm	part per million (ppm)
R	arginine
RAM	rink amide linker
R _f	retention factor
RNA	ribonucleic acid
RNase H	ribonuclease H
rpm	revolutions per minute
s	singlet
SEM	the standard error of the mean
SDS	sodium dodecyl sulfate
SPPS	solid phase peptide synthesis
Soln	solution
t	triplet
T	thymine
T _{block}	temperature of the heating block
TBTP	thiobutyltriphenylphosphonium
T ^{Bz}	N ³ -benzoylthymine
TE	Tris-EDTA
Temp.	temperature

TFA	trifluoroacetic acid
TLC	thin layer chromatography
T_m	melting temperature
TMS	tetramethylsilane
t_R	retention time
Tris	Tris(hydroxymethyl)aminomethane
Trp	tryptophan
Tyr	tyrosine
Trt	trityl
U	uracil
UV	ultraviolet



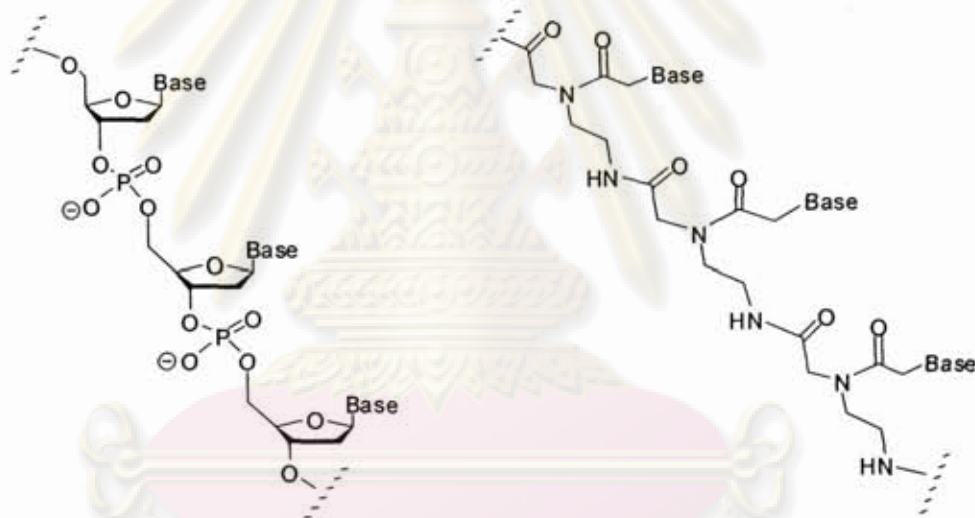
ศูนย์วิทยทรัพยากร
จุฬาลงกรณ์มหาวิทยาลัย

CHAPTER I

INTRODUCTION

1.1 Peptide nucleic acid (PNA)

Peptide nucleic acid is a synthetic analogue of DNA which was originally designed by Nielsen in 1991. [1] The deoxyribose phosphate backbone of DNA was replaced by polypeptide with the same spatial arrangement of nucleobases (**Figure 1.1**). The presence of peptide in PNA instead of deoxyribose phosphate in the DNA backbone resulted in a neutral charge species which behaves in many ways differently from the negatively charged DNA/RNA.



DNA: Deoxyribonucleic Acid aegPNA: 2-aminoethyl-glycine Peptide Nucleic Acid

Figure 1.1 Structures of DNA and aegPNA

1.2 Hybridization of PNA and DNA/RNA

PNA and DNA/RNA form hybrids following the well-known Watson-Crick base pairing rules, adenine (A) binds to thymine (T) and cytosine (C) binds to guanine (G) (**Figure 1.2**). The hydrogen bonds and base stacking held the two single stands together (**Figure 1.3**). [2] Due to the neutral backbone of PNA which avoids electrostatic repulsion, the hybrids between PNA and DNA/RNA are more stable than the hybrids between DNA and DNA or RNA [3-4], where unfavorable electrostatic

interactions can take place unless at a very high salt concentration. Moreover, PNA·DNA hybrids are much less sensitive to ionic strength of the medium than DNA duplexes. [5] The exceptionally strong binding affinity of PNA to complementary DNA/RNA is an interesting and useful property of PNA. Apart from the aforementioned properties, the stability of PNA against enzymatic degradation such as nucleases and proteases [6], make them attractive candidates for antisense and antigene applications.

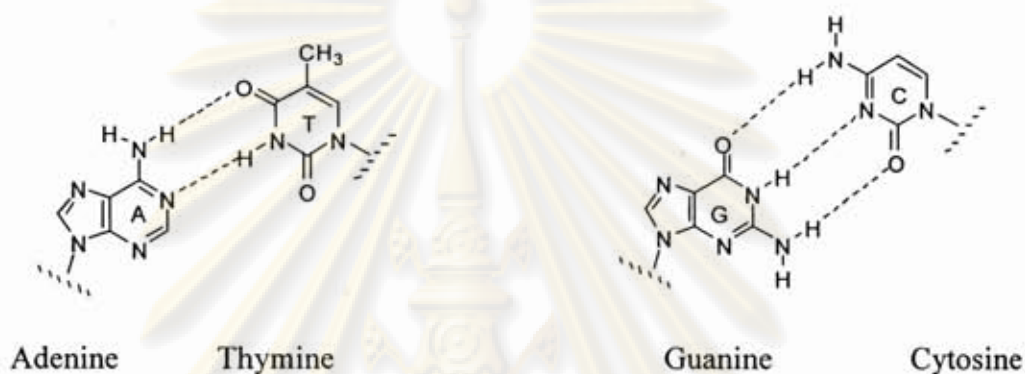


Figure 1.2 Hydrogen bonding between base pairs according to Watson-Crick base pairing rules

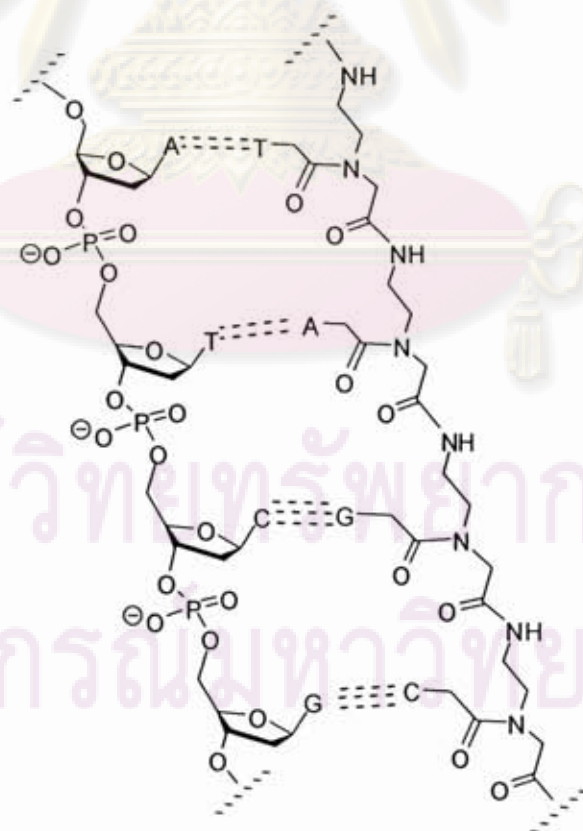


Figure 1.3 Structure of a PNA·DNA hybrid

1.3 Structure modifications of PNA

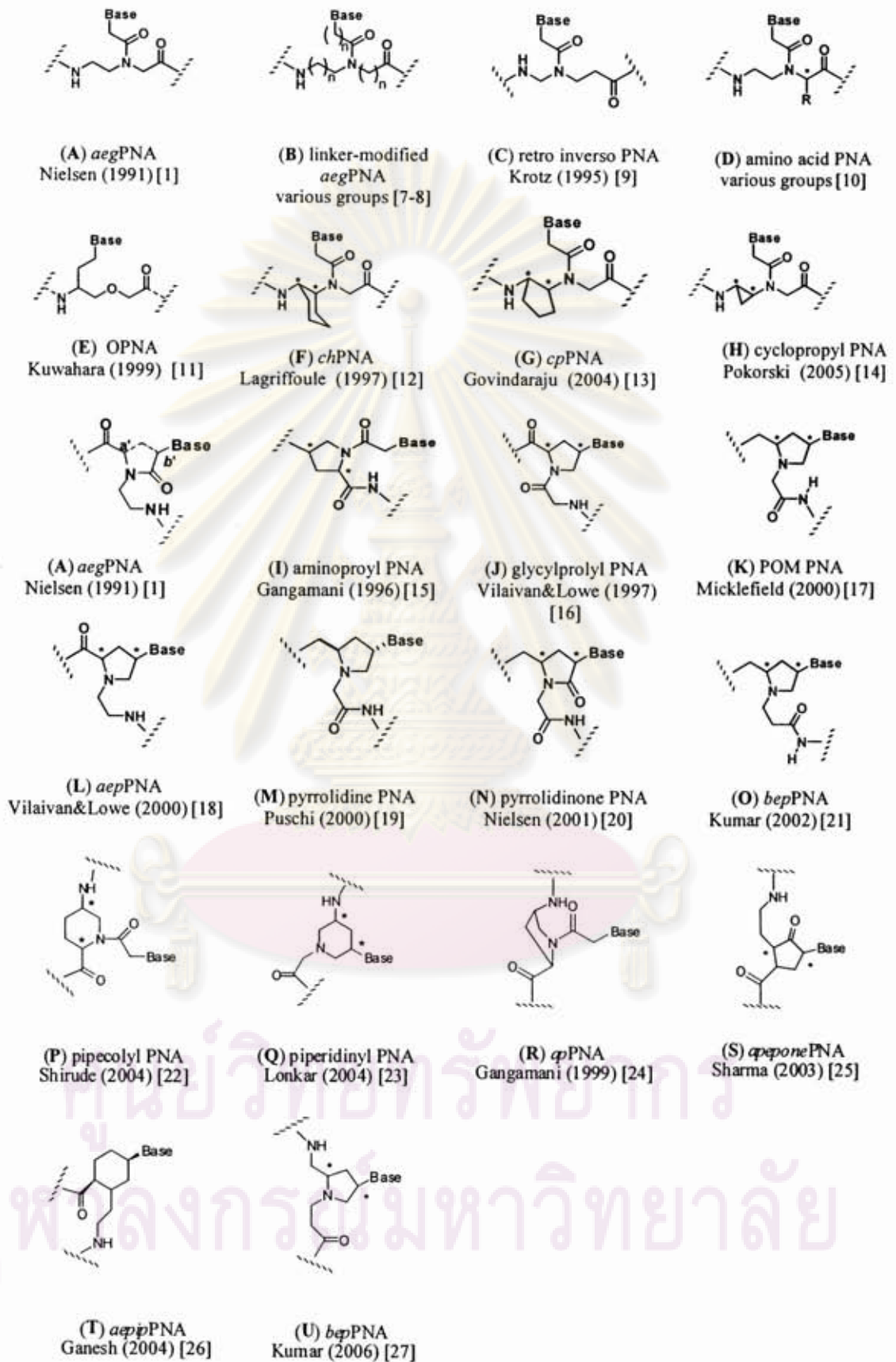


Figure 1.4 Structure modifications of PNA

The original PNA developed by Nielsen (*aegPNA*) showed a number of desirable properties for antisense/antigene applications. Various research groups have been modified the structure of *aegPNA* with the aim to improve the stability, affinity and also direction selectivity. Several alternative different polyamides backbone replacement have been proposed (**Figure 1.4**). [8-27] Examples of these modified PNAs and their properties are shown in **Table 1.1**. [28]

Table 1.1 Summary of modified PNA properties. [28]

entry	PNA modifications and properties
1	aminopropyl PNA (<i>apPNA</i>) [24]: no binding of homochiral oligomers monosubstitution stabilizes PNA·DNA duplexes stereochemistry-dependent parallel/antiparallel binding preferences
2	aminoethylpropyl PNA (<i>aepPNA</i>) [18]: cationic, improved solubility (2 <i>R</i> , 4 <i>R</i>)-T stabilizes PNA ₂ ·DNA triplexes no effect on C ₂ stereochemistry DNA duplex binding: antiparallel > parallel A/G/C/T-base-dependent binding single mismatch more destabilizing compared to control
3	aminoethylpyrrolidinone PNA (<i>aeponePNA</i>) [25]: mono-, di-, tetra-, and all modified aepone-PNA stabilize PNA ₂ ·DNA triplexes destabilize triplexes with poly r(A)
4	pyrrolidine PNA [19]: (2 <i>R</i> , 4 <i>S</i>)-A stabilize both DNA and RNA complexes (2 <i>S</i> , 4 <i>S</i>)-T destabilize DNA and RNA complexes
5	piperidinyl PNA [23]: stabilization of PNA ₂ ·DNA triplexes
6	cyclohexyl PNA (<i>chPNA</i>) [12]: destabilize PNA ₂ ·DNA triplexes and PNA ₂ ·RNA triplexes Stereochemical preferences: <i>SR</i> > <i>RS</i> for DNA, <i>SR</i> < <i>RS</i> for RNA mixed sequences: RNA >> DNA
7	cyclopentyl PNA (<i>cpPNA</i>) [13]: stabilize PNA ₂ ·DNA and PNA ₂ ·RNA triplexes stereochemical preferences: <i>SR</i> > <i>RS</i> mixed sequences: stabilize PNA·DNA and PNA·RNA duplexes.

In 2005 Vilaivan *et al.* reported a novel pyrrolidinyl PNA prolyl-ssACPC (1*S*,2*S*-2-aminocyclopentane carboxylic acid) backbone (**Figure 1.5**). The new pyrrolidinyl PNA possesses improved properties over the Nielsen PNA regarding stability and selectivity of hybridization with its complementary DNA (**Figure 1.6**). [29] For example, the hybridization between the new PNA and its complementary DNA is highly sequence specific, and the homothymine PNA prefers forming duplex rather than triplex with DNA as in Nielsen's PNA. In addition, unlike the original

PNA which can bind to DNA in both parallel and antiparallel directions, the new PNA exclusively binds to DNA in antiparallel direction.

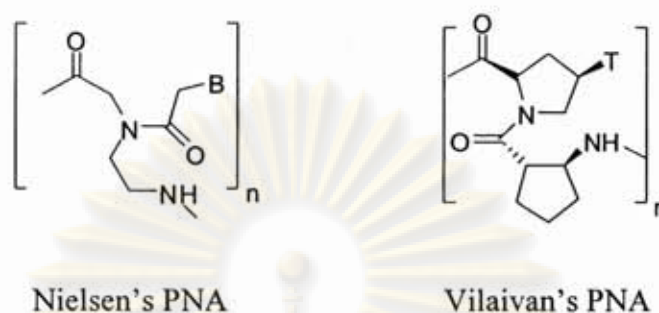


Figure 1.5 Structures of Nielsen's PNA and Vilaivan's PNA

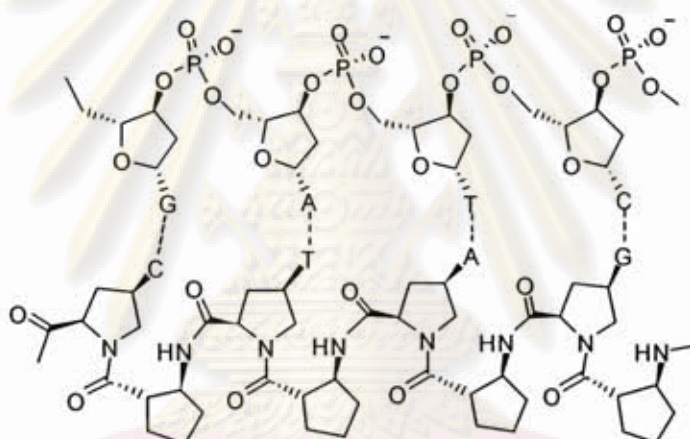


Figure 1.6 Structure of a DNA-pyrrolidinyl PNA hybrid

1.4 PNA as antisense agents

In theory, using an antisense agent to block a gene expression should be simple. The target is chosen and the complementary antisense sequence is synthesized. The antisense agent is then delivered into the cell and binds to the mRNA target, consequently inhibits gene expression (**Figure 1.7**). Antisense inhibition by natural oligonucleotides generally involves ribonuclease H (RNase H) mediates cleavage of RNA strand in oligonucleotide-RNA heteroduplex. [30] On the other hand, PNA-RNA hybrids are not recognized by RNase H [31] therefore only steric inhibition [32], which requires stoichiometric quantities of antisense PNA, is possible (**Figure 1.8**).

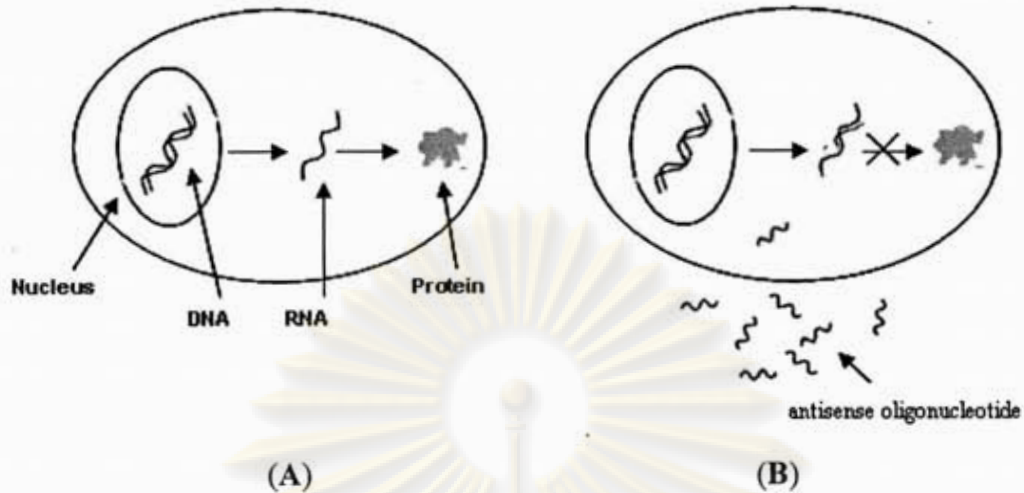


Figure 1.7 Antisense inhibition concept. (A) normal cell (B) cell treated with an antisense oligonucleotide agent [33]

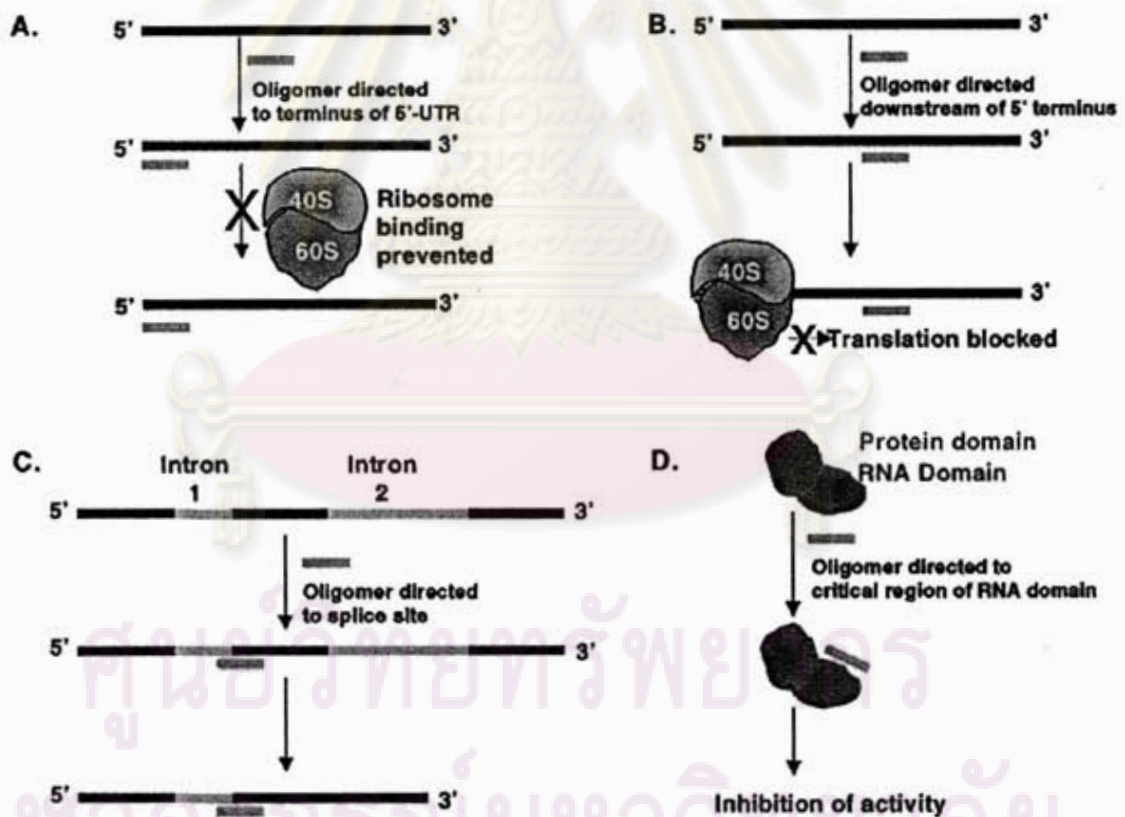


Figure 1.8 Blocking nucleic acids targets by antisense oligonucleotides (A) Inhibition of gene expression by preventing ribosomal binding (B) Inhibition of gene expression by preventing translocation of the ribosome. (C) Alteration of splicing (D) Inhibition of ribonucleoprotein [32]

1.4.1 Applications of PNA as antisense agents

The high stability and specificity of the hybrids between PNAs and RNA together with the high stability of PNA under physiological conditions are the keys for their usefulness in biological applications. Several research groups have attempted to use PNAs as tools for antisense applications. It was observed that the encoding luciferase PNAs to the 5' terminus of the untranslated region can inhibit the luciferase gene expression. [34] Various group studying *in vivo* discovered that PNAs are the potential antisense tools which can bind to a broader range of mRNA sequences. [35-38] A result of *in vitro* studying rabbit reticulocyte lysated showed that PNAs were inhibited translation at AUG start codon. [39] Studying with *E. coli* cells, Good and Nielsen [40, 41] reported that, PNAs targeted to the AUG region of mRNA corresponding to β -galactosidase and β -lactamase genes were efficient block the expression of these genes.

1.4.2 Limitations of PNA an antisense agents

The antisense strategies should be potentially useful in therapeutic applications. [42, 43] Many research groups have successfully applied PNA as antisense and antigene agents. However, the poor solubility under physiological conditions and the poor cellular uptake properties owing to their neutral backbone have limited their usefulness. Furthermore, the presence of secondary and tertiary structures of targets may hinder certain target region and could influence the antisense effect of PNA. A number of strategies have been employed in enabling the classical PNA to permeate cell membranes. Increased solubility can be achieved by modification of the PNA sequence with charged amino acid residues such as lysine. [44] Several strategies have been successfully used to transport antisense PNA through cell membranes. [45] However, the most widely used approach is to conjugate the PNA with a cell-penetrable cationic peptide carrier.

1.5 Cellular uptake strategies

A lipophilic phosphonium tag was conjugated to 11-mer PNA. [46] The phosphonium cation was taken up by mitochondria through the lipophilic lipid bilayer. Cell Penetrating Peptides (¹CPPs) such as ²Tat have been successfully used to deliver various macromolecules into cells. [48] Various polycationic peptide sequences such as poly-L-lysine can improve the cellular delivery of short synthetic oligonucleotides. [49] It was found that oligomers of arginine enter human T-cell line, Jurkat (Human acute T cell leukemia) more effectively than the analogous polymers of lysine, ornithine and histidine. [50] One of the most widely used peptide carrier for delivery of antisense agents to bacterial cell is (KFF)₃K. Attachment of (KFF)₃K to an anti-*acpP* PNA have shown improve the antisense effect in *E. coli* K12. [51] CPPs should be useful to improve therapeutic applications of PNA by increasing the cellular uptake.

1.6 Review of literatures concerning cationic carriers

1.6.1 Applications of (KFF)₃K as a carrier

In 2001 Good *et al.* [53] demonstrated the use of a cell membrane-active peptide: KFFKFFKFFK in carrying antisense PNA agents into bacterial cells. The peptide-PNA conjugates can specifically inhibit *E. coli* K12 *lacZ* expression and growth at 2 μM. The inhibition of gene expression suggested that 9- to 12-mer PNAs covalently linked to the peptide effectively entered the bacterial cells. Toxicity to the human cells (HeLa) has also been evaluated by testing the anti-*lacZ* PNA against *E. coli* grown in cell culture medium. The study was observed that at 20 μM of PNA have no cytotoxicity to the HeLa cells while a concentration of 2 μM or higher was sufficient to cure the HeLa culture from *E. coli* K12 infection.

¹ Short polycationic or amphiphilic peptides which facilitate cellular uptake of various molecular cargo. [52]

² an 86-amino-amino-acid-long nuclear protein which binds to the viral TAR region and transactivated the viral promoter

In 2004 van Boom *et al.* reported a novel artificial ribonuclease with potential cellular uptake abilities. [54] The trifunctional PNA conjugates **1a** and **1b** (Figure 1.9) contain the specific RNA-recognition domain (PNA), the RNA-cleaving domain (DETA-diethylenetriamine), and the peptide (KFF)₃K. The conjugates were assembled in a convergent synthetic route. The RNA-cleaving property of the conjugates was evaluated *in vitro* at 2 μM. The results showed efficient degradation of the target RNA at the expected sites. The cleavage efficiency strongly depended on the type of spacer connecting to the PNA and the peptide. Unfortunately, the cellular uptake of the PNA conjugate and *in vivo* RNA cleaving ability has not yet been demonstrated.

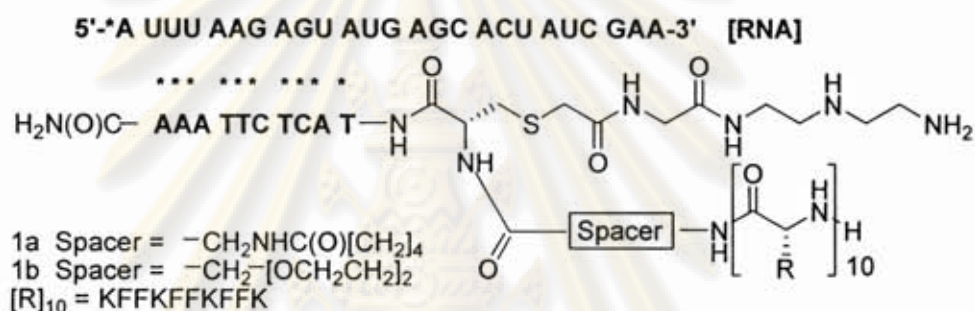


Figure 1.9 PNA-Peptide-DETA conjugates [54]

In 2004 Good *et al.* [55] studied a potential inhibition of chromosomally encoded *S. aureus* gene expression using antisense PNAs. Three PNA-peptide conjugates (Sau130, Sau131, Sau132) were designed to bind to the start codon and ³Shine-Dalgarno region of the *phoB*. *S. aureus* cultures grown in MHB were treated with PNAs along with one control mismatched PNA (Sau129). A PNA of similar composition but unrelated sequence (SP58) and the anti-*gfp* PNA (1900) were examined for comparison (Table 1.2). Sau130 caused a dose-dependent inhibition of alkaline phosphatase activity at 15 and 20 μM. The mismatched PNA showed reduction of inhibition while the unrelated sequence (SP58) exhibited no effects in gene expression (Figure 1.10). Hence, the KFF-conjugated anti-*phoB* PNA appeared to be a sequence-specific inhibitor of *S. aureus phoB* gene expression.

³

a region 6-7 nucleotides upstream of the start codon AUG in prokaryotes

Table 1.2 PNAs and antisense control of *S. aureus* gene expression and growth. [55]

	PNA designation and sequence	Anti-reporter gene peptide-PNAs	No. of bases
1900	Anti- <i>gfp</i>	H(KFFF) ₃ K-L-catagctgtttc-NH ₂	12
SP58	Unrelated	H(KFFF) ₃ K-L-cgccagttaa- NH ₂	10
SP182	Scrambled 1900	H(KFFF) ₃ K-L-acatgctgtctt- NH ₂	12
Sau129	Mismached Sau130	H(KFFF) ₃ K-L-taacataataca- NH ₂	12
Sau130	Anti- <i>phoB</i> (-6 +6)	H(KFFF) ₃ K-L-taacataagaca- NH ₂	12
Sua131	Anti- <i>phoB</i> (-2 +8)	H(KFFF) ₃ K-L-gataacataa- NH ₂	10
Sua132	Anti- <i>phoB</i> (-13 -4)	H(KFFF) ₃ K-L-acatcctect- NH ₂	10

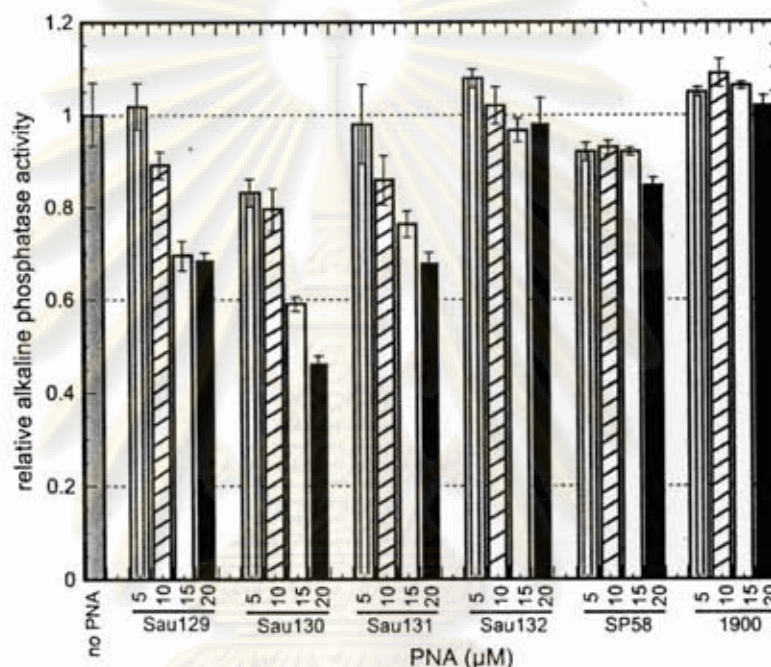


Figure 1.10 Inhibition of *phoB* expression in *S. aureus*. Relative enzyme activities are shown for cultures lacking PNA, containing anti-*phoB* PNAs (Sua130-Sua132), and containing control PNAs (Sua129, SP58, and 1900). The values indicate the level of alkaline phosphatase activity relative to cultures lacking PNA. Values are representative of the results from three independent experiments. The error bars indicate the SEM. [55]

1.6.2 Applications of Arginine rich peptides as carriers

In 2006 Koppelhus *et al.* [56] studied relative activity of different PNA-oligoarginine conjugates to promote correct expression of a recombinant luciferase gene in HeLa cells. The data in **Figure 1.11** showed that increasing the number of arginine residues in the poly-arginine peptides correlates with increased antisense

activity. However, with long Arginine oligomers conjugates such as Arg(9), toxicity appears to become a limiting factor for the activity of the poly-arginine conjugates.

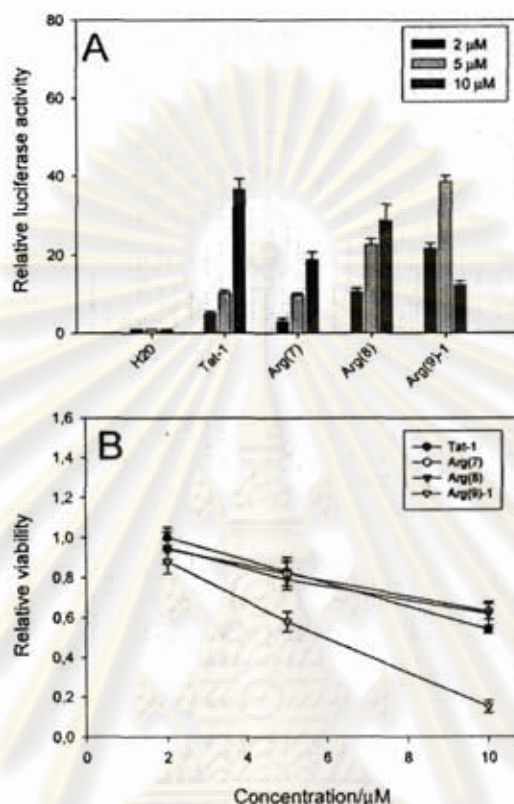


Figure 1.11 Antisense activity and toxicity of oligo-arginine-PNA conjugates, Arg(6), Arg(7), Arg(8), and Arg(9)-1 (and pTat-1) were tested head-to-head in the pLuc 705 HeLa cells in the indicated concentration (A) Cell viability was determined in parallel cultured by indirect ATP determinations. (B) Control cultures were given sterilized water in volumes equal to the volumes of conjugate solutions added to obtain the test concentrations. Luciferase activities and cell viability were normalized to the control cultures. [56]

Amino acid modifications can further increase the uptake abilities of PPII-based CPPs such as oligoarginine. Recently Schepartz *et al* [57] designed two series of cationic PPII left-handed helices with 3 residues per turn with repeating units of (PPR)_n and (PRR)_n. The uptake abilities of these fluorescein-labeled peptides in live HeLa cells were investigated by flow cytometry (Figure 1.12). The (PRR)₅ and (PRR)₆ were permeable to the cells similar to the simple R₈, R₁₀ and R₁₂ while the Tat and (PRR)₃ and (PRR)₄ only slightly permeated to the cells.

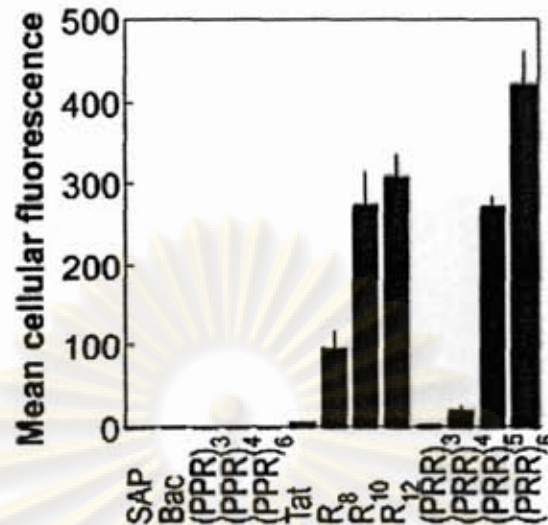
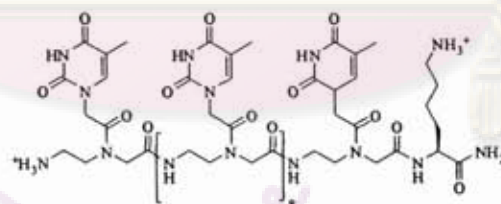
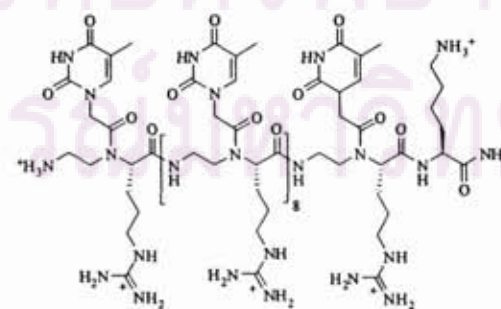


Figure 1.12 HeLa cell uptake of 1 μM fluorescein-labeled peptide after 1 h quantified by flow cytometer. Plot illustrates the mean cellular fluorescence \pm the standard error of three experiments. [57]

In 2003 Ly *et al.* [58] reported an antisense activity of a cell-permeable GPNA (guanidine-based peptide nucleic acid). The GPNA (**Figure 1.13**) at a concentration of 1 μM showed uptake efficiency to human colon cancer HCT116 cell line. Fluorescence microscope images (**Figure 1.14**) showed that GPNA entered the cell as effectively as the TAT transduction domain (amino acids 49-57). In contrast, unmodified PNA did not show uptake activity under the same condition.



Unmodified PNA: T₁₀-Lys



GPNA: (T_g)₁₀

Figure 1.13 Unmodified PNA: T₁₀-Lys and GPNA: (T_g)₁₀ [58]



Figure 1.14 Fluorescence microscope images of HCT116 cells following incubation with unmodified PNA (A: Fl-T₁₀-Lys), TAT domain (B: Fl-Tyr-Gly-Arg-Lys-Lys-Arg-Arg-Gln-Arg-Arg-Arg), and GPNA (C: Fl-(T_g)₁₀), respectively. Cells were incubated with each respective oligomer at 37 °C for 10 min at 1 μM, following by a thorough wash (5×) with PBS and fixing with 4% paraformaldehyde. Cells were then imaged with confocal fluorescence microscope. [58]

1.6.3 Applications of Tat and other CPPs as carriers

A number of different types of CPPs have been successfully used in the wide field of peptide-mediated delivery systems. Almost 50% cases used Tat peptide [59] which can deliver various molecules into mammalian cells. Tat peptide is certainly very effective *in vitro* and also local systems. [48] Recombinant of proteins consisted of Tat fragments 37-72 or 37-62 and β-galactosidase, horseradish peroxidase [60] or a Fab antibody [61] were spontaneously transported into various cell-lines. Moreover, Tat protein derived short CPPs were discovered in 1997. [62] Fragment 48-60 was found to translocate through plasma membrane. Other extensively studied CPPs include the family of polycationic sequences such as poly-lysine. Long poly-L-lysine polymers were reported to improve the cellular delivery of various proteins. [63, 64] Oligonucleotide-poly(L-lysine) conjugates have been demonstrated for uptake ability. [49] In addition, several arginine-rich peptides mainly derived from HIV and HTLV were shown a good translocating activity. [65]

1.6.4 Applications of Phosphonium cations as carriers

In 2001 Murphy *et al.* have developed a new strategy for targeting lipophilic PNA oligomers to mitochondria and used it to determine the effects of PNA on mutated mtDNA replication in manipulation of mtDNA replication and expression at A8344G MERRF point mutation. [46] A 11-mer PNA was conjugated to a lipophilic phosphonium cation, which is readily taken up the cell by mitochondria through the lipid bilayer driven by the membrane potential across the inner membrane (**Figure 1.16**). This was confirmed by using an ion-selective electrode to measure the uptake of the Phosphonium-PNA conjugates. The Phosphonium-PNA conjugate selectively inhibited the *in vitro* replication of DNA containing the A8344G point mutation that causes the human mtDNA-related diseases.

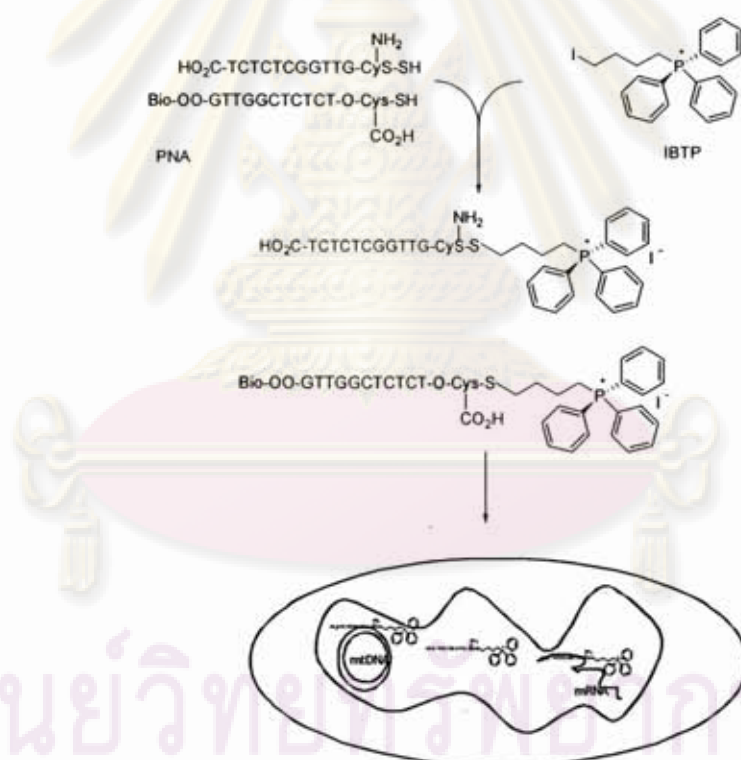


Figure 1.15 Synthesis of Phosphonium-PNA conjugates and their uptake into mitochondria

In 2007 Patino *et al.* [66] reported “a ready-to use” fluorescent-labelled cysteine-TBTP (4-thiobutyltriphenylphosphonium) synthon (**Figure 1.17**) which enables the efficient homogenous delivery of cyclic PNA into the cytoplasm of HeLa cells. As demonstrated by fluorescence microscopy, the dansyl- or fluorescein-

labelled cysteine-TBTP synthons were very useful for the cellular uptake and the intracellular localization of the antisense PNAs. Once the conjugates have entered the mitochondria, the disulfide bond was reductively cleaved resulting in releasing of the free PNA.

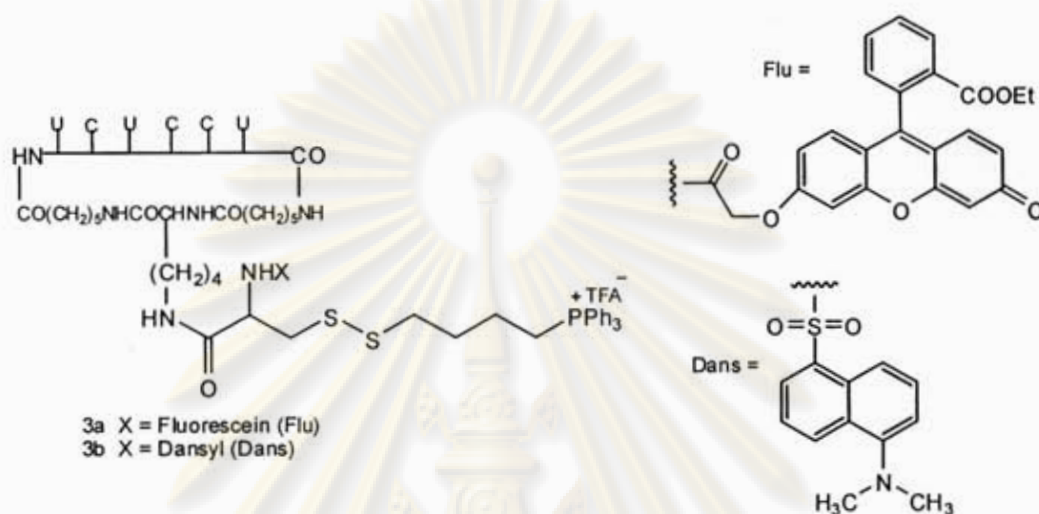


Figure 1.16 Structures of the cyclic PNA fluorescent-labelled-cysteine-TBTP conjugates

1.7 Objectives of this work

The objectives of this research are 1) to synthesize cell-penetrating peptide nucleic acid conjugates based on a novel pyrrolidinyl (1*S*, 2*S*)-ACPC PNA system 2) to determine the uptake abilities of these conjugates into *E. coli* ATCC 25922 cells. Fluorescence techniques will be used to evaluate the uptake abilities of the PNA conjugates. In addition, the stability of the pyrrolidinyl PNA towards a model protease enzyme (proteinase K) will also be investigated by HPLC.

CHAPTER II

EXPERIMENTAL SECTION

2.1 General Procedures

2.1.1 Measurements

A Metler Toledo electrical balance was used to determine the weight of all substance chemicals. Evaporation of solvent was carried out by Büchi Rotavapor R-200 with a water aspirator model B-490 or a Refco Vacubrand pump. Thin layer chromatography (TLC) performed on Merck D.C. silica gel 60 F₂₅₄ 0.2 mm. precoated aluminium plates cat. no. 1.05554. UV-visualization (254 nm) of TLC was made in-house. Flash column chromatography was performed on silica gel 230-400 mesh. Reverse phase HPLC experiments were performed on Water 600™ system equipped with gradient pump and Water 996™ photodiode array detector; optionally alternate to Rheodyne 7725 manual sample loop (100 µL sample size for analytical scale). A Polaris™ C₁₈ HPLC column 3 µm particle size 4.6 × 50 mm (Varian Inc., USA) was used for analytical purposes. The base Empower software was available for integrated the peak and data processing from HPLC analysis. Collecting fractions from HPLC were carried out manually by real time monitoring of HPLC chromatogram at a suitable absorption wavelength. The pooled fractions were dry by gentle nitrogen stream (in fume hood), or evaporation by Büchi Rotavapor R-200 with a water aspirator model B-490 or a Refco Vacubrand diaphragm pump. Melting points were investigated on a CARY 100 Bio UV-Visible spectrophotometer (Varian Inc., USA) The optical rotations ($[\alpha]_D$) were measured at the ambient temperature on a Jasco P-1010 Polarimeter using sodium light (D line, 589.3 nm) and were reported in degrees; concentrations (c) were reported as g/100 mL. ¹H NMR spectra were recorded in deuterated solvents on Varian Mercury-400 plus operating at 400 MHz. Chemical shifts (δ) are reported in part per million (ppm) relative to tetramethylsilane (TMS). Multiplicities were abbreviated as followed: singlet (s), doublet (d), triplet (t), quartet (q). Splitting patterns that could not be interpreted or easily visualized are designated as multiplet (m). MALDI-TOF mass spectra of all PNA, peptides and PNA conjugates

were obtained on a Microflex MALDI-TOF mass spectrometry (Bruker Daltonics). α -cyano-4-hydroxy cinnamic acid (CCA) was used as a matrix. The diluents for preparation of MALDI-TOF samples are 0.1% trifluoroacetic acid in acetonitrile:water (1:2).

2.1.2 Materials and Methods

All chemicals were purchased from Fluka, Merck or Aldrich Chemical Co., Ltd. The chemicals were used as received without further purification. Distilled commercial grade solvents were used for flash column chromatography, TLC analysis and extraction. Solvents for reactions and crystallization were reagent grade. Acetonitrile and methanol for HPLC experiment were HPLC grade obtained from BDH or Murch and used as received. Anhydrous N,N' -dimethylformamide ($H_2O \leq 0.01\%$) for solid phase peptide synthesis was obtained from Fluka and dried over activated 3Å molecular sieves before used. TentaGel S RAM Fmoc resin (Fluka) was used as a solid support for peptide synthesis. Trifluoroacetic acid (98%) was purchased from Fluka. The protected amino acids (Fmoc-L-Phe-OH, Fmoc-L-Cys(Trt)-OH, Fmoc-L-Agr(Mtr)-OH, Fmoc-L-Lys(Boc)-OPfp and Fmoc-L-Lys(Mtt)-OH) were obtained from Calbiochem Novabiochem Co., Ltd. 5(6)-Carboxyfluorescein N -hydroxy-succinimide ester for PNA labeling was purchased from Fluka. Nitrogen gas and hydrogen gas were obtained from Thai Industrial Gas (TIG) with high purity up to 99.5 %. MilliQ water was obtained from ultrapure water system with Millipak[®] 40 filter unit 0.22 μm , Millipore (USA). Oligonucleotides were purchased from Biodesign Unit, National Science and Technology Development Agency, Thailand. (N -Fluoren-9-ylmethoxycarbonylamino)-*cis*-4-(thymine-1-yl)-D-proline pentafluorophenyl ester (Fmoc-T-OPfp), (N -Fluoren-9-ylmethoxycarbonylamino)-*cis*-4-(N^2 -isobutyrylguanin-9-yl)-D-proline pentafluorophenyl ester (Fmoc-G^{ibu}-OPfp) and (1*S*,2*S*)-2-(N -Fluoren-9-ylmethoxycarbonyl)-aminocyclopentanecarboxylic acid pentafluorophenyl ester (Fmoc-ACPC-OPfp) were prepared by Miss Boonjira Boontha and Dr. Tirayut Vilaivan. (N -Fluoren-9-ylmethoxycarbonylamino)-*cis*-4-(N^4 -benzoyladenine-9-yl)-D-proline pentafluorophenyl ester (Fmoc-A^{Bz}-OPfp) and (N -Fluoren-9-ylmethoxycarbonylamino)-*cis*-4-(N^4 -benzoylcytosine-1-yl)-D-proline pentafluorophenyl ester (Fmoc-C^{Bz}-OPfp) were

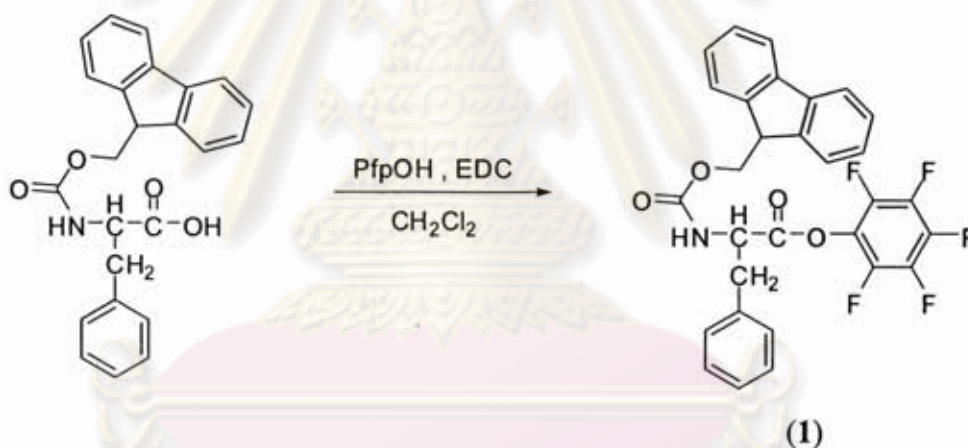
prepared by Miss Cheeraporn Ananthanawat. {2-[2-(*N*-Fluoren-9-ylmethoxycarbonyl-amino)ethoxy]ethoxy}acetic acid pentafluorophenyl ester was prepared by Miss Pratchayaporn Korkaew. Carboxybutyl(triphenylphosphonium)bromide *N*-hydroxy succinimide ester was prepared by Miss Boonjira Boontha.

2.2 Synthesis of monomers

2.2.1 Synthesis of activated peptide monomers

a) (*N*-Fluoren-9-ylmethoxycarbonyl)-*L*-phenylalanine-pentafluorophenyl ester (1)

Method I

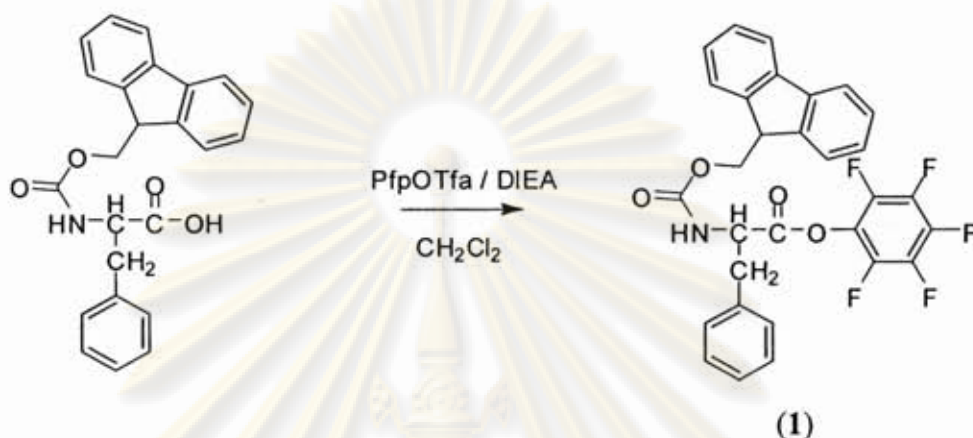


The commercially available Fmoc-L-Phe-OH (140.4 mg, 0.362 mmol) and pentafluorophenol (1.5 equiv, 99.8 mg) were dissolved in dichloromethane (2 mL) following by addition of EDC·HCl (1.5 equiv, 103.9 mg). The reaction mixture was allowed to stir at room temperature for 1 hour. The completion of the reaction was confirmed by TLC (starting material $R_f \sim 0$, product $R_f = 0.3$, hexanes:ethyl acetate 5:1). The product was purified by flash column chromatography on silica gel eluting with hexanes:ethyl acetate (5:1). After removing the solvent, the residue was stirred with hexanes for 30 minutes. After filtration and washing with hexanes, the compound (1) was obtained as a white solid (145.2 mg, 72% yield).

¹H NMR (400 MHz, CDCl₃) δ_H 3.18-3.30 (2H, dd, CHCH₂Ph), 4.08 (1H, t, CO₂CH₂CH), 4.38-4.50 (2H, dd, CO₂CH₂CH), 4.90-4.98 (1H, q, NHCHCH₂) 7.18

(2H, m, CH phenyl) , 7.19-7.40 (7H, m, 4CH Fmoc and 3CH phenyl), 7.53 (2H, m, CH Fmoc) 7.77 (2H, m, CH Fmoc)

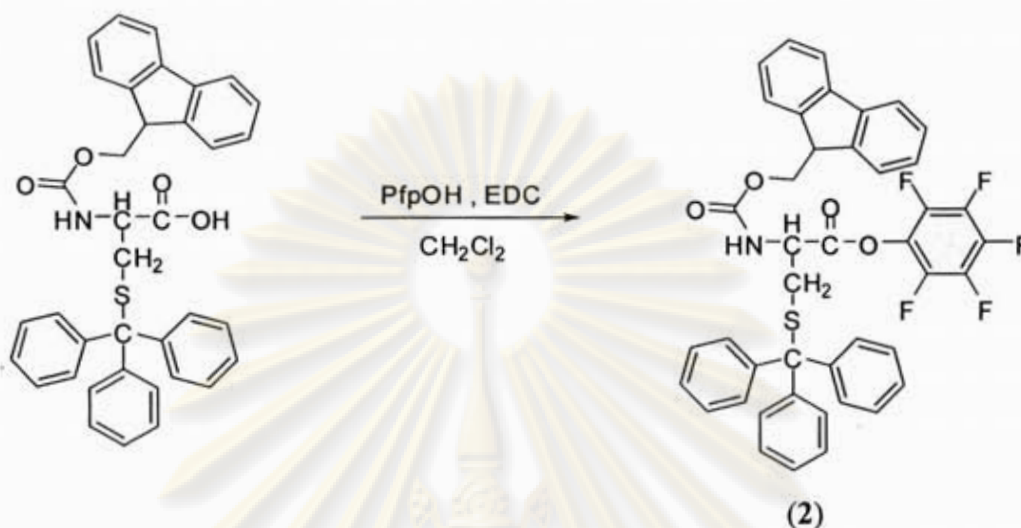
Method II



Fmoc-L-Phe-OH (195.5 mg, 0.503 mmol) was dissolved in dichloromethane. PfpOTfa (1.0 equiv, 86.2 μ L) and DIEA (1.0 equiv, 85.6 μ L) were slowly added to the solution. After 30 minutes, TLC analysis indicated that some starting material still remained. Additional portions of PfpOTfa (1.0 equiv, 86.2 μ L) and DIEA (1.0 equiv, 85.6 μ L) were added to the reaction mixture. The reaction was completed after 90 minutes according to TLC analysis. The product was purified by column chromatography on silica gel eluting with hexanes:ethyl acetate (7:1) to obtain the (N-Fluorenylmethoxycarbonyl)-L-phenylalanine-pentafluorophenyl ester (1) as a white solid (66.2 mg, 24 %) with identical NMR spectra to above.

ศูนย์วิทยทรัพยากร
จุฬาลงกรณ์มหาวิทยาลัย

b) (*N*-Fluorenylmethoxycarbonyl)-*S*-trityl-L-cysteine pentafluorophenyl ester (2)



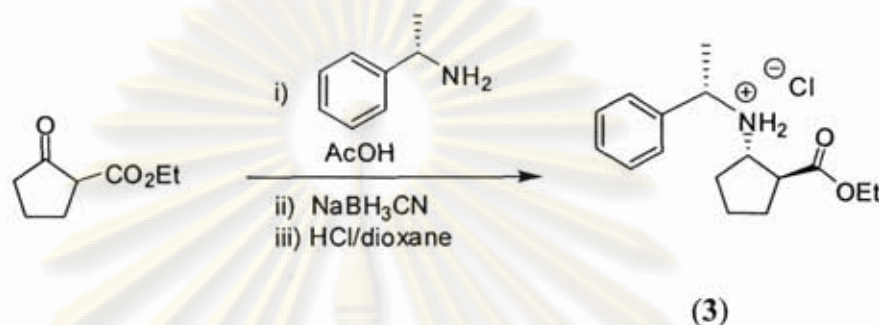
Synthesis of the title compound (2) was accomplished in the same way as described for compound (1) above. The commercially available Fmoc-L-Cys(Trt)-OH (77.9 mg, 0.133 mmol) and pentafluorophenol (1.5 equiv, 24.5 mg) were dissolved in dichloromethane (2 mL) following by adding EDC·HCl (1.5 equiv, 27.8 mg). The reaction afforded (2) (54.3 mg, 54% yield) as a light brown solid after flash column chromatography on silica gel eluting with hexanes:ethyl acetate (8:1).

¹H NMR (400 MHz, CDCl₃) δ_H 2.61-2.80 (2H, dd, CHCH₂S), 4.18 (1H, t, CHCH₂CO₂), 4.25-4.40 (2H, m, CO₂CH₂CH), 5.05 (1H, q, NHCHCH₂) 7.17 (6H, m, CH phenyl), 7.22-7.38 (13H, m, 4CH Fmoc and 9CH phenyl), 7.55 (2H, m, CH Fmoc) 7.77 (2H, m, CH Fmoc)

ศูนย์วิทยทรัพยากร
จุฬาลงกรณ์มหาวิทยาลัย

2.2.2 Synthesis of *trans*-(1*S*,2*S*)-2-aminocyclopentanecarboxylic acid (ACPC) spacer

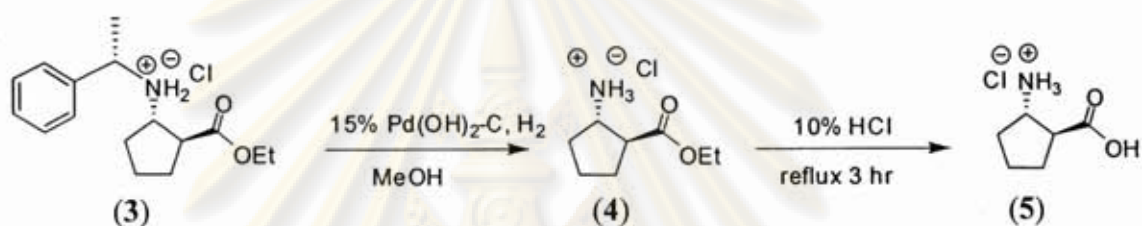
a) Ethyl (1*S*, 2*S*)-2-[(1' *S*)-phenylethyl]-aminocyclopentanecarboxylate hydrochloride (3) [67]



Ethyl cyclopentanone-2-carboxylate (4.0 mL, 27 mmol) was dissolved in absolute ethanol (32 mL) following by (*S*)-(-)- α -methylbenzylamine (3.48 mL, 30.0 mmol) and glacial acetic acid (1.54 mL, 32.0 mmol). The reaction mixture was stirred at room temperature for 2 hours to form the enamine intermediate which was monitored by TLC (7:3 hexanes/EtOAc). Next, the reaction mixture was heated to 72 °C and then sodium cyanoborohydride (3.14 g, 54.0 mmol) was slowly added over a period of 5 hours. The reaction was left at room temperature overnight. When the reaction was completed as monitored by TLC (7:3 hexanes/EtOAc, KMnO_4), the ethanol was removed by rotary evaporation to form a white sticky residue. Water (20 mL) was added to the residue and the pH was adjusted to 7 by adding solid NaHCO_3 . The mixture was extracted with dichloromethane (3×20 mL). The dichloromethane was removed by rotary evaporation to give a colorless liquid. The crude product was dissolved in 15 mL of ethyl acetate at 4 °C. A freshly prepared 4N HCl in dioxane (31 mL, prepared by slowly adding 8.50 mL of acetyl chloride to a mixture of 7.02 mL ethanol and 14.58 mL dioxane) was then added. The flask was left overnight in refrigerator to allow complete precipitation of the product. After filtration, the crude product in the form of HCl salt was obtained as a white solid (3.183 g). This material was further purified by repeated recrystallization from EtOH- H_2O until a single isomer was obtained according to ^1H NMR analysis.

^1H NMR (400 MHz, CDCl_3) δ_{H} 1.21 (3H, t, $\text{CO}_2\text{CH}_2\text{CH}_3$), 1.59 (3H, d, $^+\text{NH}_2\text{CHCH}_3$), 1.75 (2H, m, $\text{CH}_2\text{CH}_2\text{CH}_2$), 1.93 (2H, m, CH_2CHCO), 1.99 (2H, m, $^+\text{NH}_2\text{CHCH}_2$), 2.33 (1H, m, CHCO_2Et), 3.41 (1H, t, $^+\text{NH}_2\text{CHCH}_2$), 3.58 (1H, q, $^+\text{NH}_2\text{CHCH}_3$), 4.15 (2H, m, $\text{CO}_2\text{CH}_2\text{CH}_3$), 7.41-7.63 (5H, m, phenyl); $[\alpha]_{\text{D}}^{22.7} = +16.8$ ($c = 1.00$ g/100 mL CDCl_3). The optical rotation also corresponded to the authentic sample prepared previously in this laboratory $\{[\alpha]_{\text{D}}^{25} = +17.1$ ($c = 1.00$ g/100 mL CDCl_3). [68]

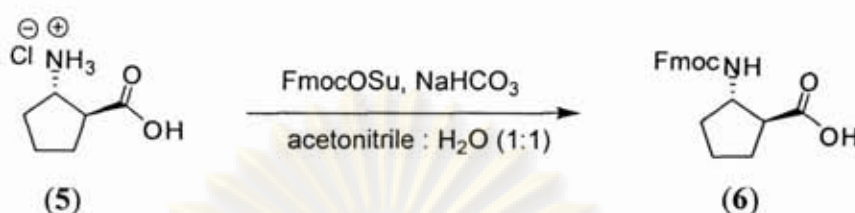
b) Ethyl (1*S*,2*S*)-2-amino-cyclopentanecarboxylate hydrochloride (5) [67]



Ethyl (1*S*,2*S*)-2-[(1'*S*)-phenylethyl]-aminocyclopentane carboxylate hydrochloride (3) (1.032 g, 3.47 mmol) was dissolved in methanol (5 mL). Palladium hydroxide on charcoal (155 mg) was added and the reaction mixture was stirred at room temperature under H_2 atmosphere overnight. The completion of the hydrogenolysis was monitored by TLC (1:3 hexanes/EtOAc). The palladium catalyst was removed by filtration. The filtrate was evaporated by rotary evaporation to obtain compound (4) as brown oil. Without further purification, the compound (4) was refluxed with 10% HCl (10 mL) for 3 hours. The mixture was allowed to cool down and the solvent was removed by rotary evaporation to obtain the title compound (5) as colorless oil which solidified to a white solid (0.406 g, 71% from 3) after stirring with acetone.

^1H NMR (400 MHz, CDCl_3) δ_{H} 1.50-1.68 [m, 2H, $\text{CH}_2\text{CH}_2\text{CH}_2$], 2.02 [m, 4H, CH_2CH_2], 2.78 [q, 1H, CHCO_2H], 3.75 [m, 1H, $\text{CH}_2\text{CHNH}_3^+$]; $[\alpha]_{\text{D}}^{22.5} = +57.0$ ($c = 1.00$ g/100 mL H_2O). The optical rotation also corresponded to the authentic samples prepared previously in this laboratory $\{[\alpha]_{\text{D}}^{25} = +61.3$ ($c = 1.00$ g/100 mL H_2O). [33]

c) (1*S*,2*S*)-2-(*N*-Fluoren-9-ylmethoxycarbonyl)-aminocyclopentanecarboxylic acid (6) [33]



The (1*S*,2*S*)-2-aminocyclopentane carboxylic acid hydrochloride (5) (406 mg, 2.46 mmol) was dissolved in water (5 mL). NaHCO₃ (2.5 equiv excess) was added until the pH of the solution was ~ 8. Acetonitrile (5 mL) was added until a homogeneous solution was obtained. Next, FmocOSu (1.012 g, 3 mmol) was slowly added with stirring at room temperature. The stirring was continued for 8 h while maintaining the pH at ~ 8 by addition of NaHCO₃. The mixture was diluted with water (20 mL) and extracted with diethyl ether (3 × 20 mL). The aqueous phase was collected and the pH was adjusted to 2 with concentrated HCl. The white suspension was extracted with dichloromethane (3 × 20 mL). The solvent was removed by rotary evaporation and the residue was dried in vacuum to afford the title compound (6) as a white solid (841.2 mg, 97 %).

¹H NMR (400 MHz, CDCl₃) δ_H 1.30-1.45 (2H, m, CH₂CH₂CH₂), 1.80-2.10 (4H, m, CH₂CH₂CH₂), 2.70 (1H, q, CHCOOH), 4.08 (1H, m, NHCH), 4.41-4.49 (2H, m, Fmoc aliphatic CH and Fmoc aliphatic CH₂) and 7.22-7.79 (8H, m, Fmoc aromatic CH); [α]^{23.7}_D = +36.1 (c = 1.00 g/100 mL MeOH). The optical rotation also corresponded to the authentic samples prepared previously in this laboratory {[α]²⁵_D = +36.4, c = 1.00g/100mL MeOH}. [68]

จุฬาลงกรณ์มหาวิทยาลัย

2.3 Synthesis of PNA conjugates

2.3.1 Preparation of the reaction pipette and apparatus for solid phase peptide synthesis

All PNA conjugate syntheses were carried out using a custom-made peptide synthesis column from Pasteur pipette as described previously. [33, 69]

Synthesis of PNA conjugates were carried out on 0.5-3.0 μmol scale. All PNAs consist of *cis*-D pyrrolidine monomers and SS-ACPC spacer. The PNAs and peptide carriers were linked by an aminoethoxyethoxyacetyl (O) linker via {2-[2-(*N*-Fluoren-9-ylmethoxycarbonyl-amino)ethoxy]ethoxy}acetic acid pentafluorophenyl ester monomer. The fluorescence labels attached at the N-termini of PNA conjugates was also linked by the same O-linker whereas the attachment of phosphonium or fluorescein at the C-termini of PNA conjugates was achieved via the free amino side chain of lysine. In a few cases, the cysteine was also attached at the C-termini of the carrier peptide sequence in order to coupling with the PNA via maleimide and thiol group reaction. [70]

2.3.2 Procedures for solid phase synthesis of PNA conjugates

The general synthesis protocol for the synthesis of PNA or PNA conjugates required three stock solutions shown below.

Stock 1: (deprotection solution) piperidine 20 μL , 1,8-diazabicyclo[5.4.0]undec-7-ene (DBU) 20 μL , and DMF 960 μL

Stock 2: (capping and coupling solution) 70 μL DIEA in 930 μL DMF

Stock 3: (activation solution) 5.5 mg HOAt in 100 μL DMF

a) Removing Fmoc protecting group from the resin

The reaction pipette containing TentaGel S RAM Fmoc resin (6.25 mg, 1.5 μmol) was prepared as described previously. [69] The resin was treated with 100 μL of the deprotection solution (stock 1) for 10 min at room temperature with occasional

agitation. After the specified period of time, the reagent was squeezed off and the reaction column was washed exhaustively with DMF.

b) Coupling of the N-terminal residues

The first amino acid (lysine, cysteine, arginine) was attached to the free amino group on the Tentagel-S-RAM resin. The activated amino acid (Fmoc-L-Lys(Boc)-OPfp, Fmoc-L-Cys(Trt)-OPfp, 6 μmol) were dissolved in a mixture of stock 2 (15 μL) and stock 3 (15 μL) for 45 min at room temperature. In case of Fmoc-L-Lys(Mtt)-OH, and Fmoc-L-Agr(Mtr)-OH, the free amino acid were treated with HATU {O-(7-azabenzotriazol-1-yl)-*N,N,N',N'*-tetramethyluronium hexafluorophosphate, 2.2 mg, 6 μmol } and 30 μL of stock 2 instead of DIEA/HOAt mixture. The coupling time remained the same. After the specified period of time, the reagent was squeezed off and the reaction column was washed exhaustively with DMF.

c) End capping

After coupling step, the resin was capped with 2 μL of acetic anhydride in 30 μL of DIEA solution (stock 2) for 5 min in order to prevent formation of deletion sequences. [71]

d) Deprotection of the Fmoc group at the N-terminus

The Fmoc-protected resin was treated with 100 μL of the deprotection solution for 10 min at room temperature with occasional agitation. After the specified period of time, the reagent was squeezed off and the reaction column was washed exhaustively with DMF. The used deprotecting reagent was kept for determination of the coupling efficiency by diluting with an appropriate volume of methanol and then the UV-absorbance of the dibenzofulvene-piperidine adduct at 264 nm was measured. The UV-absorbance of the solution obtained from the first deprotection was assumed to be 100%. Such determination of coupling efficiency was advantageous in terms of determining how the solid phase reaction progress. The efficiency should be > 95 % for each step in order to obtain acceptable yield of the PNA conjugates.

e) Coupling of PNA, SS-ACPC spacer and peptide monomers

In the same way as described for (c) – (d), the PNA monomer, or peptide (phenylalanine, arginine) monomer was attached to the free amino group of the first monomer coupling to the resin. The activated monomer (Pfp-PNA monomers, 6 μmol) were dissolved in a mixture of stock 2 (15 μL) and stock 3 (15 μL) for 45 min at room temperature. In case of Fmoc-L-Phe-OH or Fmoc-L-Arg(Mtr)-OH, the free amino acids were treated with HATU (2.2 mg, 6 μmol) and 30 μL of stock 2 instead of DIEA/HOAt mixture. Alternate couplings of the ssACPC in the same condition to the PNA monomer were subsequently performed until the complete sequence was obtained. After the specified period of time, the reagent was squeezed off and the reaction column was washed exhaustively with DMF.

f) N-terminal modification with 2-[2-(Fmoc-amino)ethoxy]ethoxy acetyl linker

The synthesis cycle was repeated until the growing peptide chain was extended to the desired sequence. After the final capping, the nucleobase side-chain protecting groups (benzoyl for C, A and isobutyryl for G) were removed by treatment with dioxane:ammonia 1:1 (2 mL) in a sealed test tube at 60 °C for 6 h. The N-terminal Fmoc group was removed by treatment with the deprotection solution as in (d). The deprotected PNA resin was further treated with 2-[2-(Fmoc-amino)ethoxy]ethoxy acetic acid pentafluorophenyl ester (5.5 mg, 10.0 μmol) dissolved in 30 μL anhydrous DMF for 30 min at room temperature with occasional agitation. After the specified period of time (2 h), the reagent was squeezed off and the reaction column was washed exhaustively with DMF.

g) Attachment of the fluorescence label

The deprotected PNA was coupled with 5(6)-fluorescein succinimidyl ester (Flu-OSu). The fluorescence label (4 equiv) was directly coupled to the N-termini of the PNA conjugates via the free amino residue under basic conditions (DIEA 10 equiv, DMF 30 μL) at room temperature for 6 hours. For attachment of fluorescein at

the C-terminal lysine, the 4-methyltrityl (Mtt) protecting group of the lysine side chain must be first removed (2% TFA in DCM, 5×1 mL). The label was then coupled under the same conditions of attachment as described above. The progress of the reaction was monitored by MALDI-TOF mass spectrometry after cleavage of a small amount of the PNA from the resin. After the reaction was completed (6 h), the resin was washed extensively with DMF. The washed resin was further treated with 1:1 ammonia/dioxane at 60 °C for 6 h to remove any non-specifically bound fluorescein.

h) Modification with phosphonium group at C-terminus

For attachment of phosphonium group to the C-termini of PNA, the 4-methyltrityl (Mtt) protecting group of lysine was removed (2 % TFA in DCM). Next, the free amino residue of lysine was coupled with carboxybutyl (triphenylphosphonium) bromide *N*-hydroxy succinimide (10.0 μ mol, 4.6 mg in 30 μ L DMF). The progress of the reaction was monitored by MALDI-TOF mass spectrometry. After the reaction was completed (2 h), the resin was washed extensively with DMF.

i) Cleavage

Trifluoroacetic acid (3×0.5 mL) was used for cleavage the resin-bond PNA at room temperature for 2 h (total period). During this period, the resin turned red, indicating that the cleavage has occurred. After the reaction completed, the trifluoroacetic acid was removed by a gentle nitrogen stream (in fume hood). The crude PNA was precipitated using diethyl ether (1 mL). After centrifugation and removal of ether, the crude PNA was allowed to dry at room temperature and stored as a solid at -20 °C until used.

For R₁₀-containing PNA, the Mtr (4-methoxy-2,3,6-trimethylbenzenesulphonyl) protecting group of arginine required treatment with TFA:thioanisole (9:1) at room temperature overnight to completely remove the protecting group. After the cleavage, the TFA and thioanisole were removed by a gentle nitrogen stream (in fume hood). The crude PNA was precipitated using diethyl ether (1 mL) as

described above. After centrifugation and removal of ether, the crude PNA was allowed to dry at room temperature and stored as a solid at $-20\text{ }^{\circ}\text{C}$ until used.

j) Purification

I) HPLC analysis

The crude PNA was dissolved in 100-200 μL deionized water or 10%-20% aqueous methanol. The solution was filtered through a nylon membrane filter (0.45 μm). Analysis and purification was performed by reverse phase HPLC, monitoring by UV-absorbance at 260 nm (also at 440 nm for the fluorescein-labeled PNA) and eluting with a gradient system of 0.01% TFA in methanol/water. The HPLC gradient system used two solvent systems which were solvent A (0.01% trifluoroacetic acid in milliQ water) and solvent B (0.01% trifluoroacetic acid in methanol). The elution began with A:B (20:80) for 5 min followed by a linear gradient up to A:B (80:20) over a period of 60 min, then hold for 5 min before reverting back to A:B (20:80).

II) SAX capture resin

In case of purification of Flu-T₃-KFF (**P4**), Flu-T₃-Phos (**P6**), Flu-T₃-K (**P7**), Flu-anti-Phos (**P14**) and Flu-anti-K (**P15**) and the purifications were achieved by anion exchanger capture using SAX. The PNA was dissolved in 100 μL of 10% v/v acetonitrile in deionized water and the pH of the solution was adjusted to basic by 10 μL of DIEA. The mixture was passed through an SAX resin column which was pre-equilibrated with deionized water. The column was then eluted with 10% acetonitrile ($5 \times 1\text{ mL}$) and 50% acetonitrile ($5 \times 1\text{ mL}$) to remove non-fluorescein tagged PNA. The PNA was then released from the column by eluting with 1% TFA in 50% MeCN: H₂O. The purity of the PNA in each elution fraction was checked by MALDI-TOF analysis.

k) Identification

After evaporation of solvents from the combined fractions at 45 °C or by gentle steam nitrogen at 40 °C, the identity of the PNA oligomer or PNA conjugates was verified by MALDI-TOF mass spectrometry. All spectra were obtained in linear positive ion mode with accelerating voltage of 25 kV. A matrix solution containing CCA in 0.1% trifluoroacetic acid in acetonitrile:water (1:2) solution was used. All spectra were processed by summing 20 individual laser shots or more.

Table 2.1 The PNAs, peptides and their conjugates

code	N → C	simple name
P1	H-KFFKFFKFFKC-NH ₂	KFF-C
P2	Fmoc-KFFKFFKFFK-NH ₂	Fmoc-KFF
P3	Fmoc-RRRRRRRRRR-NH ₂	Fmoc-R ₁₀
P4	Flu-O-TTT-O-KFFKFFKFFK-NH ₂	Flu-T ₃ -KFF
P5	Flu-O-TTT-O-RRRRRRRRRR-NH ₂	Flu-T ₃ -R ₁₀
P6	Flu-O-TTT-Lys(P ⁺)-NH ₂	Flu-T ₃ -Phos
P7	Flu-O-TTT-Lys-NH ₂	Flu-T ₃ -K
P8	H-KFFKFFKFFK-O-TTT-Lys(Flu)-NH ₂	KFF-T ₃ -Flu
P9	Flu-O-TTTTTTTTTT-O-KFFKFFKFFK-NH ₂	Flu-T ₉ -KFF
P10	H-KFFKFFKFFK-O-TTTTTTTTTT-Lys(Flu)-NH ₂	KFF-T ₉ -Flu
P11	Flu-O-TTTTTTTTTT-Lys-NH ₂	Flu-T ₉ -K
P12	Flu-O-TCATGAGGCCT-O-KFFKFFKFFK-NH ₂	Flu-anti-KFF
P13	Bz-O-TCATGAGGCCT-O-KFFKFFKFFK-NH ₂	Bz-anti-KFF
P14	Flu-O-TCATGAGGCCT-Lys(P ⁺)-NH ₂	Flu-anti-Phos
P15	Flu-O-TCATGAGGCCT-Lys-NH ₂	Flu-anti-K
P16	Bz-O-KFFKFFKFFK-O-TCATGAGGCCT-NH ₂	Bz-KFF-anti
P17	Ac-TTTTTTTTTT-Lys-NH ₂	Ac-T ₉ -K

2.4 Selected examples of PNAs, peptides or their conjugates

a) H-KFFKFFKFFKC-NH₂ (KFF-C: P1)

H-KFFKFFKFFKC-NH₂ was synthesized using the procedures described above. After deprotection of the protecting group of TentaGel S RAM Fmoc resin (4.2 mg, 1.0 μmol), the peptide monomers were coupled in the order shown in the **Table 2.2**.

Table 2.2 Synthesis of H-KFFKFFKFFKC-NH₂ (KFF-C: P1)

Cycle	Monomers	Amount	A ₂₆₄	Coupling efficiency
1	Fmoc-Cys(Trt)-OPfp	3.0 mg (4 μmol)	0.622	100
2	Fmoc-Lys(Boc)-OPfp	2.5 mg (4 μmol)	0.549	88
3	Fmoc-Phe-OPfp	2.2 mg (4 μmol)	0.583	100
4	Fmoc-Phe-OPfp	2.2 mg (4 μmol)	0.602	100
5	Fmoc-Lys(Boc)-OPfp	2.5 mg (4 μmol)	0.595	99
6	Fmoc-Phe-OPfp	2.2 mg (4 μmol)	0.596	100
7	Fmoc-Phe-OPfp	2.2 mg (4 μmol)	0.576	97
8	Fmoc-Lys(Boc)-OPfp	2.5 mg (4 μmol)	0.572	99
9	Fmoc-Phe-OPfp	2.2 mg (4 μmol)	0.547	96
10	Fmoc-Phe-OPfp	2.2 mg (4 μmol)	0.544	100
11	Fmoc-Lys(Boc)-OPfp	2.5 mg (4 μmol)	-	-

*No experiment was monitored (for all tables in this section).

After the usual cleavage, the MALDI-TOF mass spectrum of crude product of H-KFFKFFKFFKC-NH₂ (KFF-C: P1) showed $M \cdot H^+_{obs} = 1516.3$ and 3033.6 ; $M \cdot H^+_{calcd}$ (monomer) = 1515.8 , $M \cdot H^+_{calcd}$ (dimer) = 3031.6 .

ศูนย์วิทยทรัพยากร
จุฬาลงกรณ์มหาวิทยาลัย

b) Fmoc-KFFKFFKFFK-NH₂ (Fmoc-KFF: P2)

Fmoc-KFFKFFKFFK-NH₂ was synthesized using the procedures described above. After deprotection of the protecting group of TentaGel S RAM Fmoc resin (12.6 mg, 3.0 μmol), the peptide monomers were coupled in the order shown in the **Table 2.3**.

Table 2.3 Synthesis of Fmoc-KFFKFFKFFK-NH₂ (Fmoc-KFF: P2)

Cycle	Monomers	Amount	A ₂₆₄	Coupling efficiency
1	Fmoc-Lys(Boc)-OPfp	7.6 mg (12 μmol)	1.929	100
2	Fmoc-Phe-OPfp	6.6 mg (12 μmol)	1.596	83
3	Fmoc-Phe-OPfp	6.6 mg (12 μmol)	1.782	100
4	Fmoc-Lys(Boc)-OPfp	7.6 mg (12 μmol)	1.729	97
5	Fmoc-Phe-OPfp	6.6 mg (12 μmol)	1.833	100
6	Fmoc-Phe-OPfp	6.6 mg (12 μmol)	1.566	85
7	Fmoc-Lys(Boc)-OPfp	7.6 mg (12 μmol)	1.690	100
8	Fmoc-Phe-OPfp	6.6 mg (12 μmol)	1.616	96
9	Fmoc-Phe-OPfp	6.6 mg (12 μmol)	1.513	94
10	Fmoc-Lys(Boc)-OPfp	7.6 mg (12 μmol)	-	-

After the usual cleavage, the MALDI-TOF mass spectrum of crude product of Fmoc-KFFKFFKFFK-NH₂ (Fmoc-KFF: P2) showed $M \cdot H^+_{\text{obs}} = 1634.7$; $M \cdot H^+_{\text{calcd}} = 1635.9$.

ศูนย์วิทยทรัพยากร
จุฬาลงกรณ์มหาวิทยาลัย

c) **Fmoc-RRRRRRRRRR-NH₂ (Fmoc-R₁₀: P3)**

Fmoc-RRRRRRRRRR-NH₂ was synthesized using the procedures described above. After deprotection of the protecting group of TentaGel S RAM Fmoc resin (12.6 mg, 3.0 μmol), the peptide monomers were coupled in the order shown in the **Table 2.4**.

Table 2.4 Synthesis of Fmoc-RRRRRRRRRR-NH₂ (Fmoc-R₁₀: P3)

Cycle	Monomers	Amount	A ₂₆₄	Coupling efficiency
1	Fmoc-Arg(Mtr)-OH	7.3 mg (12 μmol)	1.249	100
2	Fmoc-Arg(Mtr)-OH	7.3 mg (12 μmol)	1.203	96
3	Fmoc-Arg(Mtr)-OH	7.3 mg (12 μmol)	0.999	83
4	Fmoc-Arg(Mtr)-OH	7.3 mg (12 μmol)	0.909	91
5	Fmoc-Arg(Mtr)-OH	7.3 mg (12 μmol)	0.840	92
6	Fmoc-Arg(Mtr)-OH	7.3 mg (12 μmol)	0.839	100
7	Fmoc-Arg(Mtr)-OH	7.3 mg (12 μmol)	0.815	97
8	Fmoc-Arg(Mtr)-OH	7.3 mg (12 μmol)	0.670	82
9	Fmoc-Arg(Mtr)-OH	7.3 mg (12 μmol)	0.573	86
10	Fmoc-Arg(Mtr)-OH	7.3 mg (12 μmol)	-	-

After the usual cleavage, the MALDI-TOF mass spectrum of crude product of Fmoc-RRRRRRRRRR-NH₂ (Fmoc-R₁₀: P3) showed $M \cdot H^+_{obs} = 1798.5$; $M \cdot H^+_{calcd} = 1802.1$.

ศูนย์วิทยทรัพยากร
จุฬาลงกรณ์มหาวิทยาลัย

d) Flu-O-TTT-O-KFFKFFKFFK-NH₂ (Flu-T₃-KFF: P4)

Flu-O-TTT-O-KFFKFFKFFK-NH₂ was synthesized using the procedures described above. Starting from Fmoc deprotection of resin-bound Fmoc-KFFKFFKFFKFFK (a) (0.5 μmol), the monomers were coupled in the order shown in the Table 2.5.

Table 2.5 Synthesis of Flu-O-TTT-O-KFFKFFKFFK-NH₂ (Flu-T₃-KFF: P4)

Cycle	Monomers	Amount	A ₂₆₄	Coupling efficiency
1	Fmoc-T-OPfp	1.2 mg (2 μmol)	0.845	100
2	Fmoc-ACPC-OPfp	1.1 mg (2 μmol)	0.887	100
3	Fmoc-T-OPfp	1.2 mg (2 μmol)	0.856	97
4	Fmoc-ACPC-OPfp	1.1 mg (2 μmol)	0.957	100
5	Fmoc-T-OPfp	1.2 mg (2 μmol)	-	-
6	Fmoc-ACPC-OPfp	1.1 mg (2 μmol)	-	-
7	Fmoc-egl-OPfp	2.8 mg (5 μmol)	-	-
8	5(6)-carboxyfluorescein-OSu	1.0 mg (2 μmol)	-	-

After usual cleavage and purification by SAX anion exchanger, MALDI-TOF mass spectrum of Flu-O-TTT-KFFKFFKFFK-NH₂ (Flu-T₃-KFF: P4) showed $M \cdot H^+_{\text{obs}} = 3061.9$; $M \cdot H^+_{\text{calcd}} = 3059.4$.

ศูนย์วิทยทรัพยากร
จุฬาลงกรณ์มหาวิทยาลัย

e) Flu-O-TTT-O-RRRRRRRRRR-NH₂ (Flu-T₃-R₁₀: P5)

Flu-O-TTT-O-RRRRRRRRRR-NH₂ was synthesized using the procedures described above. Starting from Fmoc deprotection of the resin-bound Fmoc-RRRRRRRRRR (a) (0.5 μmol), the monomers were coupled in the order shown in the Table 2.6.

Table 2.6 Synthesis of Flu-O-TTT-O-RRRRRRRRRR-NH₂ (Flu-T₃-R₁₀: P5)

Cycle	Monomers	Amount	A ₂₆₄	Coupling efficiency
1	Fmoc-T-OPfp	1.2 mg (2 μmol)	0.514	100
2	Fmoc-ACPC-OPfp	1.1 mg (2 μmol)	0.463	90
3	Fmoc-T-OPfp	1.2 mg (2 μmol)	0.461	100
4	Fmoc-ACPC-OPfp	1.1 mg (2 μmol)	0.347	75
5	Fmoc-T-OPfp	1.2 mg (2 μmol)	-	-
6	Fmoc-ACPC-OPfp	1.1 mg (2 μmol)	-	-
7	Fmoc-egl-OPfp	2.8 mg (5 μmol)	-	-
8	5(6)-carboxyfluorescein-OSu	1.0 mg (2 μmol)	-	-

After usual cleavage and purification by HPLC, the peak of Flu-O-TTT-O-RRRRRRRRRR-NH₂ (Flu-T₃-R₁₀: P5) appeared at $t_R = 41.1$ min. MALDI-TOF mass spectrum showed $M \cdot H^+_{obs} = 3228.3$; $M \cdot H^+_{calcd} = 3225.6$.

ศูนย์วิทยทรัพยากร
จุฬาลงกรณ์มหาวิทยาลัย

f) H-KFFKFFKFFK-O-TTT-Lys(Flu)-NH₂ (KFF-T₃-Flu: P8)

H-KFFKFFKFFK-O-TTT-Lys(Flu)-NH₂ was synthesized using the procedures described above. The monomers were coupled to the deprotected TentaGel S RAM Fmoc resin (6.25 mg, 1.5 μmol) in the order shown in the **Table 2.7**.

Table 2.7 Synthesis of H-KFFKFFKFFK-O-TTT-Lys(Flu)-NH₂ (KFF-T₃-Flu: P8)

Cycle	Monomers	Amount	A ₂₆₄	Coupling efficiency
1	Fmoc-Lys(Mtt)-OH	3.8 mg (6 μmol)	0.981	100
2	Fmoc-T-OPfp	3.6 mg (6 μmol)	0.772	79
3	Fmoc-ACPC-OPfp	3.1 mg (6 μmol)	0.773	100
4	Fmoc-T-OPfp	3.6 mg (6 μmol)	0.798	100
5	Fmoc-ACPC-OPfp	3.1 mg (6 μmol)	0.802	100
6	Fmoc-T-OPfp	3.6 mg (6 μmol)	0.832	100
7	Fmoc-ACPC-OPfp	3.1 mg (6 μmol)	0.820	99
8	Fmoc-egl-OPfp	5.5 mg (10 μmol)	0.947	100
9	Fmoc-Lys(Boc)-OPfp	3.8 mg (6 μmol)	0.923	98
10	Fmoc-Phe-OPfp	3.3 mg (6 μmol)	0.945	100
11	Fmoc-Phe-OPfp	3.3 mg (6 μmol)	0.903	96
12	Fmoc-Lys(Boc)-OPfp	3.8 mg (6 μmol)	0.767	85
13	Fmoc-Phe-OPfp	3.3 mg (6 μmol)	0.706	92
14	Fmoc-Phe-OPfp	3.3 mg (6 μmol)	0.759	100
15	Fmoc-Lys(Boc)-OPfp	3.8 mg (6 μmol)	0.672	89
16	Fmoc-Phe-OPfp	3.3 mg (6 μmol)	0.642	96
17	Fmoc-Phe-OPfp	3.3 mg (6 μmol)	0.554	86
18	Fmoc-Lys(Boc)-OPfp	3.8 mg (6 μmol)	0.546	99

The attachment of fluorescein at the C-terminal lysine was performed as follows. Firstly, deprotection of 4-methyltrityl (Mtt) protecting group was carried out using 2% TFA in DCM (5 × 1 mL). Next, the 5(6)-carboxyfluorescein-OSu (4 μmol, 2.1 mg in 30 μL of stock 2) was coupled to the C-termini of PNA conjugates in DMF. After the reaction was completed (6 h), the resin was washed extensively with DMF and then with MeOH. The washed resin was further treated with 1:1 ammonia/dioxane at 60°C for 6 h to remove any non-specifically bond fluorescein.

After usual cleavage and purification by HPLC, the peak of H-KFFKFFKFFK-O-TTT-Lys(Flu)-NH₂ (KFF-T₃-Flu: P8) appeared at *t_R* = 51.8 min.

g) Flu-O-TCATGAGGCCT-O-KFFKFFKFFK-NH₂ (Flu-anti-KFF: P12)

Flu-O-TCATGAGGCCT-O-KFFKFFKFFK-NH₂ was synthesized using the procedures described above. Starting from Fmoc deprotection of resin-bound Fmoc-KFFKFFKFFKFFK (b) (0.5 μmol), the monomers were coupled in the order shown in the table 2.8.

Table 2.8 Synthesis of Flu-O-TCATGAGGCCT-O-KFFKFFKFFK-NH₂ (Flu-anti-KFF: P12)

Cycle	Monomers	Amount	A ₂₆₄	Coupling efficiency
1	Fmoc-egl-OPfp	2.8 mg (5 μmol)	0.668	100
2	Fmoc-T-OPfp	1.2 mg (2 μmol)	0.644	96
3	Fmoc-ACPC-OPfp	1.1 mg (2 μmol)	0.727	100
4	Fmoc-C ^{Bz} -OPfp	1.4 mg (2 μmol)	0.684	94
5	Fmoc-ACPC-OPfp	1.1 mg (2 μmol)	0.719	100
6	Fmoc-C ^{Bz} -OPfp	1.4 mg (2 μmol)	0.649	90
7	Fmoc-ACPC-OPfp	1.1 mg (2 μmol)	0.656	100
8	Fmoc-G ^{Ibu} -OPfp	1.5 mg (2 μmol)	0.556	85
9	Fmoc-ACPC-OPfp	1.1 mg (2 μmol)	0.505	91
10	Fmoc-G ^{Ibu} -OPfp	1.5 mg (2 μmol)	0.439	87
11	Fmoc-ACPC-OPfp	1.1 mg (2 μmol)	0.467	100
12	Fmoc-A ^{Bz} -OPfp	1.5 mg (2 μmol)	0.330	71
13	Fmoc-ACPC-OPfp	1.1 mg (2 μmol)	0.283	86
14	Fmoc-G ^{Ibu} -OPfp	1.5 mg (2 μmol)	0.294	100
15	Fmoc-ACPC-OPfp	1.1 mg (2 μmol)	0.244	83
16	Fmoc-T-OPfp	1.2 mg (2 μmol)	0.238	98
17	Fmoc-ACPC-OPfp	1.1 mg (2 μmol)	0.234	98
18	Fmoc-A ^{Bz} -OPfp	1.5 mg (2 μmol)	0.238	100
19	Fmoc-ACPC-OPfp	1.1 mg (2 μmol)	0.199	84
20	Fmoc-C ^{Bz} -OPfp	1.4 mg (2 μmol)	0.270	100
21	Fmoc-ACPC-OPfp	1.1 mg (2 μmol)	0.212	79
22	Fmoc-T-Opfp	1.2 mg (2 μmol)	0.184	87
23	Fmoc-ACPC-OPfp	1.1 mg (2 μmol)	0.182	99
24	Fmoc-egl-OPfp	2.8 mg (5 μmol)	-	-
25	5(6)-carboxyfluorescein-OSu	1.0 mg (2 μmol)	-	-

After usual cleavage and purification by HPLC (*t_R* 21.2 min), MALDI-TOF mass spectrum showed a peak at $M \cdot H^+_{\text{obs}} = 5769.5$; $M \cdot H^+_{\text{calcd}} = 5763.7$.

h) Bz-O-TCATGAGGCCT-O-KFFKFFKFFK-NH₂ (Bz-anti-KFF: P13)

Bz-O-TCATGAGGCCT-O-KFFKFFKFFK-NH₂ was synthesized using the procedures described above. Starting from Fmoc deprotection of the resin-bound Fmoc-KFFKFFKFFK-resin (c) (0.5 μmol), the monomers were coupled in the order shown in the Table 2.9.

Table 2.9 Synthesis of Bz-O-TCATGAGGCCT-O-KFFKFFKFFK-NH₂ (Bz-anti-KFF: P13)

Cycle	Monomers	Amount	A ₂₆₄	Coupling efficiency
1	Fmoc-egl-OPfp	2.8 mg (5 μmol)	0.511	100
2	Fmoc-T-OPfp	1.2 mg (2 μmol)	0.552	100
3	Fmoc-ACPC-OPfp	1.1 mg (2 μmol)	0.436	100
4	Fmoc-C ^{Bz} -OPfp	1.4 mg (2 μmol)	0.416	95
5	Fmoc-ACPC-OPfp	1.1 mg (2 μmol)	0.404	100
6	Fmoc-C ^{Bz} -OPfp	1.4 mg (2 μmol)	0.465	100
7	Fmoc-ACPC-OPfp	1.1 mg (2 μmol)	0.452	100
8	Fmoc-G ^{Ibu} -OPfp	1.5 mg (2 μmol)	0.413	91
9	Fmoc-ACPC-OPfp	1.1 mg (2 μmol)	0.484	100
10	Fmoc-G ^{Ibu} -OPfp	1.5 mg (2 μmol)	0.351	73
11	Fmoc-ACPC-OPfp	1.1 mg (2 μmol)	0.391	100
12	Fmoc-A ^{Bz} -OPfp	1.5 mg (2 μmol)	0.362	93
13	Fmoc-ACPC-OPfp	1.1 mg (2 μmol)	0.336	100
14	Fmoc-G ^{Ibu} -OPfp	1.5 mg (2 μmol)	0.364	100
15	Fmoc-ACPC-OPfp	1.1 mg (2 μmol)	0.344	100
16	Fmoc-T-OPfp	1.2 mg (2 μmol)	0.245	71
17	Fmoc-ACPC-OPfp	1.1 mg (2 μmol)	0.288	100
18	Fmoc-A ^{Bz} -OPfp	1.5 mg (2 μmol)	0.260	90
19	Fmoc-ACPC-OPfp	1.1 mg (2 μmol)	0.252	100
20	Fmoc-C ^{Bz} -OPfp	1.4 mg (2 μmol)	0.247	98
21	Fmoc-ACPC-OPfp	1.1 mg (2 μmol)	0.254	100
22	Fmoc-T-Opfp	1.2 mg (2 μmol)	0.263	100
23	Fmoc-ACPC-OPfp	1.1 mg (2 μmol)	0.256	100
24	Fmoc-egl-OPfp	2.8 mg (5 μmol)	-	-
25	5(6)-carboxyfluorescein-OSu	1.0 mg (2 μmol)	-	-

After usual cleavage and purification by HPLC (*t_R* 52.0-58.9 min), MALDI-TOF mass spectrum showed a peak at $M \cdot H^+$ obs = 5515.5; $M \cdot H^+$ calcd = 5509.7.

i) **Flu-O-TCATGAGGCCT-Lys(P⁺)-NH₂ (Flu-anti-Phos: P14)**

Flu-O-TCATGAGGCCT-Lys(P⁺)-NH₂ was synthesized using the procedures described above. The monomers were coupled to the deprotected TentaGel S RAM Fmoc resin (6.25 mg, 1.5 μmol) in the order shown in the **Table 2.10**.

Table 2.10 Synthesis of Flu-O-TCATGAGGCCT-Lys(P⁺)-NH₂ (Flu-anti-Phos: P14)

Cycle	Monomers	Amount	A ₂₆₄	Coupling efficiency
1	Fmoc-Lys(Mtt)-OH	3.8 mg (6 μmol)	0.981	100
2	Fmoc-T-OPfp	3.8 mg (6 μmol)	0.772	79
3	Fmoc-ACPC-OPfp	3.1 mg (6 μmol)	0.773	100
4	Fmoc-C ^{Bz} -OPfp	4.3 mg (6 μmol)	0.798	100
5	Fmoc-ACPC-OPfp	3.1 mg (6 μmol)	0.802	100
6	Fmoc-C ^{Bz} -OPfp	4.3 mg (6 μmol)	0.832	100
7	Fmoc-ACPC-OPfp	3.1 mg (6 μmol)	0.820	99
8	Fmoc-G ^{Ibu} -OPfp	4.4 mg (6 μmol)	0.947	100
9	Fmoc-ACPC-OPfp	3.1 mg (6 μmol)	0.923	98
10	Fmoc-G ^{Ibu} -OPfp	4.4 mg (6 μmol)	0.945	100
11	Fmoc-ACPC-OPfp	3.1 mg (6 μmol)	0.903	96
12	Fmoc-A ^{Bz} -OPfp	4.4 mg (6 μmol)	0.767	85
13	Fmoc-ACPC-OPfp	3.1 mg (6 μmol)	0.706	92
14	Fmoc-G ^{Ibu} -OPfp	4.4 mg (6 μmol)	0.759	100
15	Fmoc-ACPC-OPfp	3.1 mg (6 μmol)	0.672	89
16	Fmoc-T-OPfp	3.8 mg (6 μmol)	0.642	96
17	Fmoc-ACPC-OPfp	3.1 mg (6 μmol)	0.554	86
18	Fmoc-A ^{Bz} -OPfp	4.4 mg (6 μmol)	0.546	99
19	Fmoc-ACPC-OPfp	3.1 mg (6 μmol)	0.483	89
20	Fmoc-C ^{Bz} -OPfp	4.3 mg (6 μmol)	0.490	100
21	Fmoc-ACPC-OPfp	3.1 mg (6 μmol)	0.417	85
22	Fmoc-T-OPfp	3.8 mg (6 μmol)	0.404	97
23	Fmoc-ACPC-OPfp	3.1 mg (6 μmol)	0.411	100
24	Fmoc-egl-OPfp	5.5 mg (10 μmol)	-	-
25	5(6)-carboxyfluorescein-OSu	3.1 mg (6 μmol)	-	-

After treatment of the resin with 1:1 ammonia/dioxane to remove any non-specifically bound fluorescein, the attachment of phosphonium group at the C-terminal lysine was performed as follows. Firstly, deprotection of 4-methyltrityl (Mtt) protecting group was carried out using 2% TFA in DCM (5 × 1 mL). Next, the carboxybutyl (triphenylphosphonium) bromide *N*-hydroxysuccinimide (10 μmol, 4.6

mg in 30 μ L DMF) was coupled to the C-termini of PNA conjugates in DMF. After the reaction was completed (2 h), the resin was washed extensively with DMF and then with MeOH.

After usual cleavage and purification by SAX anion exchanger, MALDI-TOF mass spectrum of Flu-O-TCATGAGGCCT-Lys(P⁺)-NH₂ (Flu-anti-Phos: **P14**) showed $M \cdot H^+_{\text{obs}} = 4555.5$; $M \cdot H^+_{\text{calcd}} = 4556.0$.

j) Flu-O-TCATGAGGCCT-Lys-NH₂ (Flu-anti-K: P15)

Flu-TCATGAGGCCT-Lys-NH₂ was synthesized using the procedures described above. After deprotection of the protecting group of TentaGel S RAM Fmoc resin (4.2 mg, 1.0 μ mol), the monomers were coupled in the order shown in the **Table 2.11**.

Table 2.11 Synthesis of Flu-O-TCATGAGGCCT-Lys-NH₂ (Flu-anti-K: **P15**)

Cycle	Monomer	Amount	A ₂₆₄	Coupling efficiency
1	Fmoc-Lys(Boc)-OPfp	2.5 mg (4 μ mol)	0.748	100
2	Fmoc-T-OPfp	2.5 mg (4 μ mol)	0.731	98
3	Fmoc-ACPC-OPfp	2.1 mg (4 μ mol)	0.725	99
4	Fmoc-C ^{Bz} -OPfp	2.9 mg (4 μ mol)	0.727	100
5	Fmoc-ACPC-OPfp	2.1 mg (4 μ mol)	0.639	88
6	Fmoc-C ^{Bz} -OPfp	2.9 mg (4 μ mol)	0.750	100
7	Fmoc-ACPC-OPfp	2.1 mg (4 μ mol)	0.645	86
8	Fmoc-G ^{Ibu} -OPfp	2.9 mg (4 μ mol)	0.640	99
9	Fmoc-ACPC-OPfp	2.1 mg (4 μ mol)	0.626	98
10	Fmoc-G ^{Ibu} -OPfp	2.9 mg (4 μ mol)	0.542	87
11	Fmoc-ACPC-OPfp	2.1 mg (4 μ mol)	0.573	100
12	Fmoc-A ^{Bz} -OPfp	3.0 mg (4 μ mol)	0.322	56
13	Fmoc-ACPC-OPfp	2.1 mg (4 μ mol)	0.318	999
14	Fmoc-G ^{Ibu} -OPfp	2.9 mg (4 μ mol)	0.325	100
15	Fmoc-ACPC-OPfp	2.1 mg (4 μ mol)	0.315	97
16	Fmoc-T-OPfp	2.5 mg (4 μ mol)	0.329	100
17	Fmoc-ACPC-OPfp	2.1 mg (4 μ mol)	0.296	90
18	Fmoc-A ^{Bz} -OPfp	3.0 mg (4 μ mol)	0.198	67
19	Fmoc-ACPC-OPfp	2.1 mg (4 μ mol)	0.310	100
20	Fmoc-C ^{Bz} -OPfp	2.9 mg (4 μ mol)	0.300	97
21	Fmoc-ACPC-OPfp	2.1 mg (4 μ mol)	0.302	100
22	Fmoc-T-OPfp	2.5 mg (4 μ mol)	0.290	96
23	Fmoc-ACPC-OPfp	2.1 mg (4 μ mol)	-	-

24	Fmoc-egl-OPfp	5.5 mg (10 μ mol)	-	-
25	5(6)-carboxyfluorescein-OSu	2.1 mg (4 μ mol)	-	-

After usual cleavage and purification by SAX anion exchanger, MALDI-TOF mass spectrum of Flu-O-TCATGAGGCCT-Lys-NH₂ (Flu-anti-K: P15) showed $M \cdot H^+_{\text{obs}} = 4207.6$; $M \cdot H^+_{\text{calcd}} = 4206.9$.

2.5 T_m experiments of PNA-DNA hybrids [72]

A CARY 100 Bio UV-Visible spectrophotometer (Varian Ltd.) equipped with a thermal melt system was used for T_m experiments. The samples for T_m measurement were prepared by mixing DNA and PNA solutions together to give a final concentration of 1.0 μ M (ratio of PNA:DNA = 1:1) in 10 mM sodium phosphate buffer (pH 7.0). The total volumes were adjusted to be 750 μ L by an addition of degassed MilliQ water. The samples were transferred to 10 mm quartz cells and equilibrated at the starting temperature for 10 min. The A_{260} was recorded in steps from 20 \rightarrow 90 \rightarrow 20 \rightarrow 90 $^{\circ}$ C (block temperature) with a temperature increment of 1 $^{\circ}$ C/min and hold time of 10 min after each cycle. The results taken from the last heating cycle were used and were normalized by dividing the absorbance at each temperature by the initial absorbance. The temperatures recorded were the block temperature and were corrected using a direct read out from temperature probe.

Correct temperature and normalized absorbance were defined as follows.

$$\text{Correct.Temp} = (0.9696 \times T_{\text{block}}) - 0.8396$$

$$\text{Normalized Abs.} = \text{Abs}_{\text{obs}}/\text{Abs}_{\text{init}}$$

T_m was obtained from derivative plot after smoothing in KaleidaGraph 3.6 (Synergy Software) and analysis of the data was performed on a PC compatible computer using Microsoft Excel XP (Microsoft). The T_m values were accurate within ± 0.5 $^{\circ}$ C.

2.6 Cell uptake ability studies

The experiments here carried out at Department of Microbiology, Faculty of Pharmacy, Mahidol University, Bangkok, under supervision of Dr. Mullika T. Chomnawang and Miss Piyatip Khuntayaporn.

2.6.1 Measurements

E. coli ATCC 25922 cells were cultured in water bath model sv 1422 (memmert). Optical density of overnight cell cultures was measured at 600 nm by a NovaspecII spectrophotometer (Pharmacia Biotech.). Cytotoxicity evaluation of treated cell cultures in 96-well plate by measuring optical density at 590 nm was performed on an Emax microplate reader (Molecular devices, USA). Fluorescence experiments were performed on a Spectramax Gemini EM spectrofluorometer (Molecular Devices, USA) (excitation wavelength of 480 nm and emission wavelength of 510 nm). A Vortex Genie 2 (Scientific Industries, USA) was used in the washing step for removal of excess PNAs from *E. coli* cells. The separated cells were examined under an Epi-fluorescence Microscope (Olympus BX51). Separation of pellet and supernatant were performed on a digital microcentrifuge model Denville 260D (Scientific Inc.). A dry bath incubator model MD-01N (Major Science, Taiwan) was used for incubation the lysis culture at desired temperature. All chemicals, tips and Eppendorfs were sterilized in a Labo Autoclave (SANYO) before use.

2.6.2 General procedures

Colonies of *E. coli* ATCC 25922 (**Figure 2.1**) were cultured in Difco™⁴ LB Broth, Lenox containing Tryptone (10.0 g/L), yeast extract (5.0 g/L) and sodium chloride (5.0 g/L). The cells grow up in LB broth 5 mL in a sealed test tube with shaking in a water bath at 37 °C for 15-17 hours. After this period, the *E. coli* cells were diluted into a test tube by LB Broth to the concentration which provided OD₆₀₀ = 0.49-0.51 (~ 10⁸⁵ CFU/mL) then the cells were again diluted with LB Broth to 0.1× or 0.01× dilution (~ 10⁷ or ~ 10⁶ CFU/mL) with a total volume of 5 mL. The cell dilution stocks were plated in 96-well plates at a volume of 80 µL per well. The cells (3 wells: a tested PNA) were incubated with PNA conjugates and the control (20 µL of 25 µM) to a final concentration of 5 µM and total volume of the culture = 100 µL.

⁴ Nutritionally rich media developed by Lennox for the growth and maintenance of pure cultures of recombinant strains of *E. coli*

⁵ colony-forming unit - a measure of viable cell in which a colony represents an aggregate of cells derived from a single progenitor

Moreover, addition 20 μL of water into cell culture is necessary for determination of background fluorescence intensity. The plates were stored at 37° C for 2, 4 or 8 hours (1 cultivation: 1 experiment).

The concentration of stock solutions of PNA and Flu-PNA were defined as follows

$$\text{conc.} = \frac{A_{260}}{\epsilon_{260}}$$

$$\epsilon_{260} \text{ PNA-Flu} = \epsilon_{260} \text{ Nucleobases of PNA} + \epsilon_{260} \text{ Flu}$$

$$\epsilon_{260} (\times 10^3 \text{ cm}^{-1}/\text{M}): \text{A} = 15.4, \text{T} = 8.8, \text{C} = 7.4, \text{G} = 11.5, \text{Flu} = 41.0$$



Figure 2.1 Colonies of *E. coli* ATCC 25922

2.6.3 Evaluation of uptake abilities

After the incubation period, the cell cultures were centrifuged at 10,000 rpm for 10 minutes. The supernatant consisting of culture medium and free PNA conjugates were collected. To evaluate the uptake abilities of the PNA conjugates in cell cultures, the pelletized bacterial cells were washed and lysed by either of the lysis method below.

Method I: The cells were washed with 0.1 M PBS pH 7.2 (200 μL) followed by 0.01% TE buffer pH 8.5 (30 μL). The separated cells were examined under fluorescence microscope and lysed using 15% sucrose (in 50 mM Tris-50 mM EDTA pH 8.5, 80 μL) at -4 °C for 5 min, following by lysozyme (5 mg/mL in 0.01% TE buffer pH 8.5, 20 μL) at -4 °C for 30 min and then 0.1% Triton X-100 (in 50 mM Tris-50 mM EDTA pH 8.5, 60 μL) at -4 °C for 30 min. To separate the lysis solution

for determination of uptake ability, the mixture was centrifuged at 14,000 rpm for 5 minutes. The cell debris was examined by fluorescence microscopy to ensure the complete cell lysis. Fluorescence of the supernatant ("lysis solution") was measured to determine the uptake ability of PNA conjugates.

Method II: The cells were washed with 0.1 M PBS pH 7.2 (200 μ L). The separated cells were lysed using 6.7% sucrose (in 50 mM Tris-1 mM EDTA pH 8.0, 69.0 μ L) at 37 $^{\circ}$ C for 10 min, following by lysozyme 10 mg/mL (in 25 mM Tris pH 8.0, 17.2 μ L) at 37 $^{\circ}$ C for 5 min and 20% SDS w/v (in 50 mM Tris-20 mM EDTA pH 8.0, 5.2 μ L) at 37 $^{\circ}$ C for 10 min. To obtain the lysis solution for determination of uptake ability, the mixture was centrifuged at 10,000 rpm for 10 minutes. Fluorescence of the supernatant ("lysis solution") was measured (2 measurements: 1 well) to determine the uptake ability of PNA conjugates.

The fluorescence intensity recorded of each solution was corrected or adjusted by background fluorescence subtraction and converted into percentage as follows

Adjusted fluorescence = Fluorescence of lysis solution – Fluorescence of background

$$\% \text{ Fluorescence} = \frac{\text{Adjusted fluorescence} \times 100\%}{\text{Adjusted fluorescence of cell culture at 0 h}}$$

2.7 Determination of PNA stabilities toward proteases

2.7.1 Measurements

Reverse phase HPLC experiments were performed on Water 600TM system equipped with gradient pump and Water 996TM photodiode array detector. A PolarisTM C₁₈ HPLC column 3 μ m particle size 4.6 \times 50 mm (Varian Inc., USA) was used for analytical purposes (10 μ L of sample size). The base Empower software was available for integrated the peak and data processing from HPLC analysis. The chromatogram monitoring was carried out at a suitable absorbance (215 nm for the control and 260 nm for the PNA). The eluting gradient system consisted of 0.01% TFA in methanol (A) and in water (B). The elution started with A:B (10:90) for 5 min followed by a linear gradient up to A:B (90:10) over a period of 60 min. The UV absorption pattern of each peak was determined to identify the degradation fragments.

2.7.2 General procedures

Proteinase K (fungal, > 20 units/mg) was purchased from Inditrogen (USA). Rat Adrenocorticoid hormone, fragment 4-10 (ACTH 4-10: Met-Glu-His-Phe-Arg-Trp-Gly) were obtained from sigma. The ACTH 4-10 was dissolved in milliQ water to obtain a stock solution of 1 mg/mL. The stock solution was diluted to 0.2 mg/mL (207.8 μ M). The diluted stock was freshly prepared on the day the experiments were to be performed. The proteinase K (10 mg) was dissolved in storage buffer (1 mL) containing 50% (v/v) glycerol, 10 mM Tris-HCl pH 7.5 and CaCl₂ (2 mg)

2.7.3 Evaluation of Ac-TTTTTTTTT-Lys-NH₂ (Ac-T₉-K: P17) stabilities toward proteinase K

The stabilities of the PNA towards proteinase K were investigated using HPLC analysis. ACTH 4-10 was used as a control. ACTH 4-10 was dissolved in water to make a stock solution of 0.2 mg/mL (207.8 μ M). A solution of P17 (Ac-T₉-K, final conc. = 30 μ M) and ACTH 4-10 (final conc. = 100 μ M) in water was prepared and was incubated at 37°C for 5 min. HPLC analysis of the mixture was performed using the gradient described above, monitored at 215 nm, revealed the presence of two non-overlapping peaks at 40.4 min (ACTH) and 45.6 min (PNA) respectively.

To determine the stability of the PNA and the control under the test conditions, the PNA and ACTH mixture was prepared in 100 mM Tris-HCl buffer pH 7.5 and was incubated at 37 °C for 1 and 20 h without proteinase K. HPLC analysis was used to confirm the stabilities of the PNA and the peptide under the tested conditions before digestion of proteinase K.

To determine the stabilities of the PNA toward proteinase K, the enzyme at different concentrations (0.5, 0.05, 0.005, 0.0005 mg/mL) was added to the mixtures of the PNA and ACTH in 100 mM Tris-HCl buffer pH 7.5 in a total reaction volume of 14 μ L. The mixtures were incubated at 37 °C from 5 min to 18.5 h. After the specified period of time, the reaction was stopped using 1 μ L of 1.0 M HCl. The stabilities of PNA toward the enzyme compared to the control were again investigated by HPLC.

CHAPTER III

RESULTS AND DISCUSSION

3.1 Synthesis of activated peptide monomers

3.1.1 Synthesis of activated phenylalanine monomer

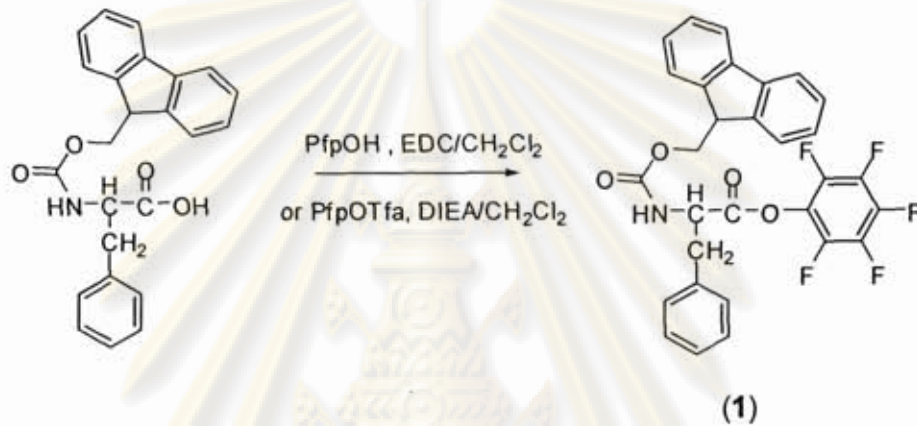


Figure 3.1 Synthesis of (N-Fluoren-9-ylmethoxycarbonyl)-L-phenylalanine-pentafluorophenyl ester (1)

The commercially available Fmoc-Phe-OH was activated by reacting with PfpOH and EDC as described previously for the synthesis of PNA monomers. [33] This reaction was complete within 1 h according to TLC analysis. The product was purified by flash column chromatography, which had to be carried out quickly to avoid decomposition of the product on the column. The product, (N-Fluoren-9-ylmethoxycarbonyl)-L-phenylalanine-pentafluorophenyl ester (1), was obtained in 72 % yield as a white solid (**Figure 3.1**).

The same compound could be obtained by the reaction between Fmoc-Phe-OH and PfpOTfa in the presence of DIEA as described previously for the synthesis of PNA monomer. [68] The product (1) was obtained after purification as described above in 24 % yield which was identical in all respects to the product obtained from the former method. TLC analysis of the pooled fractions from flash column chromatography confirmed that the product was obtained. The R_f value of the product was 0.3 while the R_f value of the starting material (Fmoc-Phe-OH) was 0.0 under the

elution condition (SiO₂, 7:1 Hexanes:EtOAc). The identity of the product was further confirmed by ¹H-NMR spectrum which was fully consistent with the expected structure (see Chapter 2 for details of the NMR spectrum).

3.1.2 Synthesis of activated cysteine monomer

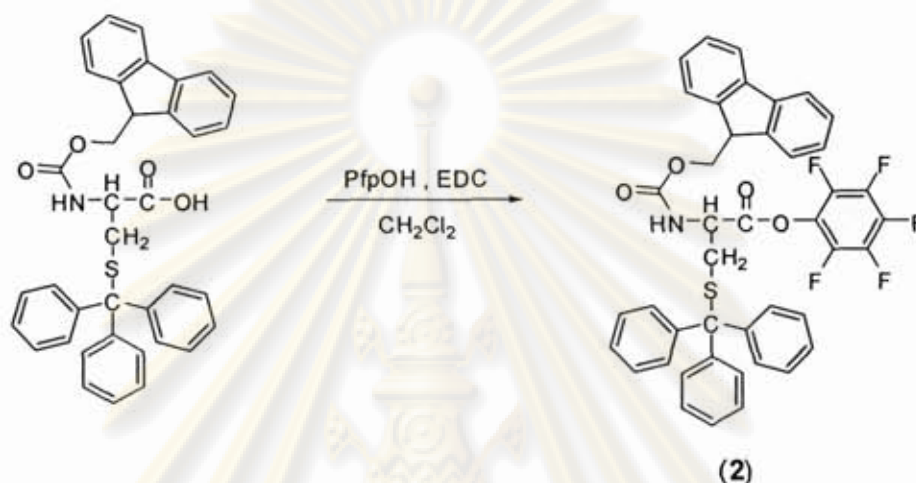


Figure 3.2 Synthesis of (N-Fluorenylmethoxycarbonyl)-L-cysteine-pentafluorophenyl ester (2)

Similar to phenylalanine monomer, the commercially available Fmoc-Cys(Trt)-OH was reacted with PfpOH and EDC to give the pentafluorophenyl ester product (2) in 54 % yield as a light brown solid (Figure 3.2). TLC analysis (8:1 Hexanes:EtOAc) revealed a less polar product ($R_f = 0.3$) compared to the starting material ($R_f \sim 0.0$), which confirmed that the expected product had formed. The identity of the product was also further confirmed by ¹H-NMR spectrum which was fully consistent with the expected structure (see Chapter 2 for details of the NMR spectrum).

3.2 Synthesis of activated PNA monomers

The four Pfp-PNA monomers were synthesized and purified previously as reported by Miss Boonjira Boontha, Miss Cheerporn Ananthanawat, and Dr. Tirayut Vilaivan. [29] The purity of the compounds were checked by ¹H-NMR and used as received without further purification.

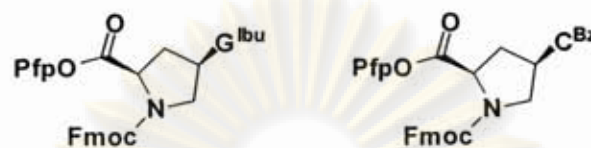


Figure 3.3 PNA monomers

3.3 Synthesis of ACPC spacer

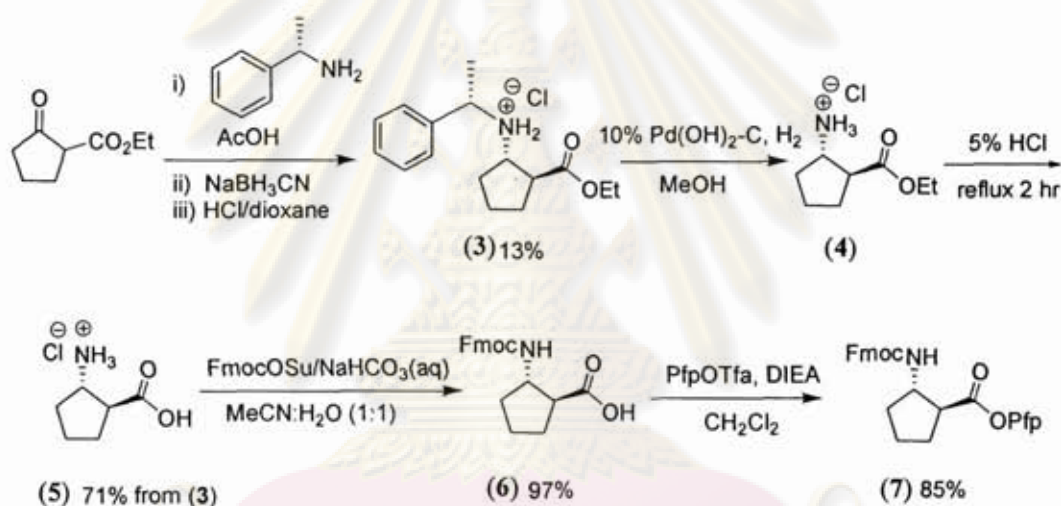


Figure 3.4 Synthesis of ACPC spacer

The β -amino acid spacer (*ss*ACPC) was synthesized following the procedure reported by Gellman. [67] The commercially available ethyl cyclopentanone-2-carboxylate was reacted with (*S*)-(-)- α -methylbenzylamine in the presence of glacial acetic acid to give an enamine intermediate which was stereoselectively reduced with sodium cyanoborohydride to obtain the β -aminoester (**3**). The desired diastereomer, ethyl (1*S*,2*S*)-2-[(1'*S*)-phenylethyl]-aminocyclopentane carboxylate hydrochloride (**3**), was separated from the mixture with other stereoisomers by crystallization of the corresponding hydrochloride salt to obtain the product in 13% yield (**Figure 3.4**). The NMR spectrum (**Figure 3.5**) of the product confirmed that the (1*S*,2*S*,1'*S*)-isomer was indeed obtained. [68] The optical rotation value $\{[\alpha]_D^{23} = +16.8$ ($c = 1.00$ g/100 mL

CDCl_3)} corresponded well to that of the authentic sample prepared previously in this laboratory $\{[\alpha]_{\text{D}}^{25} = +17.1$ ($c = 1.00$ g/100 mL CDCl_3)}.

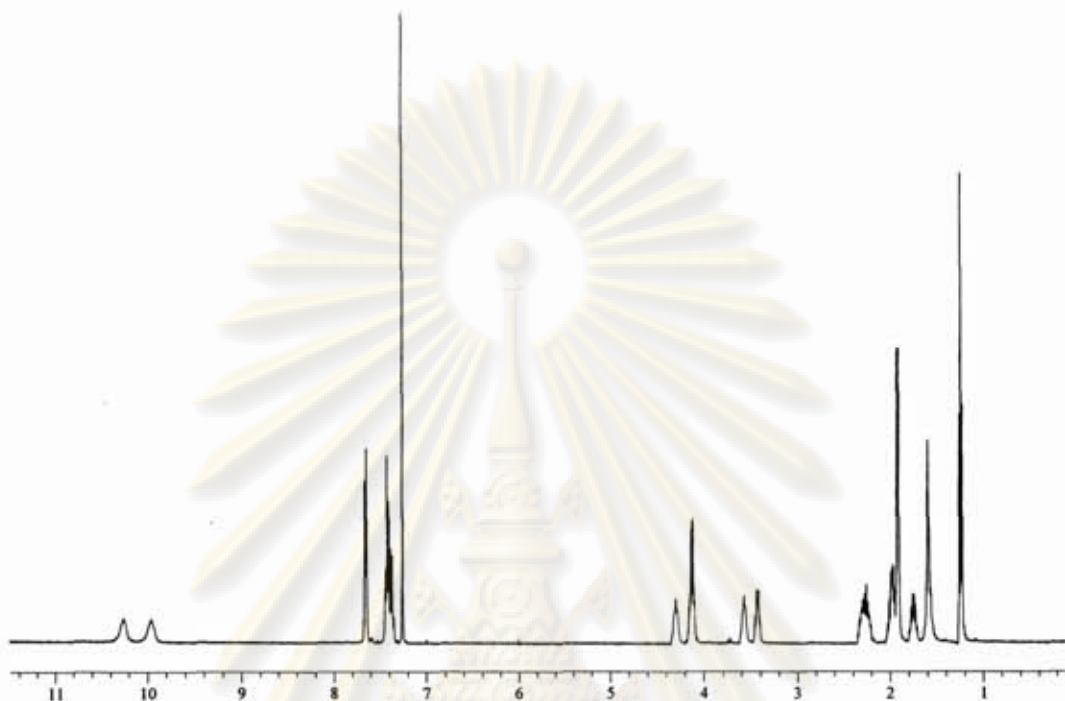


Figure 3.5 ¹H-NMR spectrum of ethyl (1*S*,2*S*)-2-[(1'*S*)-phenylethyl]-aminocyclopentane carboxylate hydrochloride (**3**)

The free amine (**4**) was obtained by catalytic hydrogenolysis of (**3**) to remove the *S*-methylbenzylamine auxiliary. Hydrolysis of (**4**) in refluxing aqueous HCl gave the free amino acid (**5**) as hydrochloride salt in 71 % yield (from **3**). The amino group in (**5**) was protected with Fmoc using FmocOSu under mildly basic condition (aqueous NaHCO_3) as described previously. [68, 33] The resulting Fmoc-protected ACPC (**6**) was obtained as a white solid in 97% yield. The ¹H NMR spectrum (**Figure 3.6**) of the compound (**6**) corresponded well with literature values. [68] The specific rotation value $\{[\alpha]_{\text{D}}^{23.7} = +36.1$ ($c = 1.00$ g/100 mL MeOH)} was also in good agreement with that of the authentic samples prepared previously in this laboratory $\{[\alpha]_{\text{D}}^{25} = +36.4$ ($c = 1.00/100$ mL MeOH)}.

The Pfp-ACPC spacer (**7**) was synthesized and purified (85% yield) by Miss Boonjira Boontha. After column chromatography and recrystallization, the Pfp-ACPC spacer (**7**) was obtained as a white solid (**Figure 3.4**).

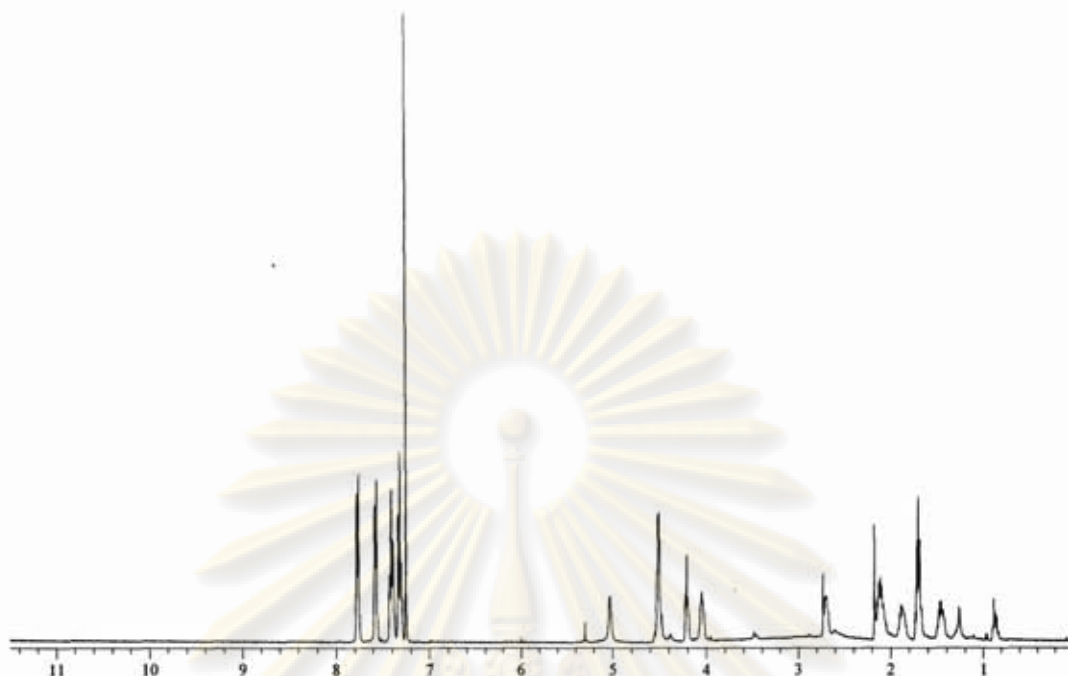


Figure 3.6 $^1\text{H-NMR}$ spectrum of (1*S*,2*S*)-2-(*N*-Fluorenylmethoxycarbonyl)-aminocyclopentanecarboxylic acid (**6**)

3.4 Synthesis of PNA conjugates by solid phase peptide synthesis

Solid phase synthesis of PNA conjugate was carried out according to the standard protocol previously developed in this laboratory. [33, 69] For the synthesis of PNA conjugates carrying carrier peptides at the C-termini (**P4**, **P5**, **P9**, **P12** and **P13**), the following protocol was employed. The appropriate activated Fmoc-protected amino acids (Lys, Phe, Arg) were coupled to the resin until the desired peptide sequence was obtained. A diethyleneglycol (aminoethoxyethoxyacetyl, O-linker) was then added to increase the distance between the peptide and the PNA. After deprotection of Fmoc group of the O-linker, the PNA part was synthesized by coupling of the PNA monomers and the spacer alternately until the desired PNA conjugate sequence was obtained. If further labeling with fluorescein was not desired (for **P13**), the PNA was then capped by benzylation with benzoic anhydride to improve stability and facilitate purification. On the other hand, if labeling was to be performed, another O-linker was inserted followed by coupling with 5(6)-carboxyfluorescein succinimidyl ester to afford the labeled PNA conjugates. The labeled PNA conjugates was then treated with 1:1 aqueous ammonia:dioxane at 60 °C

for 6 h to remove the nucleobase side chain protection and any non-specifically bound fluorescein before cleavage from the solid support.

For attachment of peptide to PNA at the N-termini (**P8**, **P10** and **P16**) the following protocol was employed. Fmoc-Lys(Mtt)-OH (or Fmoc-T-OPfp for **P16**) was first coupled to the resin followed by the PNA monomer and the spacer alternately until the desired PNA sequence was obtained. After completion of the PNA synthesis, coupling of the O-linker was performed as described previously. After removal of Fmoc group of the O-linker, the activated peptide monomers (Lys, Phe, Arg) were sequentially coupled until the desired PNA conjugate sequence was obtained. If further labeling with fluorescein was not desired (for **P16**), the Fmoc of PNA was deprotected then the PNA was capped by benzylation with benzoic anhydride as describe above. On the other hand, if labeling was to be performed, after removal of the Mtt group of protected lysine at the C-termini by treatment with 2% TFA in dichloromethane, the PNA conjugate was coupled with 5(6)-carboxyfluorescein succinimidyl ester. The PNA conjugate was then treated with 1:1 aqueous ammonia:dioxane at 60 °C for 6 h prior to the final cleavage from the solid support as described previously. [73] This ammonia treatment also caused concomitant cleavage of the Fmoc group.

The control PNA: Flu-O-TTT-Lys-NH₂ (**P7**, abbreviated as Flu-T₃-K) and Flu-O-TTTTTTTTTT-Lys-NH₂ (**P11** abbreviated as Flu-T₉-K) were synthesized as described in the literature. [71]

Synthesis of PNA modified with phosphonium label at the C-termini (**P6** and **P14**) required incorporation of Fmoc-Lys(Mtt)-OH as the first residue before the PNA synthesis started After completion of the standard PNA synthesis, for PNA containing A, G, C bases, treatment with 1:1 aqueous ammonia:dioxane at 60 °C for 6 h to remove the nucleobase side chain protection before coupling to the phophonium was required. For T₃ and T₉ PNA, after completion of the PNA synthesis the Mtt group was removed by 2% TFA in dichloromethane. The phosphonium group was introduced to the PNA on solid support using carboxybutyl triphenylphosphonium bromide [74, 75] with out requiring any activating reagent. If N-terminal labeling with fluorescein was required, the protocol described earlier was adopted.

In all cases, after the ammonia treatment, the support-bound PNA was treated with 95% trifluoroacetic acid in order to cleave the desired PNA from the solid

support. After 2 h treatment, the trifluoroacetic acid was removed by gentle nitrogen stream. The crude residue was precipitated with diethyl ether followed by purification with C-18 reverse phase HPLC. An example of chromatogram is shown in **Figure 3.7**. The concentration of the pooled fractions was determined spectrophotometrically. The identity of the synthesized PNA was confirmed by MALDI-TOF mass spectrometry (**Figure 3.8** and **Table 3.2**)

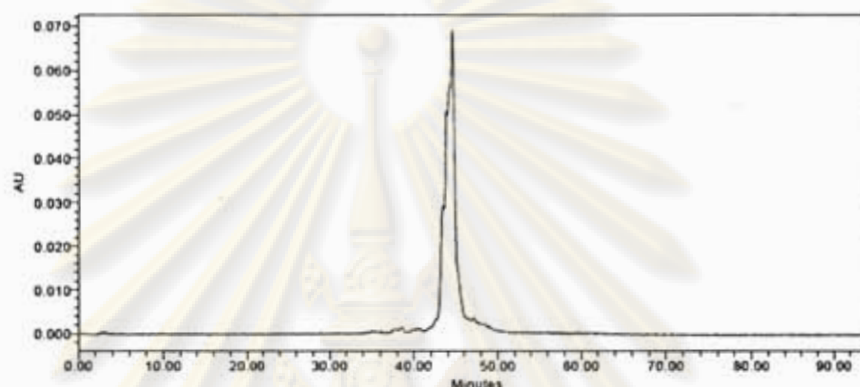


Figure 3.7 HPLC chromatogram of crude product of Flu-TTT-RRRRRRRRRR-NH₂ (Flu-T₃-R₁₀: **P5**)

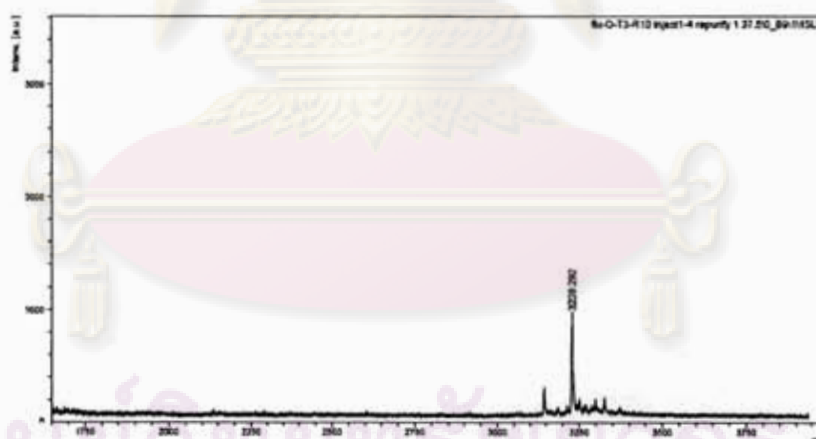


Figure 3.8 MALDI-TOF mass spectrum of purified Flu-TTT-RRRRRRRRRR-NH₂ (Flu-T₃-R₁₀: **P5**). $M \cdot H^+_{\text{obs}} = 3228.3$; $M \cdot H^+_{\text{calcd}} = 3225.6$

In case of purification of N-terminal fluorescein modified PNA including Flu-O-TTT-O-KFFKFFKFFK-NH₂ (**P4**, abbreviated as Flu-T₃-KFF), Flu-O-TTT-Lys(P⁺)-NH₂ (**P6**, abbreviated as Flu-T₃-Phos), Flu-T₃-K (**P7**), Flu-O-TCATGAGGCCT-Lys(P⁺)-NH₂ (**P14**, abbreviated as Flu-anti-Phos), and Flu-O-TCATGAGGCCT-Lys-NH₂ (**P15**, abbreviated as Flu-anti-K), the purifications were

achieved by a newly developed anion-exchange capture technique using strongly basic ion-exchange silica (SAX, Varian Inc.). In this technique, the solution of fluorescein-labeled PNA was first treated with DIEA until pH ~ 10 to ensure that the fluorescein label is in its anionic form. This solution was then passed through a short column containing the SAX support which will trapped only the full length PNA which carried the negatively-charged fluorescein label. The captured fluorescein labeled PNA was then released from the column by eluting with 1% TFA in 50% MeCN:H₂O. The acidic eluent caused protonation of the fluorescein label therefore the labeled PNA can no longer be absorbed by the anion exchanger. The purity of PNA purified in this way was excellent and was comparable to the HPLC-purified PNA. However, some labeled PNA such as Flu-O-TTT-O-RRRRRRRRRR-NH₂ (**P5**, abbreviated as Flu-T₃-R₁₀) and Flu-O-TCATGAGGCCT-O-KFFKFFKFFK-NH₂ (**P12**, abbreviated as Flu-anti-KFF) precipitated under basic conditions and could not be purified by this method.

A cysteine labeled KFF peptide H-KFFKFFKFFKC-NH₂ (**P1**, abbreviated as KFF-C) was also synthesized with the aim to link to the PNA in a convergent fashion by thiol-maleimide interaction (**Figure 3.9**). [70] Unfortunately, this compound dimerized easily as revealed by MALDI-TOF analysis ($M \cdot H^+_{\text{obs}} = 1516.3, 3033.6$; $M \cdot H^+_{\text{calcd}} = 1515.8$). The dimer was probably formed as a result of air oxidation and thus this approach was not pursued further. Accordingly, it was decided to focus on the synthesis of PNA conjugates by sequential coupling strategies as described above.

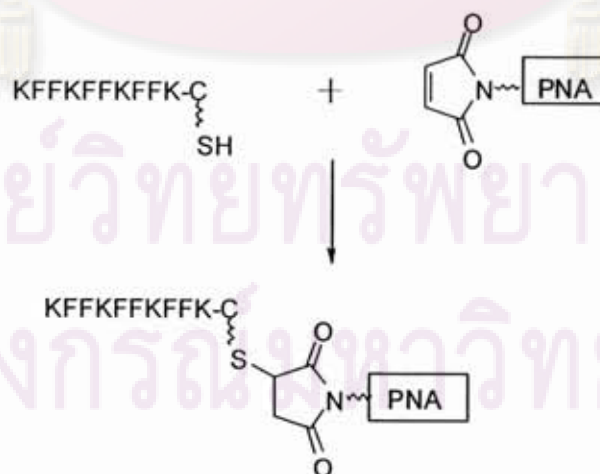


Figure 3.9 Synthesis of PNA-peptide conjugated using convergent fashion by thiol-maleimide interaction

Table 3.1 Percent coupling efficiency of PNAs, peptides and their conjugates

code	N → C	simple name	% efficiency * (overall)
P2	Fmoc-KFFKFFKFFK-NH ₂	Fmoc-KFF	78
P3	Fmoc-RRRRRRRRRR-NH ₂	Fmoc-R ₁₀	46
P4	Flu-O-TTT-O-KFFKFFKFFK-NH ₂	Flu-T ₃ -KFF	-**
P5	Flu-O-TTT-O-RRRRRRRRRR-NH ₂	Flu-T ₃ -R ₁₀	-
P6	Flu-O-TTT-Lys(P ⁺)-NH ₂	Flu-T ₃ -Phos	-
P7	Flu-O-TTT- Lys-NH ₂	Flu-T ₃ -K	85
P8	H-KFFKFFKFFK-O-TTT-Lys(Flu)-NH ₂	KFF-T ₃ -Flu	87
P9	Flu-O-TTTTTTTTTT-O-KFFKFFKFFK- NH ₂	Flu-T ₉ -KFF	40
P10	H-KFFKFFKFFK-O-TTTTTTTTTT-Lys(Flu)-NH ₂	KFF-T ₉ -Flu	41
P11	Flu-O-TTTTTTTTTT-Lys-NH ₂	Flu-T ₉ -K	51
P12	Flu-O-TCATGAGGCCT-O-KFFKFFKFFK-NH ₂	Flu-anti-KFF	22
P13	Bz-O-TCATGAGGCCT-O-KFFKFFKFFK-NH ₂	Bz-anti-KFF	39
P14	Flu-O-TCATGAGGCCT-Lys(P ⁺)-NH ₂	Flu-anti-Phos	42
P15	Flu-O-TCATGAGGCCT-Lys-NH ₂	Flu-anti-K	39
P16	Bz-O-KFFKFFKFFK-O-TCATGAGGCCT-NH ₂	Bz-KFF-anti	20
P17	Ac-TTTTTTTTTT-Lys-NH ₂	Ac-T ₉ -K	53

* calculated from the initial absorbance of dibenzofulvene-piperidine adduct from deprotection of Fmoc lysine with the absorbance obtained from Fmoc deprotection of the last cycle.

** no data available

ศูนย์วิทยทรัพยากร
จุฬาลงกรณ์มหาวิทยาลัย

Table 3.2 t_R and mass spectral data of the PNAs peptides and their conjugates used in this study

PNA	t_R^a (min)	mass		
		$M.H^+_{obs}^b$	$M.H^+_{calcd}^c$	% error ^d
P2	not purified	1634.7	1635.9	0.073
P3	not purified	1798.5	1802.1	0.200
P4	Purified by SAX	3061.9	3059.4	0.082
P5	42.1	3228.3	3225.6	0.084
P6	Purified by SAX	1992.4	1996.87	0.224
P7	Purified by SAX	1646.7	1646.7	0.000
P8	51.8	-	-	-
P9	59.0	-	-	-
P10	58.3	-	-	-
P11	35.8	-	-	-
P12	cannot be purified	-	-	-
P13	cannot be purified	-	-	-
P14	purified by SAX	4555.5	4556.0	0.011
P15	purified by SAX	4207.6	4206.9	0.017
P16	51.8	-	-	-
P17	44.4	-	-	-

^a Condition for reverse-phase HPLC: C-18 column 3 μ m particle size 4.6 x 50 mm; gradient system of 0.01% TFA in MeOH/water 20:80 to 80:20 in 60 min; hold time 5 min.

^b matrix solution containing CCA in 0.1% TFA in acetonitrile:water (1:2) solution

^c calculated mass for $[M+H]^+$

^d $(M.H^+_{calcd} - M.H^+_{obs})/M.H^+_{calcd} \times 100\%$

^{*} No MALDI-TOF analysis result was obtained due to instrumental breakage, however, the T_m experiment have been used to confirm the hybridization between the synthesized P9-P11/P16-P17 and their complementary DNA targets.

In order to study the antisense effect on the cellular delivery of the PNA-conjugates, it was necessary to ensure that the linear coupling of the PNA conjugates is practical for mixed base sequence. As a synthetic model, synthesis of an antisense PNA sequence TCATGAGGCCT designed to *waaP* gene [76] of *Pseudomonas aeruginosa* [77] was also carried out. A series of the antisense sequence PNA attached to cations or peptide carriers were also synthesized (P12-P16). Nevertheless, attempts to synthesize the sequence Flu-O-TCATGAGGCCT-O-KFFKFFKFFK-NH₂ (P12

abbreviated as Flu-anti-KFF) were not successful. The very low yield of crude product as monitored by MALDI-TOF mass spectrometry along with the poor solubility of the conjugate complicated the purification by HPLC and SAX. However, the presence of a mass peak at $m/z = 5769.5$ ($M \cdot H^+_{\text{calcd}} = 5763.7$) confirmed that the synthesized crude PNA consisted of the desired PNA. In case of Bz-O-TCATGAGGCCT-O-KFFKFFKFFK-NH₂ (**P13**, abbreviated as Bz-anti-KFF), a minor mass peak at $m/z = 5515.0$ ($M \cdot H^+_{\text{calcd}} = 5509.7$) confirmed that the desired PNA was present in the crude product. Unfortunately, the HPLC chromatograms of these PNA conjugates were rather complex, and without the mass spectrometer available, it was difficult to know exactly which peak to collect. Therefore these two PNA conjugates (**P12** and **P13**) could not be successfully prepared in pure forms.

In case of Bz-O-KFFKFFKFFK-O-TCATGAGGCCT-NH₂ (**P16**, abbreviated as Bz-KFF-anti) the crude product was purified by reverse phase HPLC which showed a major peak at t_R 35.8. The identity of the PNA was confirmed by T_m experiment with complementary DNA (see Section 3.5 and **Table 3.3**). For Flu-O-TCATGAGGCCT-Lys(P⁺)-NH₂ (**P14**, abbreviated as Flu-anti-Phos), the crude product was purified by SAX anion exchanger. MALDI-TOF analysis (see Appendix) confirms that the PNA was successfully obtained.

3.5 Study of the hybridization properties of PNA conjugates by UV-melting technique

The ability of the synthesized PNA conjugates to form hybrids with DNA was determined by UV-melting technique. [78] The transition from of the duplex to the single strand form occurs within a narrow temperature range (typically 10-20°C) and can be easily monitored by measuring the temperature-dependent UV absorbance at 260 nm. The temperature at the midpoint of the transition is called melting temperature or T_m . The stability of the duplex can be estimated from the T_m value. The higher T_m indicated the more stable duplex. Thus, T_m experiments can be used to confirm the hybridization between the synthesized PNAs/PNA conjugates and their complementary DNA targets (**Table 3.3**). Representative T_m and first derivative curves are shown in **Figures 3.10-3.11**. In case of T₃ PNAs (**P4-P8**), no T_m experiment was carried out since the T_m would be too low to be observed.

Table 3.3 T_m values of hybrids between PNAs/PNA conjugates and their complementary DNA targets

PNA	T_m with DNA ($^{\circ}\text{C}$)	
	DNA sequence 5'→3'	T_m ($^{\circ}\text{C}$)
Flu-anti-K (P15)	AGGCCTCATGA	62.2
Flu-anti- Phos (P14)	AGGCCTCATGA	62.0
Bz-KFF-anti (P16)	AGGCCTCATGA	58.3
Flu-T ₉ -KFF (P9)	AAAAAAAAAA	74.8
KFF-T ₉ -Flu (P10)	AAAAAAAAAA	74.8
Flu-T ₉ -K (P11)	AAAAAAAAAA	74.8
Ac-T ₉ -K (P17)	AAAAAAAAAA	79.7

Condition PNA:DNA = 1:1, [PNA] = 1.0 μM , 10 mM sodium phosphate buffer, pH 7.0, heating rate 1.0 $^{\circ}\text{C}/\text{min}$

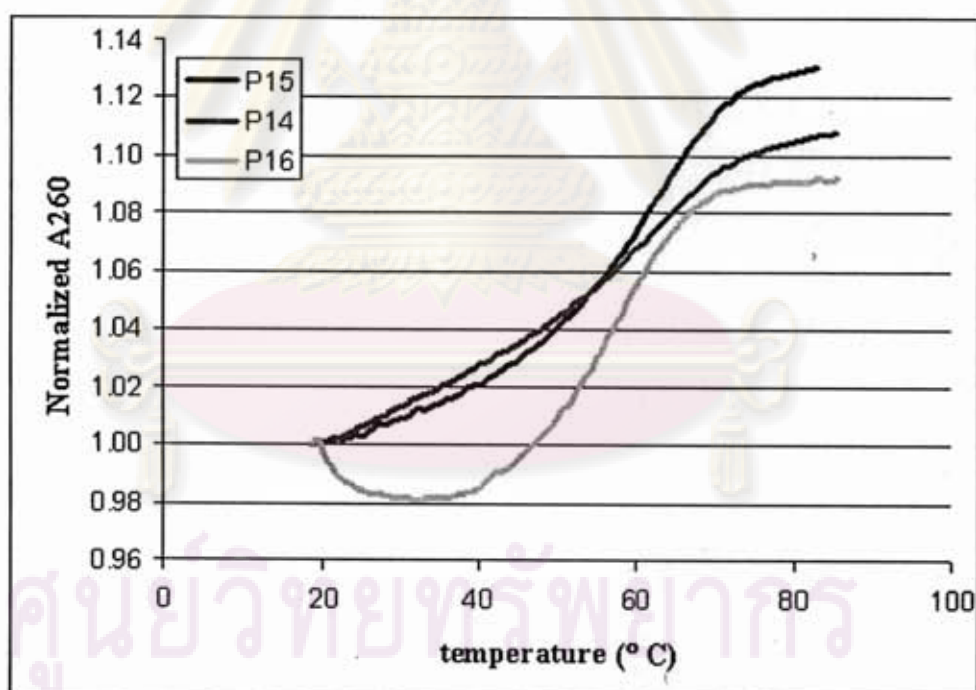


Figure 3.10 T_m curves of Flu-anti-K (P15), Flu-anti-Phos (P14) and Bz-anti-KFF (P16) with d(AGGCCTCATGA) (perfect match DNA). Experimental conditions: PNA:DNA = 1:1, [PNA] = 1.0 μM , 10 mM sodium phosphate buffer, pH 7.0, heating rate 1.0 $^{\circ}\text{C}/\text{min}$.

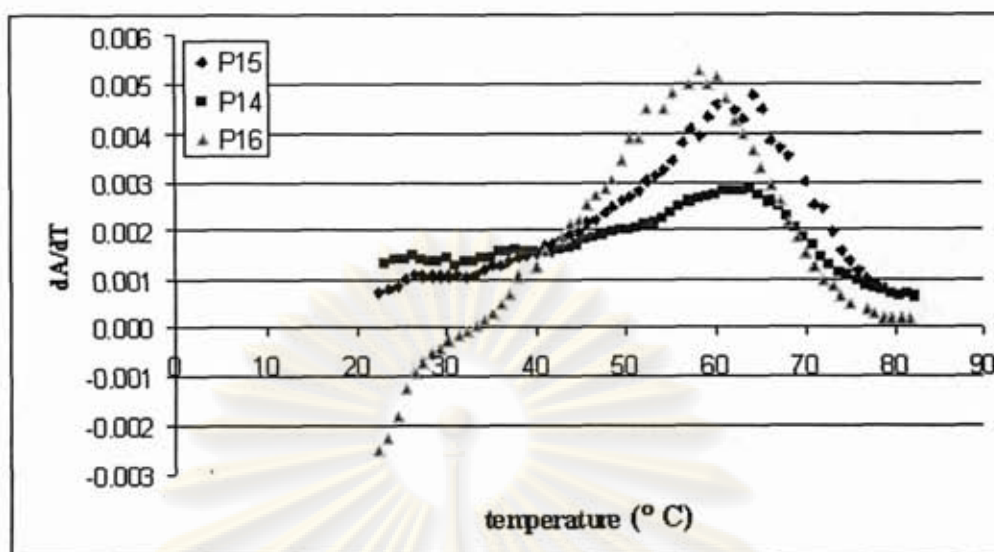


Figure 3.11 First-derivative T_m plots of Flu-anti-K (P15), Flu-anti-Phos (P14) and Bz-anti-KFF (P16) with d(AGGCCTCATGA) (perfect match DNA). Experimental conditions: PNA:DNA = 1:1, [PNA] = 1.0 μ M, 10 mM sodium phosphate buffer, pH 7.0, heating rate 1.0 $^{\circ}$ C/min.

3.6 Uptake ability studies

3.6.1 Theory and Experimental Design

To exhibit the desired antisense effects, the antisense agents must be able to reach the gene targets within the cell. This requires passing through a lipophilic negative-surface charge cell membrane. In general, PNA cannot permeate bacterial cell membrane easily. [79] *E. coli* is probably one of the most extensively studied. [80] Many peptide have been used successfully as carriers for delivery of PNAs to *E. coli* cells including (KFF)₃K. [79] On the other hand, polyarginine (R₁₀) was shown to be an effective cell-penetrating peptide in mammalian cells. [57] It is, however, unknown whether these peptide carriers would still be effective in delivering the new pyrrolidiny ssACPC PNA. Here we designed and synthesized ssACPC PNA conjugates with well known carriers including R₁₀, (KFF)₃K and phosphonium at varying positions (P4, P5, P6, P8, P9 and P10). At this stage no antisense effect was investigated therefore the sequence of the PNA was chosen to be the simplest ones, T₃ and T₉ PNA controls with the same T₃ and T₉ sequences, without the carrier groups (P7 and P11) were also synthesized to compare the uptake abilities by *E. coli* cells.

To enable direct observation of the cellular uptake by fluorescence spectroscopy, All PNAs used in this study were labeled with fluorescein (Flu) via an amide linkage between 5(6)-carboxyfluorescein and the amino group of the PNA (or free amino group of lysine attached to the PNA at C-termini for **P10**). The tested PNA conjugates or the control (20 μL of 25 μM) and water (20 μL) were incubated with the diluted *E. coli* ATCC 25922 cells ($\sim 10^7$ or $\sim 10^6$ CFU/mL) in LB Broth (80 μL) to a total volume of 100 μL for the specified period. The optical density (at 590 nm) of cell growth was monitored for cytotoxicity evaluation (Section 3.10). After the incubation time, the mixtures were centrifuged and the pelletized bacterial cells were washed with 0.1 M PBS pH 7.2 (200 μL) in order to remove the excess PNAs/PNA conjugates. In some experiments, the washed cells were examined under fluorescence microscope. The collected washed cells were lysed using either method I or method II as described in Section 3.8. The fluorescence intensity (at the excitation wavelength of 480 nm and the emission wavelength of 510 nm) of the lysis solution was measured in order to determine the uptake efficiency of PNA conjugates. The fluorescence intensities of the lysis solutions were compared to the initial fluorescence intensities of cell growth at 0 h which were adjusted to be 100% (see Section 2.6). High fluorescence intensity indicated the higher uptake ability but the figure should not be over 100%.

3.6.2 Cationic peptides (KFF and R₁₀) as carriers

In order to evaluate the cellular delivery of PNA conjugates, a series of PNA conjugates with cationic peptides were synthesized and tested in the *E. coli* ATCC 25922 cells. In the first experiments, the very short and simple T₃ sequence was first studied. The simple, unconjugated PNA with fluorescein label Flu-T₃-K (**P7**) was used as a negative control sequence. In the experiment, three sets of cell dilution at $0.01\times$ ($\sim 10^6$ CFU/mL) of the stock cell ($\text{OD}_{600}=0.5$, $\sim 10^8$ CFU/mL) were treated with the two PNA conjugates (**P4** and **P5**) and the PNA control at the final concentration of PNA = 5 μM at 37 °C for 4 h.

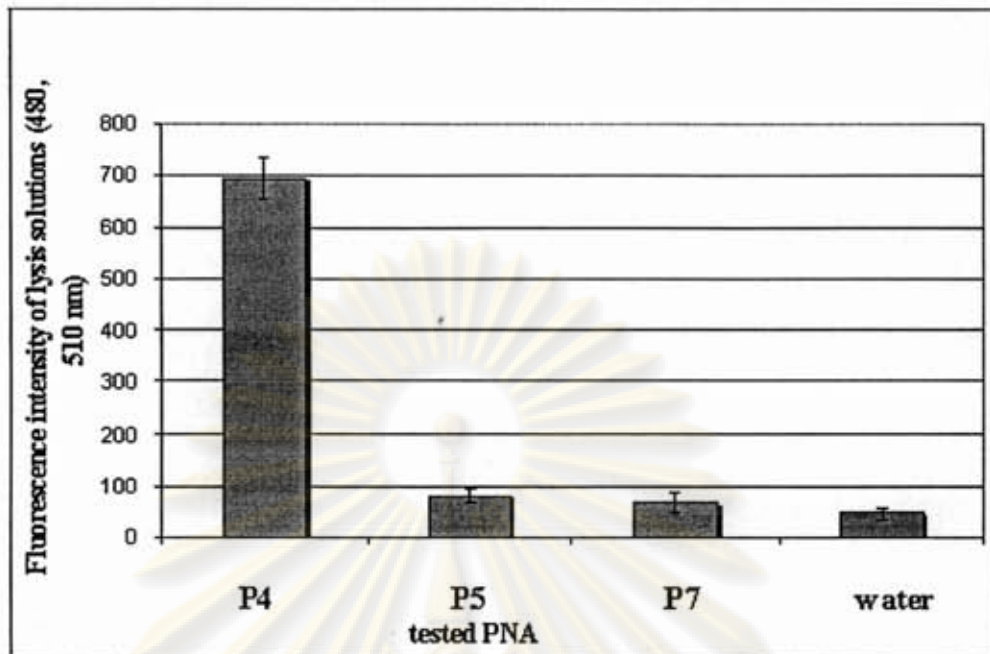


Figure 3.12: Fluorescence intensities of the solutions obtained from lysis of the *E. coli* ATCC 25922 cells after treatment with PNA conjugates (5 μ M, 37 $^{\circ}$ C, 4 h) Flu-T₃-KFF (**P4**), Flu-T₃-R₁₀ (**P5**), Flu-T₃-K (**P7**) and none (water).

The treated cells were then lysed using the following protocol (method I). The pelletized cells were thoroughly washed with PBS followed by TE buffer. The cells were then lysed using 15% sucrose at -4 $^{\circ}$ C for 5 min, followed by lysozyme (5 mg/mL) at -4 $^{\circ}$ C for 30 min and then 0.1% Triton X-100 at -4 $^{\circ}$ C for 30 min. Fluorescence intensities of the lysed cell solutions at 4 h were then measured (**Figure 3.12**). The (KFF)₃K was considered to be a good carrier since the significant fluorescence intensity was observed with the cells treated with the PNA conjugate Flu-T₃-KFF (**P4**). The cell-permeation properties of the conjugate (**P4**) was further confirmed by fluorescence microscopy (**Figure 3.13**). No adjusted fluorescence intensity was observed for the control PNA (**P7**), under identical conditions. The results clearly showed that (KFF)₃K could be a potential cell-penetrating carrier for the PNA. By contrast, R₁₀ was found to be a poor carrier because the fluorescence intensity of the lysed cells after treatment with the PNA Flu-T₃-R₁₀ conjugate (**P5**), was similar to the control (**P7**) and the background (water).

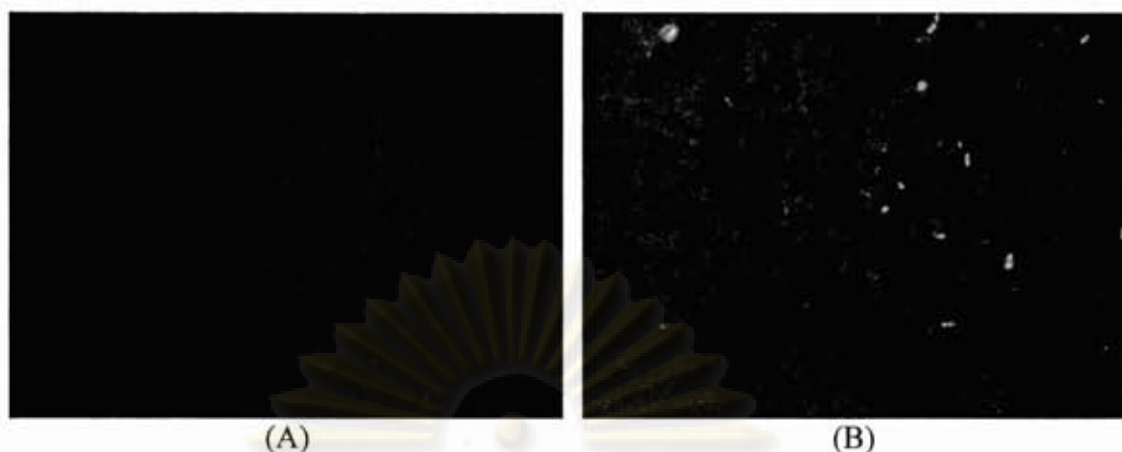


Figure 3.13 Fluorescence microscopy images of *E. coli* ATCC 25922 cells (A) treated with 5 μ M of Flu-T₃-K (P7) at 37 °C for 4 h (control) (B) treated with 5 μ M of Flu-T₃-KFF (P4) at 37 °C for 4 h.

3.6.3 Phosphonium as a carrier

The positively charged and lipophilic triphenylalkylphosphonium group has been previously used for PNA delivery to target human mtDNA L-chain (np 8339-8349). [46] The use of phosphonium group as carrier appeared to be attractive mainly because of the simplicity in labeling of PNA with phosphonium by solid-phase methodology. [74, 75] To determine whether the phosphonium-PNA conjugate could be taken up by the *E. coli* ATCC 25922 cells, the uptake experiment of cell dilution at $0.1 \times (\sim 10^7 \text{ CFU/mL})$ of the stock cell ($\text{OD} = 0.5$ at 600 nm, $\sim 10^8 \text{ CFU/mL}$) was carried out in a similar fashion to the experiment described above. The uptake abilities were determined from the fluorescence intensity of the cells lysis after treatment with the Flu-T₃-Phos conjugate (P6) at a concentration of 5 μ M for 4 and 8 h. In addition, the fluorescence intensities of supernatants which contain culture medium and the non-uptaken excess PNA conjugates were also measured and compared with KFF conjugates and unmodified PNA.

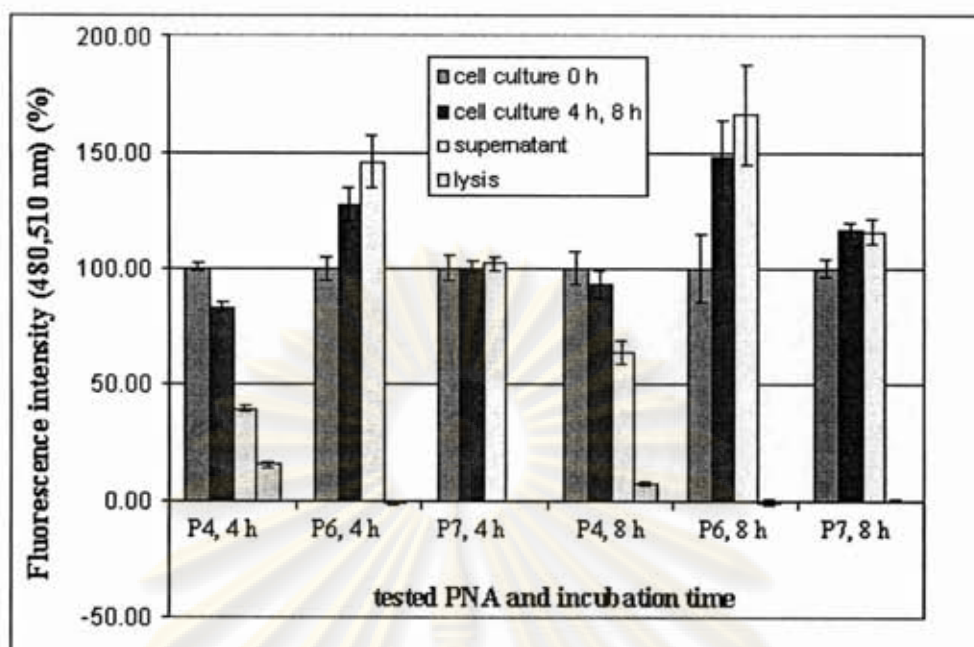


Figure 3.14 Percentages of fluorescence intensities of the solutions obtained from cell cultures at 0 h, 4 h, 8 h, supernatant and lysis of the 0.1× dilution cells after treatment with 5 μ M of Flu-T₃-KFF (P4), Flu-T₃-Phos (P6) and the control: Flu-T₃-K (P7) at 37 °C for 4 h.

The results shown in **Figure 3.14** suggested that phosphonium-PNA conjugate cannot be uptaken by *E. coli* cells at both 4 and 8 h. Another important thing to note was that the fluorescence intensity of the lysis solution obtained from cells treated with Flu-T₃-KFF conjugate (P4) at 8 h (7.4%, compared to the starting cells culture at 0 h) was lower than at 4 h (15.7%, compared to the starting cells culture at 0 h). The progressively lower fluorescence intensity observed against time may be the consequence of the ability of *E. coli* cells to digest or excrete the PNA from their cells. In addition, from this experiment an unexpected increment of fluorescence intensities of cell culture and also in supernatant of cell lysis after treatment with Flu-T₃-Phos conjugate (P6) both at 4 and 8 h were observed. No satisfactory explanation can be offered at these stages, but it was clear that phosphonium was much less effective carrier than KFF for delivery of the PNA to *E. coli* cells.

In this experiment the cells dilution was changed from 0.01× to 0.1× dilution in order to compare the efficiency of the uptake ability of the KFF PNA conjugate (P4) at 4 h. At 0.01× dilution the fluorescence intensity of the lysis solution was 9.8% while at 0.1× dilution the fluorescence intensity was increased to 15.7%. This might

be because the more cells are available for excess PNA which can effective entering the cells.

3.7 Uptake studies with longer PNA (9 mer)

3.7.1 Comparison of uptake abilities of Flu-O-TTT-O-(KFF)₃K-NH₂ (P4) and Flu-O-TTTTTTTTTT-O-(KFF)₃K-NH₂ (P9)

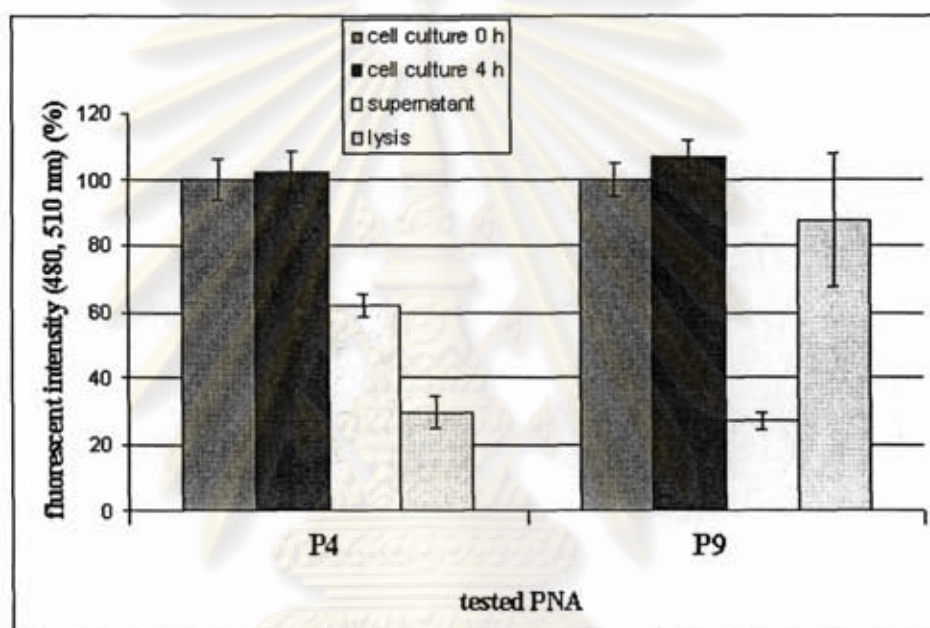


Figure 3.15 Percentages of fluorescence intensities of the solutions obtained from cell cultures at 0 h, 4 h, supernatant and lysis of the 0.01× dilution cells after treatment with 5 μM of Flu-T₃-KFF (P4) and Flu-T₉-KFF (P9) at 37 °C for 4 h.

The fluorescence intensities (percent uptaken into cells with reference to the fluorescence intensity of cell treated at 0 h) of lysis solutions of cell treated with Flu-T₃-KFF (P4) and Flu-T₉-KFF (P9) at the cell dilution of 0.01× were compared as shown in **Figure 3.15**. The results demonstrated that despite the increased length of the PNA part, Flu-T₉-KFF (P9) could be uptaken into the cells efficiently (**Figure 3.15**). It can therefore be concluded that the KFF carrier was able to carry long PNA to *E. coli* cells at least as efficiently as with short PNA.

3.8 Comparison of two different lysis methods (I and II)

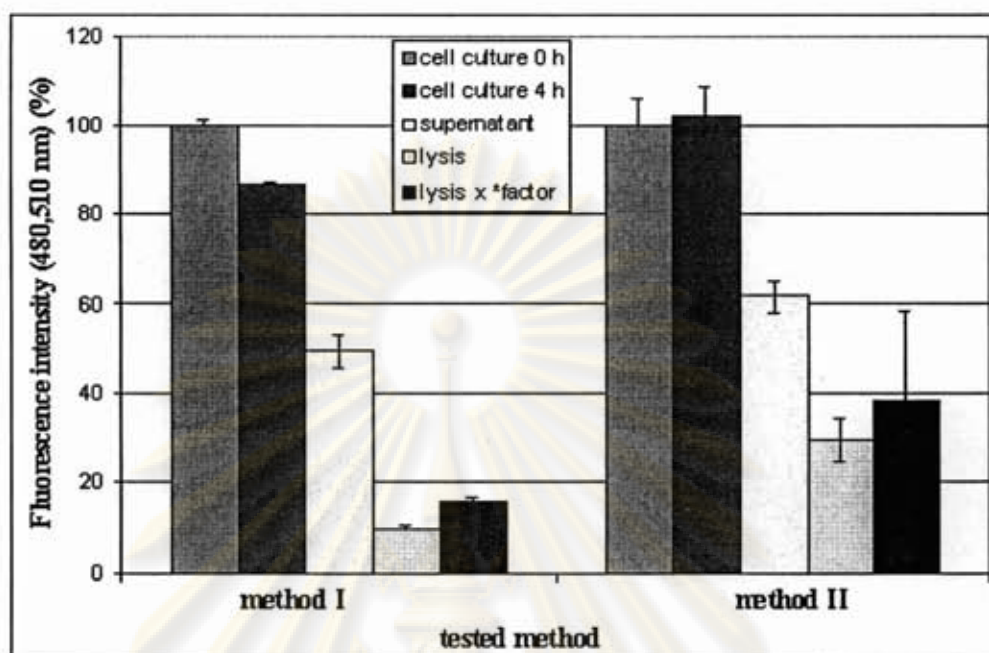


Figure 3.16 Percentages of fluorescence intensities of the solutions obtained from lysis by method I and method II of the $0.01\times$ dilution cells after treatment with $5\ \mu\text{M}$ of Flu-T₃-KFF (P4) at $37\ ^\circ\text{C}$ for 4 h.

* total volume of lysis solution/total volume of cell culture 0 h

The efficiency of two different lysis methods was compared to ensure the complete cell lysing. After incubation $0.01\times$ dilution of *E. coli* cells with the PNA Flu-T₃-KFF (P4), the cells were centrifugally washed with PBS. The pelletized cells were lysed using the method I described earlier (Section 3.6.2) or method II. In the method II, the cells were washed with only PBS buffer. The lysis step required 6.7% sucrose, 10 mg/mL lysozyme followed 20% SDS w/v to a total volume of $120\ \mu\text{L}$ at $37\ ^\circ\text{C}$. The total lysis time was 20 min. The advantage of the lysis method II was that the experiment time was considerably reduced.

The fluorescence intensities of cell culture at 0 h, 4 h, supernatant, and lysis solution were compared in Figure 3.16. The fluorescence intensities of lysis solutions were also adjusted by lysis factor in order to enable direct comparison between two methods. The result clearly demonstrates that the lysis method II was more effective than method I (up to 2-fold) in shorter lysis time, therefore the method II was chosen for the lysis *E. coli* cells in subsequent experiments.

3.9 Position requirement of peptide (KFF)₃K as a carrier of PNA

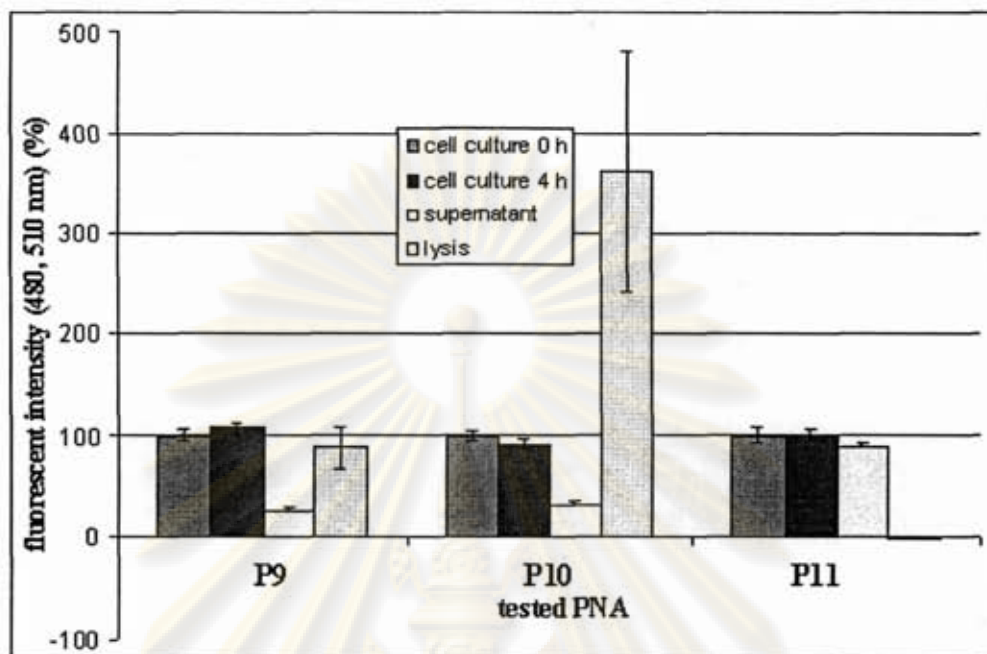


Figure 3.17 Percentages of fluorescence intensities of the solutions obtained from lysis of the 0.01× dilution cells after treatment with 5 μM of Flu-T₉-KFF (**P9**), KFF-T₉-Flu (**P10**) and the control: Flu-T₉-K (**P11**) at 37 °C for 4 h

The position of the peptide attached to the PNA (C- vs N-terminus) has been found to greatly influence the antisense activities of the PNA conjugates. [81] To determine the position requirement of the (KFF)₃K carrier, the PNA conjugates Flu-T₉-KFF (**P9**) and KFF-T₉-Flu (**P10**) conjugates carrying the KFF sequence at the C and the N-termini of the PNA respectively, were synthesized and their cell-penetrating properties were studied. The fluorescein-labeled unconjugated PNA Flu-T₉-K (**P11**) was used as the control in this study. The *E. coli* cells at a concentration of 0.01× dilution from the stock cell culture were treated with the PNA conjugates for 4 h. After the incubation period, the cells were washed with PBS and were lysed using method II. The total volume of the lysis solutions were adjusted to 100 μL. The fluorescence intensities of the cell culture, supernatant and lysis solution recorded are shown in **Figure 3.17**. The results showed that the Flu-T₉-KFF conjugate (**P9**) could be efficiently uptaken into *E. coli* cells (up to 88%). As expected, no uptaking was observed in the control PNA (**P11**). However, suspicious results were obtained with

the KFF-T₉-Flu conjugate (**P10**) which showed % fluorescence over 350% compare to the fluorescence intensity of cell culture at 0 h.

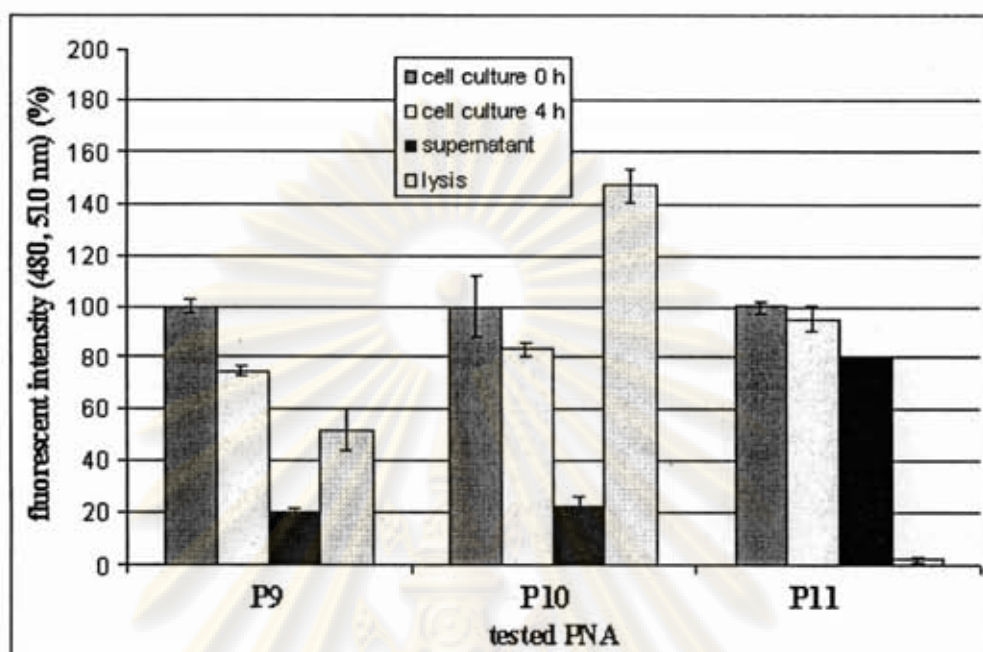


Figure 3.18 Percentages of fluorescence intensities of the solutions obtained from lysis of the 0.1× dilution cells after treatment with 5 μM of Flu-T₉-KFF (**P9**), KFF-T₉-Flu (**P10**) and the control: Flu-T₉-K (**P11**) at 37 °C for 4 h.

To confirm this, the *E. coli* cells at a different dilution (0.1×) were treated with the Flu-T₉-KFF (**P9**) and KFF-T₉-Flu (**P10**) conjugates again. Although the concentration of *E. coli* cells was increased from 0.01× to 0.1×, the fluorescence intensity of the lysis solution from cells treated with the KFF-T₉-Flu (**P10**) was still over 100% (148%) whereas the fluorescence intensity of the lysis solution of the Flu-T₉-KFF was 52% (**Figure 3.18**). Since the PNA **P10** was found to be poorly soluble in aqueous medium and acetonitrile was needed to improve solubility of the PNA, these suspicious results might be due to solubility problems or other additional factors like instability of the PNA conjugate under the assay conditions. It is therefore not possible to conclude about the role of the position of the carrier peptide to the uptake ability. However, it is probably safer to choose the more well-behaved C-terminal KFF conjugate such as **P9** for future antisense studies.

3.10 Evaluation of Cytotoxicities

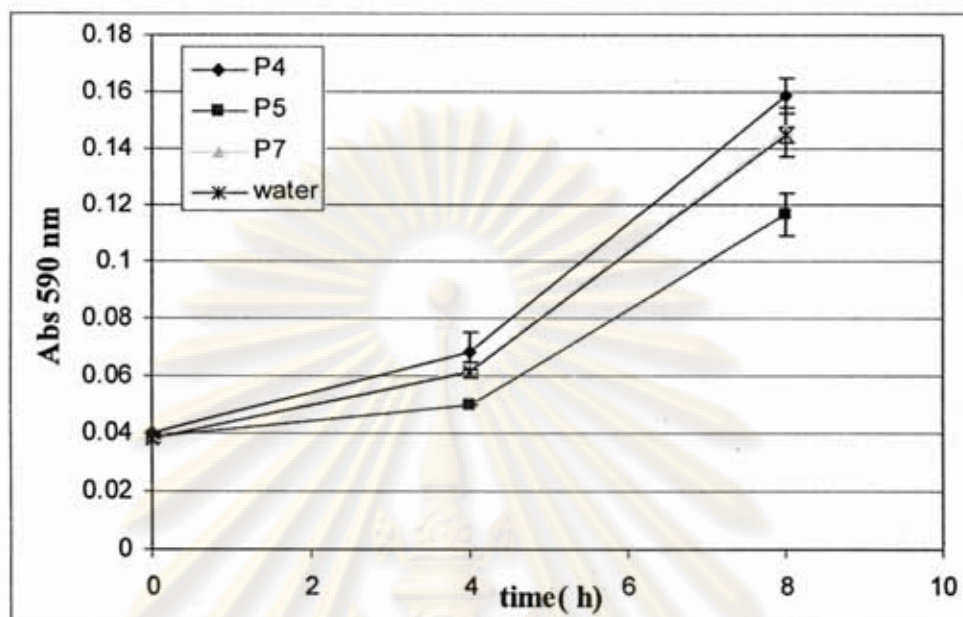


Figure 3.19 Cytotoxic effects of PNA conjugates. *E. coli* ATCC 25922 at 0.01× dilution cells were treated with Flu-T₃-KFF (P4), Flu-T₃-R₁₀ (P5), Flu-T₃-K (P7), and none (water), for 4 and 8 h, and then the absorbance at 590 nm was measured.

To determine the cytotoxic effects of the PNA conjugates, the UV absorbance of bacterial cell growth were monitored by measuring the UV absorbance at 590 nm against time (Figure 3.19). The results were encouraging as Flu-T₃-KFF conjugate (P4) apparently showed no toxicity. The cell growth was similar to the control and the background. Variance analysis (P-value > 0.1) confirmed that the graphs of P4, P7 and water were not different to others. On the other hand, the Flu-T₃-R₁₀ conjugate (P5) should be considered as somewhat toxic because a reduced rate of cell growth was observed.

In addition, the cytotoxic effect of the phosphonium labeled PNA Flu-T₃-Phos (P6) was also investigated at a different *E. coli* cells dilution (0.1×). From the Figure 3.20, it can be seen that all PNA did not effect the cell growth of the *E. coli*. These results suggested that phosphonium labeled, KFF conjugate and unmodified PNA are not cytotoxic.

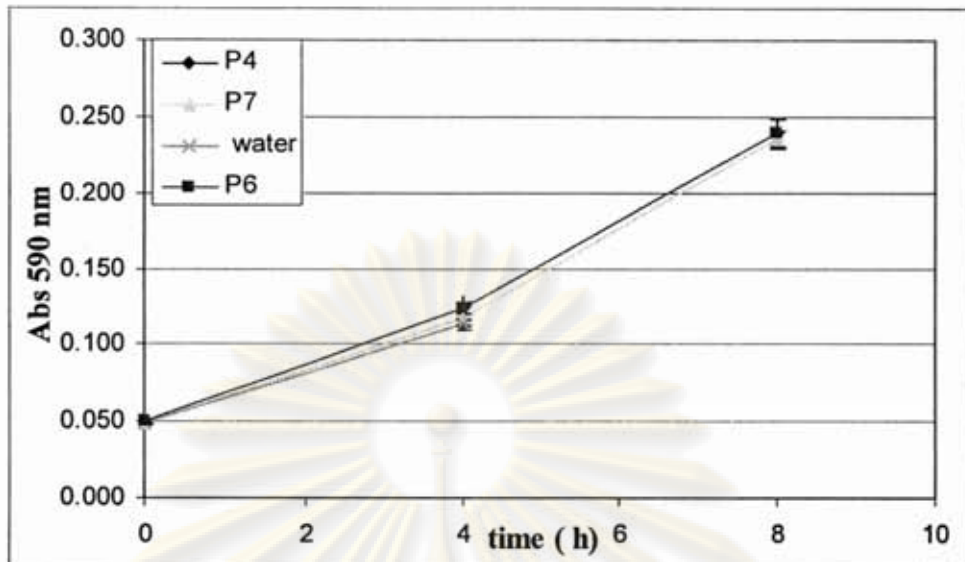


Figure 3.20 Cytotoxic effects of PNA conjugates. *E. coli* ATCC 25922 at 0.1× dilution cells were treated with Flu-T₃-KFF (P4), Flu-T₃-K (P7), none (water) and Flu-T₃-Phos (P6) for 4 and 8 h, and then the absorbance at 590 nm was measured.

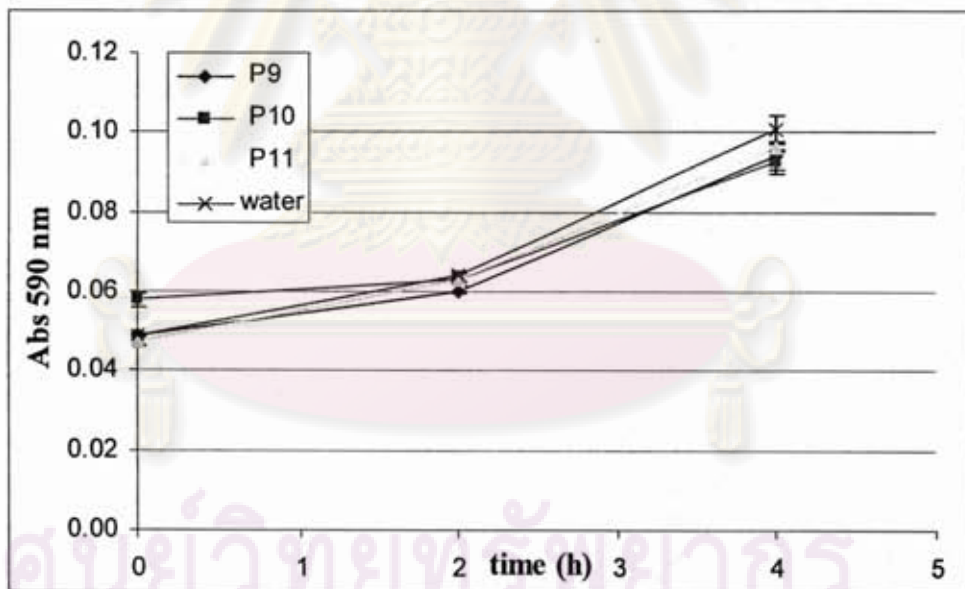


Figure 3.21 Cytotoxic effects of PNA conjugates. *E. coli* ATCC 25922 0.1× dilution cells were treated with Flu-T₉-KFF (P9), KFF-T₉-Flu (P10), Flu-T₉-K (P11) and none (water), for 2 and 4 h, and then the absorbance at 590 nm was measured.

The cytotoxic effects of the T₉ PNA conjugates to *E. coli* cells growth at 0.1× dilution were also investigated. **Figure 3.21** shows optical density at 590 nm of treated cell culture at 0, 2 and 4 h. Both Flu-T₉-KFF (P9) and Flu-T₉-K (P11) did not

show any significant difference to the background. In case of KFF-T₉-Flu (**P10**), a noticeable difference in initial optical density at 0 h was observed. This may be because of the poor solubility of KFF-T₉-Flu (**P10**) in the cell culture medium which can increase the overall optical density to some extent.

3.11 Determination of stabilities of PNA toward cellular enzymes

3.11.1 Theory and experiment design

Stability of PNA under physiological conditions needs to be considered for *in vivo* or cell culture studies. The stability of PNA in the media is an interesting point since bacterial or other cells may have ability to produce a number of enzymes such as peptidases which may have possibility to digest the PNA. To fully utilize the cell-penetrating properties of the *ssACPC* PNA conjugates in *E. coli* cells, the stability of the PNA needs to be demonstrated. To ensure that the PNA is stable under the studied condition, this research aim to study the stability of the novel PNA toward protease enzymes. The enzyme proteinase K - a broad-specificity serine protease - was chosen as a model enzyme.

The simple unlabelled and unconjugated PNA Ac-T₉-K (**P17**) was first tested for its stability towards proteinase K. A simple peptide: ACTH 4-10 (Adrenocorticotrope Hormone Fragment 4-10: Met-Glu-His-Phe-Arg-Trp-Gly) was also used as the positive control for this study. [82] HPLC analysis (UV detector) was used to evaluate the stability of the PNA relative to the control peptide. Monitoring the ACTH 4-10 was carried out at 215 nm while the PNA was monitored at 260 nm. [82]

3.11.2 Stabilities of PNA toward proteinase K

Initially, the HPLC conditions that can resolve the PNA and the ACTH 4-10 control were optimized. The aqueous solutions of PNA **P17** and ACTH 4-10 were mixed in different ratios and subjected to HPLC analysis using MeOH:H₂O with 0.01% TFA gradient (10% MeOH for 5 min then linear gradient to 90% MeOH over 60 min). The PNA (30 μM) and ACTH 4-10 (100 μM) was found to be the optimum

ratio which provided ~ 1:1 absorption intensities at 215 nm (**Figure 3.22**). The UV absorption pattern (**Figure 3.23**) of the peak at 45.6 min showed maximum absorption at 271.6 nm indicated that this peak is the PNA. The UV pattern of the peak at 40.4 min showed a maximum absorption at ~ 220 nm and a minor absorption at 289.4 (Trp) indicated that this peak is ACTH 4-10.

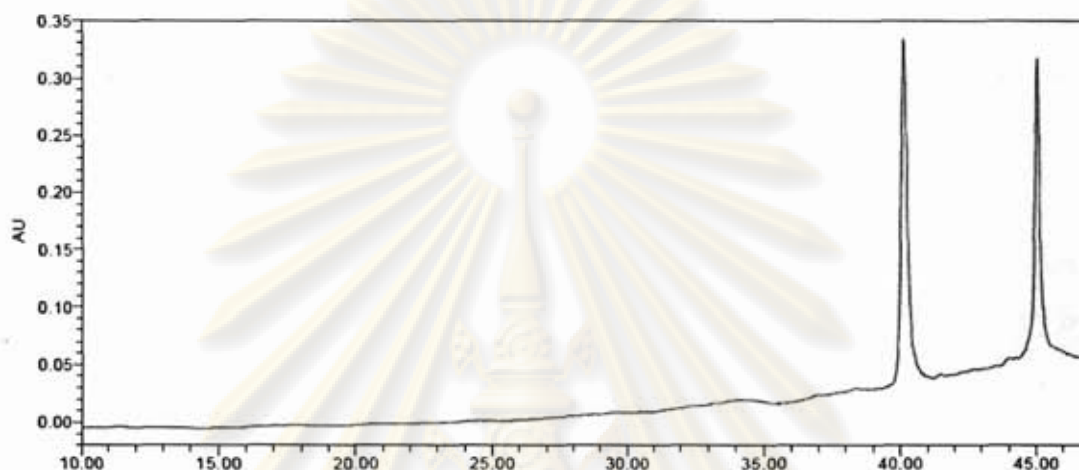


Figure 3.22 HPLC chromatogram (215 nm) of a mixture containing ACTH 4-10 (100 μM , $t_R = 40.4$ min) and P17 (30 μM , $t_R = 45.6$ min).

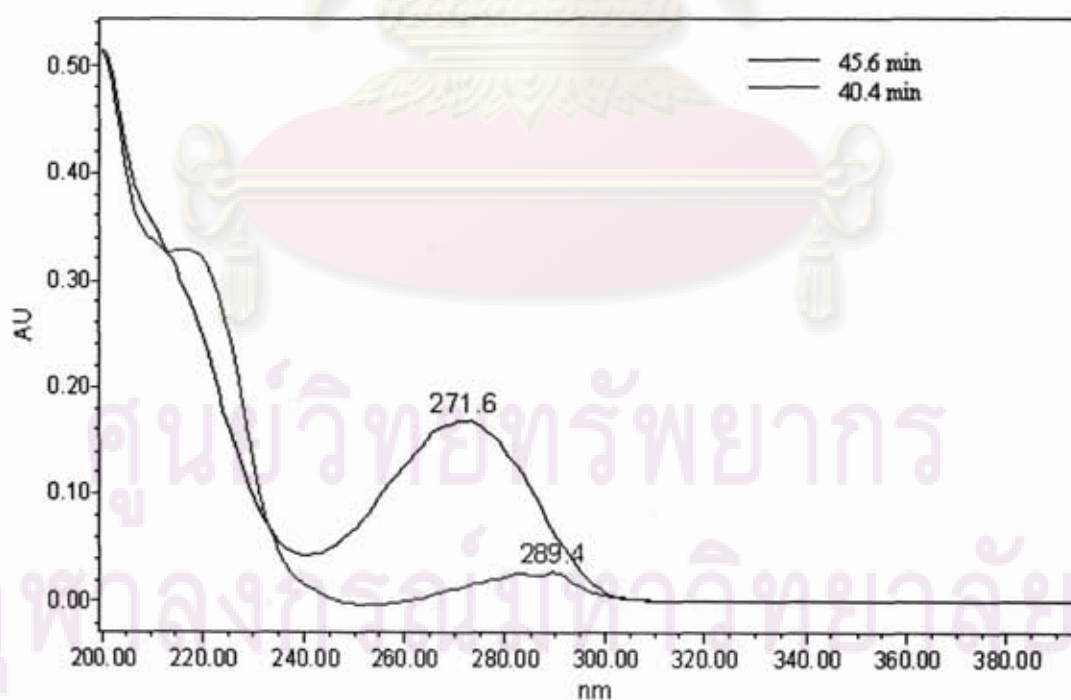


Figure 3.23 UV absorption patterns of HPLC peaks from the analysis of ACTH 4-10 (100 μM) and P17 (30 μM) mixture shown in **Figure 3.22**

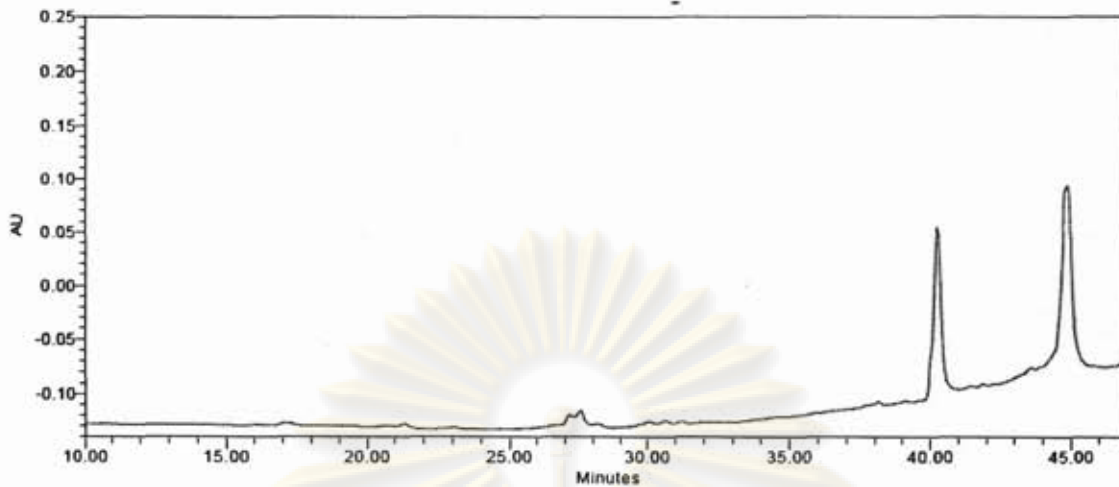


Figure 3.24 HPLC chromatogram (215 nm) of the PNA-peptide mixture without proteinase K treatment. Conditions: P17 30 μM and ACTH 4-10 100 μM in 100 mM Tris-HCl pH 7.5 at 37° C for 20 h.

The next experiment was carried out in order to test the stability of PNA and the peptide control under the incubation conditions in the absence of proteinase K. The PNA and the control were dissolved in 100 mM Tris-HCl buffer pH 7.5 to a final concentration of 30 μM and 100 μM respectively (total volume at 15 μL). The solution was incubated at 37 °C for 1 h and 20 h. After the incubation time, the solution was analyzed by HPLC. The results clearly showed that the PNA and the control peptide are stable under the incubation conditions for at least 20 h. No noticeable degradation was found for both the PNA and the peptide (**Figure 3.24**).

The stabilities of PNA and the peptide control in the presence of proteinase K at various concentrations were next evaluated. Proteinase K was added to the same PNA-peptide mixture to the desired concentration (total volume of at 14 μL). The solution was incubated at 37 °C for the specified period of time. After that, 1 μL of 1.0 μM HCl was added to stop the reaction and the quenched reaction mixture was analyzed by HPLC.

จุฬาลงกรณ์มหาวิทยาลัย

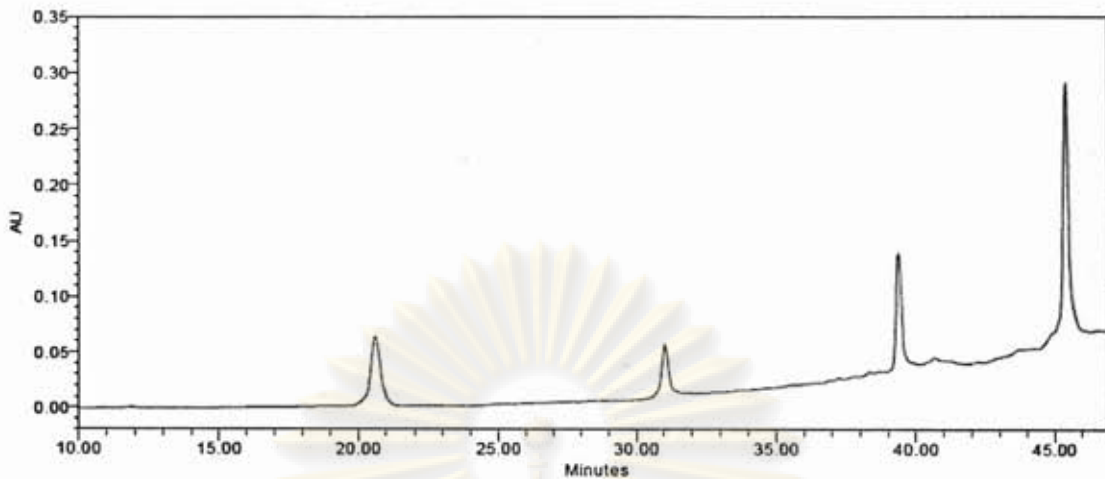


Figure 3.25 HPLC chromatogram (215 nm) of the PNA-peptide mixture with proteinase K treatment. Conditions: P17 30 μM , ACTH 4-10 100 μM and proteinase K at final conc. = 0.0005 mg/mL (0.015⁶ units/mL) in 100 mM Tris-HCl pH 7.5 at 37° C for 20 min.

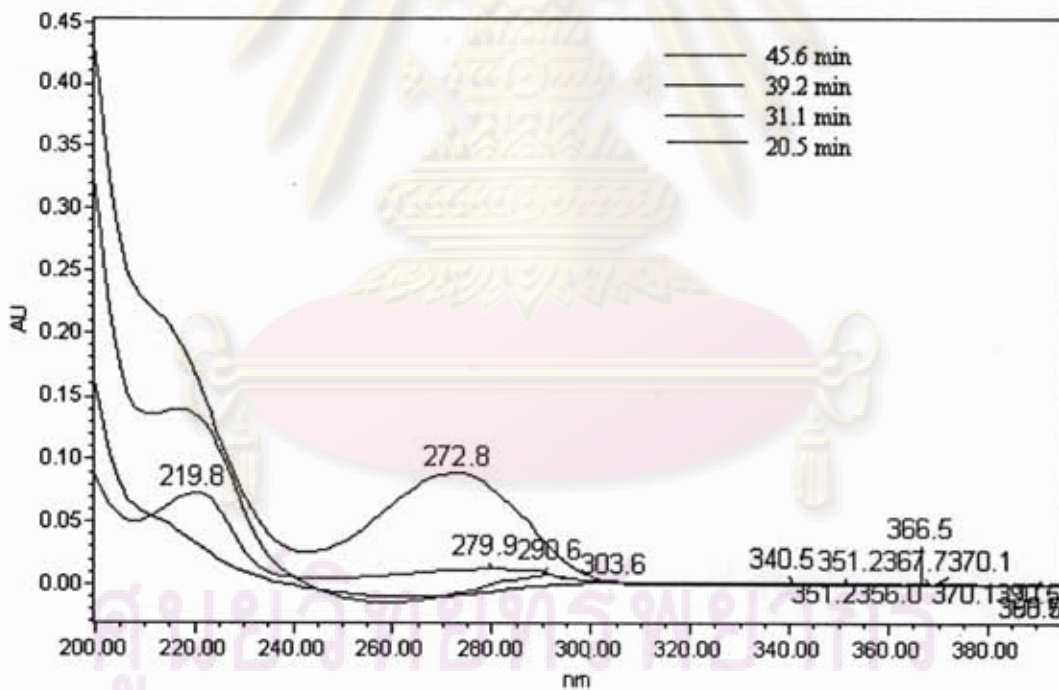


Figure 3.26 UV absorption patterns of HPLC peaks from the analysis of ACTH 4-10 (100 μM) and P17 (30 μM) mixture after proteinase K treatment as shown in **Figure 3.25**.

⁶ One Unit is defined as that amount of the enzyme that catalyzes the conversion of 1 micromole of substrate per minute. The conditions also have to be specified: one usually takes a temperature of 30°C and the pH value and substrate concentration that yield the maximal substrate conversion rate. [83]

The result presented in **Figure 3.25** shown that in the presence of proteinase K at 0.0005 mg/mL (0.015 units/mL) the control was significantly degraded while the PNA still remained intact (37 °C for 20 min). The UV absorption pattern (**Figure 3.26**) of the peak at 20.5 min ensured that the peak was a degraded product from the control (39.2 min) since both showed the same absorption patterns. Another peak at 31.1 min was also observed which could not be arisen from degradation of the PNA because no absorption at ~ 270 nm was found. The peak at 31.1 min was more likely to derive from degradation of the peptide control. The relative intensities of the **P17** peak at 45.6 min and the peptide peak at 39.2 min also support the conclusion that the PNA was stable under the conditions at which a significant amount of the control peptide was degraded by proteinase K.

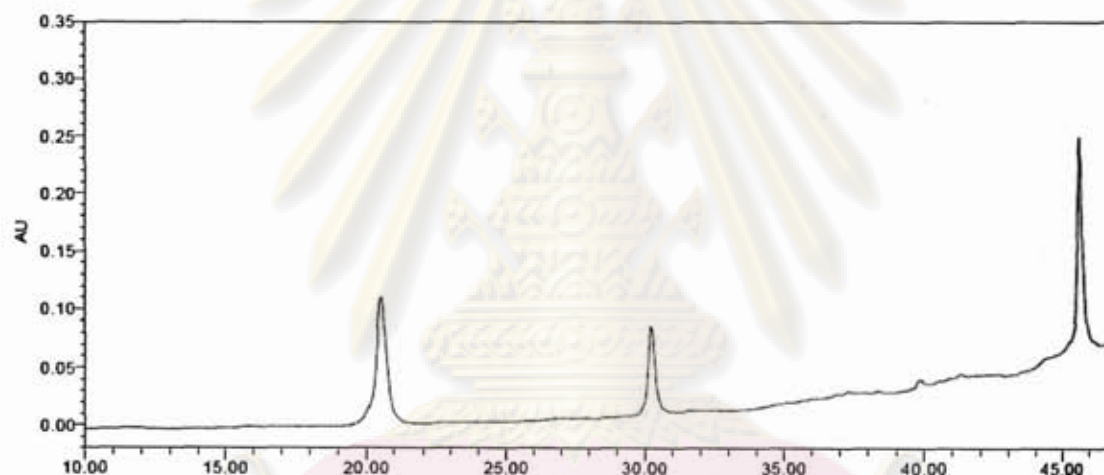


Figure 3.27 HPLC chromatogram (215 nm) of the PNA-peptide mixture with proteinase K treatment. Conditions: **P17** 30 μ M, ACTH 4-10 100 μ M and proteinase K at final conc. 0.005 mg/mL (0.15 units/mL) in 100 mM Tris-HCl pH 7.5 at 37° C for 5 min.

Next, the concentration of proteinase K was increased from 0.0005 mg/mL (0.015 units/mL) to 0.005 mg/mL (0.15 units/mL) and the incubation period was reduced from 20 min to 5 min. **Figure 3.27** clearly showed that under these conditions, the control was completely cleaved into two fragments. No degradation of PNA could be observed. In order to confirm the excellent stability of PNA towards proteinase K, the concentration of the enzyme was increased to a final concentration

of 0.5 mg/mL (15 units/mL) and the incubation times were varied from 5 min, 1 h, 3.5 h and 18.5 h.

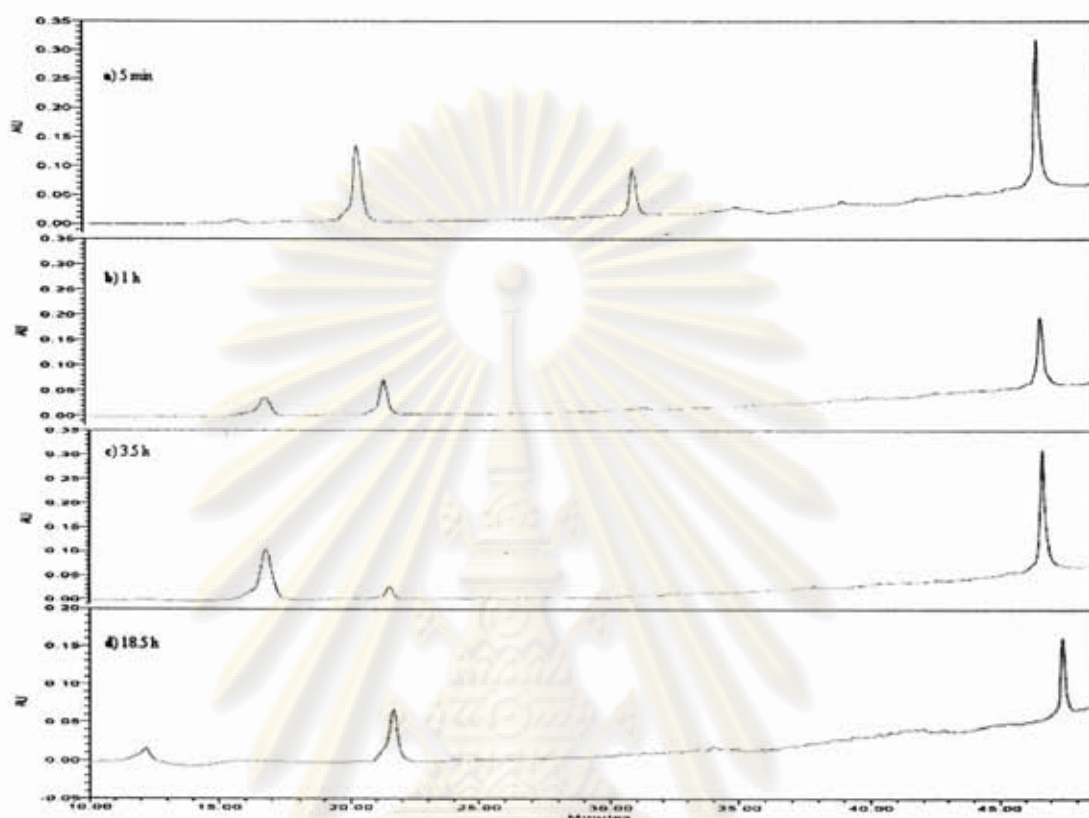


Figure 3.28 HPLC chromatogram (215 nm) of the PNA-peptide mixture with proteinase K treatment. Conditions: P17 30 μ M, ACTH 4-10 100 μ M and proteinase K at final conc. = 0.5 mg/mL (15 units/mL) in 100 mM Tris-HCl pH 7.5 at 37° C for (a) 5 min, (b) 1 h, (c) 3.5 h and (d) 18.5 h.

After 5 min treatment of the peptide mixture with proteinase K at the concentration of 0.5 mg/mL (15 units/mL), the HPLC chromatogram was similar to at 0.005 mg/mL, 5 min {**Figures 3.27 and 3.28 (a)**}. Under both conditions, the peptide control peak at ~ 40 min completely disappeared while the PNA peak at ~ 45 min still remained and no fragmentation of the PNA has been observed.

After leaving for 1 h, the peak at ~ 30 min was degraded with the appearance of a new peak at 16.2 min {**Figure 3.28 (b)**}. The UV patterns in **Figure 3.29** demonstrated that both peaks at 16.2 and 20.9 min should derive from the control peptide since they contain no characteristic absorbance of PNA at ~ 270 nm. When the incubation time was increased to 3.5 h {**Figure 3.28 (c)**}, the result was similar to

the 1 h incubation, except for the noticeable difference in the ratio of the peaks at 16.2 and 20.9 min {**Figure 3.28 (b)** and **Figure 3.28 (c)**}.

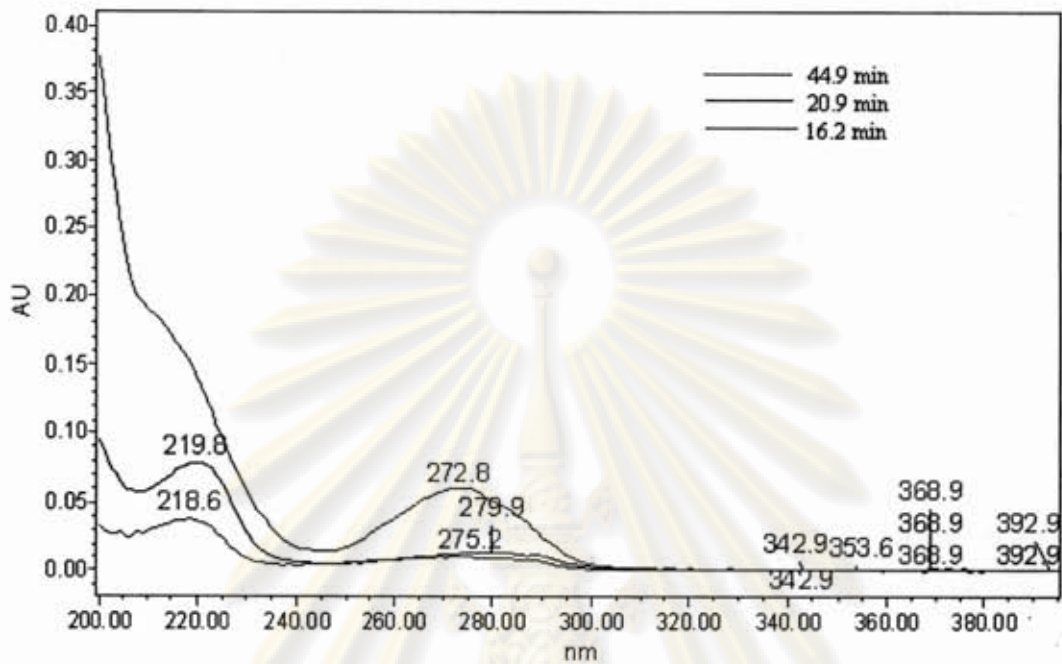


Figure 3.29 UV absorption patterns of HPLC peaks from the analysis of ACTH 4-10 (100 μM) and P17 (30 μM) mixture after proteinase K treatment for 1 h as shown in **Figure 3.28 (b)**.

The stability of PNA after extended exposure to high concentration of proteinase K was also evaluated. **Figure 3.28 (d)**, after the digestion period was increased to 18.5 h, A noticeable degradation of the PNA could be observed as shown by the presence of a new peak at 12.2 min with a maximum absorbance at 265.7 nm. Nevertheless, the PNA peak at 47.1 min was still not completely degraded (**Figure 3.30**). As a result, the PNA appeared to be stable in media containing a very high concentration of proteinase K (0.5 mg/mL, 15 units/mL) overnight. The results from **Figure 3.27** and **Figure 3.28 (d)** suggested that the PNA was much more stable than the control towards proteolytic enzymes.

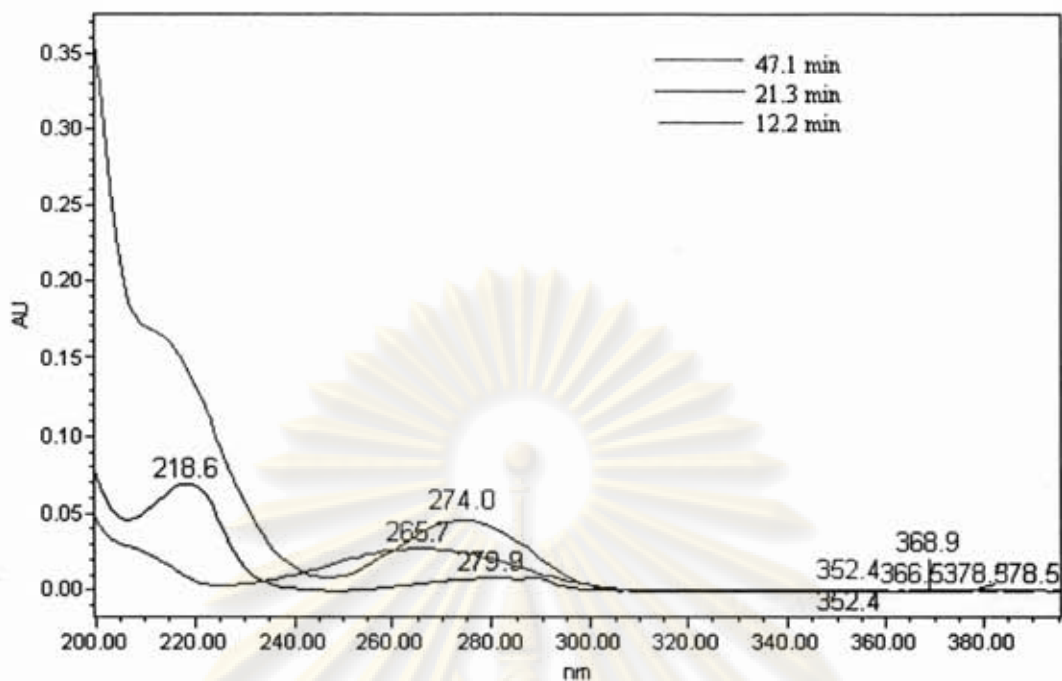


Figure 3.30 UV absorption patterns of HPLC peaks from the analysis of ACTH 4-10 (100 μM) and P17 (30 μM) mixture after proteinase K treatment for 18.5 h as shown in **Figure 3.28 (d)**.

Of course, the stabilities of the PNAs and their conjugates toward proteases and nucleases should also be next considered if times and resources are available. However, even without experimental results, it is probably safe to assume that the PNA will be very unlikely to be substrates of nucleases due to the absence of phosphate ester bonds.

ศูนย์วิทยทรัพยากร
จุฬาลงกรณ์มหาวิทยาลัย

CHAPTER IV

CONCLUSION

In this research, a novel pyrrolidiny (1*S*, 2*S*)-ACPC PNA attached to various carriers have been successfully synthesized by linear coupling using standard solid phase peptide synthesis. A series of PNA conjugates with cationic peptides namely (KFF)₃K, R₁₀ and a lipophilic cation: phosphonium cation (P⁺) were synthesized and tested in the *E. coli* ATCC 25922 cells. To determine the cell penetrating properties of the PNA conjugates into the *E. coli* cells at 5 μM (4 h, 37°C), three model PNA conjugates, Flu-O-TTT-O-(KFF)₃K-NH₂, Flu-O-TTT-O-R₁₀-NH₂ and Flu-O-TTT-Lys(P⁺)-NH₂ were labeled with fluorescein in order to enable direct observation of the cellular uptake by fluorescence spectroscopy. The unconjugated PNA with fluorescein label Flu-O-TTT-Lys-NH₂ was used as a negative control. It was demonstrated that, the (KFF)₃K was a good carrier, the cell-permeation properties of the conjugate was further confirmed by fluorescence microscopy. In contrast, R₁₀ was found to have low cellular delivery. No cytotoxicity was observed for Flu-O-TTT-O-(KFF)₃K-NH₂ and Flu-O-TTT-Lys(P⁺)-NH₂ according to cell growth rates. On the other hand, Flu-O-TTT-O-R₁₀-NH₂ retarded the cell growth therefore it was considered to be toxic to *E. coli* cells.

The longer PNA-KFF conjugate namely Flu-O-TTTTTTTTTT-O-(KFF)₃K-NH₂ were prepared with the aim to study the PNA length requirement. The results demonstrated that despite the increased length of the PNA part, Flu-O-TTTTTTTTTT-O-(KFF)₃K-NH₂ could be uptaken into the cells efficiently. The percent uptake ability compare to initial fluorescent intensity at 88 % indicated that the Flu-O-TTTTTTTTTT-O-(KFF)₃K-NH₂ can be uptaken into the cells even better than Flu-O-TTT-O-(KFF)₃K-NH₂. It can therefore be concluded that the KFF carrier was able to carry long PNA to *E. coli* cells at least as efficiently as with short PNA

Attempts to determine the importance of the position of attachment of the (KFF)₃K carrier failed. Over 100% fluorescent intensity was observed for N-termini conjugates H-(KFF)₃K-TTTTTTTTTT-Lys(Flu)-NH₂, possibly due to precipitation or degradation of the PNA under the test conditions. On the other hand, (KFF)₃K

attached to the PNA at C-termini was potential to deliver the PNA conjugates: Flu-O-TTTTTTTTTT-O-(KFF)₃K-NH₂ into the cells.

Synthesis of mixed base PNA-KFF conjugates Flu-O-TCATGAGGCCT-O-(KFF)₃K-NH₂ was not successful because of poor yield and complication of purifying the poorly soluble PNA. However, two additional sequences, Bz-O-(KFF)₃K-O-TCATGAGGCCT-NH₂ and Flu-O-TCATGAGGCCT-Lys(P⁺)-NH₂, designed to exhibit antisense effect on *Pseudomonas aeruginosa* were successfully prepared. Preliminary experiments in collaboration with Miss Piyatip Khuntayaporn and Dr Mullika T. Chomnawang are yet to revealed any observable antisense effects.

Finally, the stability of the novel PNA towards a proteolytic enzyme was evaluated using Ac-TTTTTTTTTT-Lys-NH₂ and Proteinase K as models. The peptide control (ACTH 4-10) was rapidly degraded under conditions 0.15 units/mL proteinase K at 37°C within 5 min. By contrast, the PNA was stable under the same conditions. The PNA appeared to be stable even treatment with 15 units/mL of proteinase K for prolonged period (18.5 h) at 37°C.



ศูนย์วิทยทรัพยากร
จุฬาลงกรณ์มหาวิทยาลัย

REFERENCES

- [1] Nielsen, P. E.; Egholm, M.; Berg, R. H.; and Buchardt, O. Sequence-selective recognition of DNA by strand displacement with a thymine-substituted polyamide. Science. 254 (1991): 1497-1500.
- [2] Watson, J. D.; and Crick, F. H. C. A Structure for deoxyribose nucleic acid. Nature. 171 (1953): 737-738.
- [3] Egholm, M.; Buchardt, O.; Christensen, L.; Behren, C.; Freier, S. M.; Driver, D. A.; Berg, R. H.; Kim, S. K.; Norden, B.; and Nielsen, P. E. PNA hybridizes to complementary oligonucleotides obeying the Watson-Crick hydrogen-bonding rules. Nature. 365 (1993): 566-568.
- [4] Giesen, U.; Kleider, W.; Berding, C.; Geiger, A.; Orum, H.; and Nielsen, P. E. A formula for thermal stability (T_m) prediction of PNA/DNA duplexes. Nucleic Acids Res. 26 (1998): 5004-5006.
- [5] Tomac, S.; Sarkar, M.; Ratilainen, T.; Wittung, P.; Nielsen, P.; Norden, B.; and Graslund, A. Ionic effects on the stability and conformation of peptide nucleic acid complexes. J. Am. Chem. Soc. 118 (1996): 5544-5552.
- [6] Demidov, V. V.; Potaman, V. N.; Frank-Kamenetskii, M. D.; Egholm, M.; Buchardt, O.; Sonnichsen, S. H.; and Nielsen, P. E. Stability of peptide nucleic acids in human serum and cellular extracts. Biochem. Pharmacol. 48 (1994): 1310-1313.
- [7] Hyrup, B.; Egholm, M.; Nielsen, P. E.; Wittung, P.; Norden, P. B.; and Buchardt, O. Structure-activity studies of the binding of modified peptide nucleic acids (PNAs) to DNA. J. Am. Chem. Soc. 116 (1994): 7964-7970.
- [8] Hyrup, B.; Egholm, M.; Buchardt, O.; and Nielsen, P. E. A flexible and positively charged PNA analogue with an ethylene-linker to the nucleobase: synthesis and hybridization properties. Bioorg. Med. Chem. Lett. 6 (1996): 1083-1088.
- [9] Krotz, A. H.; Buchardt, O.; and Nielsen, P. E. Synthesis of "retro-inverso" peptide nucleic acids: 2. oligomerization and stability. Tetrahedron Lett. 36 (1995): 6941-6944.
- [10] Haaima, G.; Lohse, A.; Buchardt, O.; and Nielsen, P. E. Peptide nucleic acids (PNAs) containing thymine monomers derived from chiral amino acids:

- hybridization and solubility properties of D-lysine PNA. Angew. Chem. Int. Ed. Engl. 35 (1996): 1939-1942.
- [11] Kuwahara, M.; Arimitsu, M.; and Sisido, M. Sequence-specific hybridization between two different types of peptide nucleic acids. Bull. Chem. Soc. Jpn. 72 (1999): 1547-1552.
- [12] Lagriffoule, P.; Wittung, P.; Eriksson, M.; Jensen, K. K.; Norden, B.; Buchardt, O.; and Nielsen, P. E. Peptide nucleic acids with a conformationally constrained chiral cyclohexyl-derived backbone. Chem. Eur. J. 3 (1997): 912-919.
- [13] Govindaraju, T.; Kumar, V. A.; and Ganesh, K. N. (1S,2R/1R,2S)-*cis*-cyclopentyl PNA (*cp*PNA) as constrained PNA analogues: synthesis and evaluation of aeg-*cp* PNA chimera and stereopreferences in hybridization with DNA/RNA. J. Org. Chem. 69 (2004): 5725-5734.
- [14] Pokorski, J. K.; Myers, M. C.; and Appella, D. H. Cyclopropane PNA: observable triplex melting in a PNA constrained with a 3-membered ring. Tetrahedron Lett. 46 (2005): 915-917.
- [15] Gangamani, B. P.; Kumar, V. A.; and Ganesh, K. N. Synthesis of N^α -(purinyl/pyrimidinyl acetyl)-4-aminoproline diastereomers with potential use in PNA synthesis. Tetrahedron. 52 (1996): 15017-15030.
- [16] Lowe, G.; Vilaivan, T.; and Westwell, M. S. Hybridization studies with chiral peptide nucleic Acids. Bioorg. Chem. 25 (1997): 321-329.
- [17] Hickman, D. T.; Micklefield, J.; King, P. M.; Slater, J. M.; and Cooper, M. A. Unusual RNA and DNA binding properties of a novel pyrrolidine-amide oligonucleotide mimic (POM). Chem. Commun. (Cambridge). 22 (2002): 2251-2252.
- [18] Vilaivan, T.; Khongdeesameor, C.; Harnyuttanakorn, P.; Westwell, M. S.; and Lowe, G. Synthesis and properties of chiral peptide nucleic acids with a *N*-aminoethyl-D-proline backbone. Bioorg. & Med. Chem. Lett. 10 (2000): 2541-2545.
- [19] Püschl, A.; Tedeschi, T.; and Nielsen, P. E. Pyrrolidine PNA: a novel conformationally restricted PNA analogue. Org. Lett. 2 (2000): 4161-4163.
- [20] Püschl, A.; Boesen, T.; Zuccarell, G.; Dahl, O.; Pitsch, S.; and Nielsen, P. E. Synthesis of pyrrolidinone PNA: a novel conformationally restricted PNA

- analogue. *J. Org. Chem.* 66 (2001): 707-712.
- [21] Govindaraju, T.; and Kumar, V. A. Backbone extended pyrrolidine peptide nucleic acids (*bepPNA*): design, synthesis and DNA/RNA binding studies. *Chem. Commun.* 2005: 495-497.
- [22] Shirude, P. S.; Kumar, V. A.; and Ganesh, K.N. Chimeric peptide nucleic acids incorporating (2*S*,5*R*)-aminoethyl pipercolyl units: synthesis and binding studies. *Tetrahedron Lett.* 45 (2004): 3085-3088.
- [23] Lonkar, P. S.; and Kumar, V.A. Design and synthesis of conformationally frozen peptide nucleic acid backbone: chiral piperidine PNA as a hexitol nucleic acid surrogate. *Bioor. Med. Chem. Lett.* 14 (2004): 2147-2149.
- [24] Gangamani, B.P.; D'Costa, M.; Kumar, V. A.; and Ganesh, K. N. Conformationally restrained chiral PNA conjugates: synthesis and DNA complementation studies. *Nucleosides & Nucleotides*.18 (1999): 1409-1411.
- [25] Sharma, N.; and Ganesh, K.N. Expanding the repertoire of pyrrolidyl PNA analogues for DNA/RNA hybridization selectivity: aminoethylpyrrolidinone PNA (*aepone-PNA*). *Chem. Commun.* (2003): 2484-2485.
- [26] Shirude, P. S.; Kumar, V. A.; and Ganesh, K. N. (2*S*,5*R*/2*R*,5*S*)-Aminoethylpipercolyl *aepip-aegPNA* chimera: synthesis and duplex/triplex stability. *Tetrahedron.* 60 (2004): 9485-9491.
- [27] Govindaraju, T.; and Kumar, V. A. Backbone extended pyrrolidine PNA (*bepPNA*): a chiral PNA for selective RNA recognition. *Tetrahedron.* 62 (2006): 2321-2330.
- [28] Kumar, V. A.; and Ganesh, K.A. Conformationally constrained PNA analogues: structure evolution toward DNA/RNA binding selectivity. *Acc. Chem. Res.* 38 (2005): 404-412.
- [29] Suparpprom, C.; Srisuwannaket, C.; Sangvanich, P.; and Vilaivan, T. Synthesis and oligodeoxynucleotide binding properties of pyrrolidinyl peptide nucleic acids bearing prolyl-2-aminocyclopentanecarboxylic acid (ACPC) backbones. *Tetrahedron Lett.* 46 (2005): 2833-2837.
- [30] Norden, B.; and Ray, A. Peptide Nucleic Acid (PNA): Its medical and biotechnical applications and promise for the Future. *FASEB J.* 14 (2000): 1041-1059.

- [31] Knudsen, H.; and Nielsen, P. E. Antisense properties of duplex- and triplex-forming PNAs. Nucleic Acids Res. 24 (1996): 494-500.
- [32] Braasch, D. A.; and Corey, D. R. Novel antisense and peptide nucleic acid strategies for controlling gene expression. Biochemistry. 42 (2002): 4503-4510.
- [33] Suparpprom, C. Synthesis and nucleic acid binding properties of novel peptide nucleic acids carrying beta amino acid spacer. Doctoral dissertation, Department of Chemistry, Graduated School, Chulalongkorn University, 2006.
- [34] Doyle, D. F.; Braasch, D. A.; Simmons, C. G.; Janowski, B. A.; and Corey, D. R. Inhibition of gene expression inside cells by peptide nucleic acids: effect of mRNA target sequence, mismatched bases, and PNA length. Biochemistry. 40 (2001): 53-64.
- [35] Pooga, M.; Ursel, S.; Hallbrink, M.; Valkna, A.; Saar, K.; Rezaei, K.; Kahl, U.; Hao, J. K.; Xu, X. J.; Wiesenfeld-Hallin, Z.; Hokfelt, T.; Bartfai, T.; and Langel, U. Cell penetrating PNA constructs regulate galanin receptor levels and modify pain transmission *in vivo*. Nat. Biotechnol. 16 (1998): 857-861.
- [36] Branden, L. J.; Mohamed, A. J.; and Smith, C. I. E. A peptide nucleic acid-nuclear localization signal fusion that mediates nuclear transport of DNA. Nat. Biotechnol. 17 (1999): 784-787.
- [37] Dias, N.; Dheur, S.; Nielsen, P.E.; Gryaznov, S.; van Aerschot, A.; Herdewijn, P.; Helene, C.; and Saison-Behmoaras, T. E. Antisense PNA tridecamers targeted to the coding region of Ha- mRNA arrest polypeptide chain elongation. J. Mol. Biol. 294 (1999): 403-416.
- [38] Tyler, B. M.; Jansen, K.; McCormick, D. C. L.; Boules, M.; Stewart, J. A.; Zhao, L.; Lacy, B.; Cusack, B.; Fauq, A.; and Richelson, E. Peptide nucleic acids targeted to the neurotensin receptor and administered i.p. cross the blood-brain barrier and specifically reduce gene expression. Proc. Natl. Acad. Sci. USA. 96 (1999): 7053-7058.
- [39] Obika, S.; Nanbu, D.; Hari, Y.; Andoh, J.; Morio, K.; Doi, T.; and Imanishi, T. Stability and structural features of the duplexes containing nucleoside analogues with a fixed N-type conformation, 2'-O,4'-C-methylene ribonucleosides. Tetrahedron Lett. 39 (1998): 5401-5404.

- [40] Good, L.; and Nielsen, P. E. Inhibition of translation and bacterial cell growth by peptide nucleic acid targeted to ribosomal RNA. Proc. Natl. Acad. Sci USA. 95 (1998): 2073-2075.
- [41] Good, L.; and Nielsen, P. E. Antisense inhibition of gene expression in bacteria by PNA targeted to mRNA. Nat. Biotechnol. 16 (1998): 355-358.
- [42] Wang, B.; and Kuramitsu, H. K. Inducible antisense RNA expression in the characterization of gene functions in *Streptococcus* mutants. Infect Immun. 73 (2005): 3568-3576.
- [43] Ji, Y.; Zhang, B.; Van, S. F.; Horn; Warren, P.; Woodnutt, G.; Burnham, M. K.; and Rosenberg, M. Identification of critical staphylococcal genes using conditional phenotypes generated by antisense RNA. Science. 293 (2001): 2266-2269.
- [44] Good, L. Antisense antibacterials. Exp. Opin. Ther. Patents. 12 (2002): 1173-1179.
- [45] Lundin, K. E.; Good, L.; Stromberg, R.; Graslund, A.; and Smith, C. L. Biological activity and biotechnological aspects of peptide nucleic acid. Adv. Genet. 56 (2006): 1-51.
- [46] Murphy, P.; Muratovska, A.; Lightowers, R.; Taylor, R.; Turnbull, D.; Smith, R.; Wilce, J.; and Martin, S. Targeting peptide nucleic acid (PNA) oligomers to mitochondria within cells by conjugation to lipophilic cations: implications for mitochondria DNA replication, expression and disease. Nucleic Acids Res. 29 (2001): 1852-1863.
- [47] Langel. U. Cell-penetrating peptides: processes and applications, pp 424: CRC press, 2002.
- [48] Vives, E. Present and future of cell-penetrating peptide mediated delivery system: "is the Trojan horse too wild to go only to Troy?" J. Control. Release. 109 (2005): 77-85.
- [49] Leonetti, J. P.; Degols, G.; and Lebleu, B. Biological activity of oligonucleotide-poly(L-lysine) conjugates: mechanism of cell uptake. Bioconjugate Chem. 1 (1990): 149-153.
- [50] Mitchell, D. J.; Kim, D. T.; Steinman, L.; Fathman, C. G.; and Rothbard, J. B. Polyarginine enters cells more efficiently than other polycationic homopolymers. J. Pept. Res. 56 (200): 318-325.

- [51] Tan, X. X.; Actor, J. K.; and Chen, Y. Peptide nucleic acid antisense oligomer as a therapeutic mouse intraperitoneal infection. Antimicrob Agents Chemother. 49 (2005): 3203-3207.
- [52] Available from: http://en.wikipedia.org/wiki/Cell_penetrating_peptide [2009, February 5]
- [53] Good, L.; Awasthi, S. K.; Dryselius, R.; Larsson, O.; and Nielsen, P. E. Bactericidal antisense effects of peptide-PNA conjugates. Nat. Biotechnol. 19 (2001): 360-364.
- [54] Petersen, L.; de Koning, M. C.; van Kuik-Romeijn, P.; Weterings, J.; Pol, C. J.; Platenburg, G.; Overhand, M.; van der Marel, G. A.; and van Boom, J. H. Synthesis and *in vitro* evaluation of PNA-peptide-DETA conjugates as potential cell penetrating artificial ribonucleases. Bioconjugate chem. 15 (2004): 576-582.
- [55] Nekhotiaeva, N.; Awasthi, S. K.; Nielsen, P. E.; and Good, L. Inhibition of *Staphylococcus aureus* gene expression and growth using antisense peptide nucleic acids. Mol. ther. 4 (2004): 652-659.
- [56] Bendifallah, N.; Rasmussen, F. W.; Zachar, V.; Ebbesen, P.; Nielsen, P. E.; and Koppelhus, U. Evaluation of cell-penetrating peptides (CPPs) as vehicles for intracellular delivery of antisense peptide nucleic acid (PNA). Bioconjugate chem. 17 (2006): 750-758.
- [57] Daniels, D. S.; and Schepartz, A. Intrinsically cell-permeable miniature proteins based on a minimal cationic PPII motif. J. Am. Chem. Soc. 2007, 129 (2007): 14578-14579.
- [58] Zhou, P.; Wang, M.; Du, L.; Fisher, G. W.; Waggoner, A.; and Ly, D. H. Novel binding and efficient cellular uptake of guanidine-based peptide nucleic acids (GPNA). J. Am. Chem. Soc. 125 (2003): 6878-6879.
- [59] Dietz, G. P.; and Bahr, M. Delivery of bioactive molecules into the cell: the Trojan horse approach. Mol. Cell. Neurosci. 27 (2004): 85-131.
- [60] Fawell, S.; Seery, J.; Daikh, Y.; Moore, C.; Chen, L. L.; Pepinsky, B.; and Barsoum, J. Tat-mediated delivery of heterologous proteins into cells. Proc. Natl. Acad. Sci. USA. 92 (1994): 664-668.
- [61] Anderson, D. C.; Nichols, E.; Manger, R.; Woodle, D.; Barry, M.; and Fritzberg, A. R. Tumor cell retention of antibody Fab fragments is enhanced by an

- attached HIV TAT protein-derived peptide. Biochem. Biophys. Res. Commun. 194 (1993): 876-884.
- [62] Vives, E.; Brodin, P.; and Lebleu, B. A truncated HIV-1 Tat protein basic domain rapidly translocates through the plasma membrane and accumulates in the cell nucleus. J. Biol. Chem. 272 (1997): 16010-16017.
- [63] Shen, W. C.; and Ryser, H. J. Conjugation of poly-L-lysine to albumin and horseradish peroxidase: a novel method of enhancing the cellular uptake of proteins. Proc. Natl. Acad. Sci. USA. 75 (1978): 1872-1876.
- [64] Shen, W. C.; Ryser, H. J. Poly (L-lysine) and poly (D-lysine) conjugates of methotrexate: different inhibitory effect on drug resistant cells. Mol. Pharmacol. 16 (1979): 614-622.
- [65] Futaki, S.; Suzuki, T.; Ohashi, W.; Yagami, T.; Tanaka, S.; Ueda, K.; and Sugiura, Y. Arginine-rich peptides. An abundant source of membrane-permeable peptides having potential as carriers for intracellular protein delivery. J. Biol. Chem. 276 (2001): 5836-5840.
- [66] Mehiri, M.; Caldarelli, S.; Giorgio, A. D.; Barouillet, T.; Doglio, A.; Condom, R.; and Patino, N. A "ready-to-use" fluorescent-labelled-cysteine-TBTP (4-thiobutyltriphenylphosphonium) synthon to investigate the delivery of non-permeable PNA (peptide nucleic acids)-based compounds to cells. Bioorg. chem. 35 (2007): 313-326.
- [67] Le Place, P, R.; Umezawa, N.; Lee, H.-S.; and Gellman, S. H. An efficient route to either enantiomer of *trans*-2-aminocyclopentanecarboxylic acid. J. Org. Chem. 66 (2001): 5629-5632.
- [68] Kanjanawarut, R. Synthesis of gold nanoparticles modified with polyamide nucleic acids. Master's Thesis, Department of Petrochemistry and Polymer Science, Graduate School, Chulalongkorn University, 2007.
- [69] Srisuwannaket, C. Synthesis and DNA-binding properties of pyrrolidinyl peptide nucleic acids bearing (1S, 2S)-2-aminocyclopentane carboxylic acids spacer. Doctoral dissertation, Department of Chemistry, Graduate School, Chulalongkorn University, 2005.
- [70] Haralambidis, J.; Tregear, G.; and Ede, N. Routine preparation of thiol oligonucleotides: application to the synthesis of oligonucleotide-peptide hybrids. Bioconjugate Chem. 5 (1994): 373-378.

- [71] Korkaew, P. Solid-phase capture of PNA-DNA hybrids for determination of DNA base sequences. Master's Thesis, Department of Chemistry, Graduate School, Chulalongkorn University, 2007.
- [72] Vilaivan, T.;Lowe, G., A novel pyrrolidiny PNA showing high sequence specificity and preferential binding to DNA over RNA. J. Am. Chem. Soc. **2004**, 124(32), 9326-9327.
- [73] Ngamviriyavong, P. Synthesis of peptide nucleic acid containing aminoethyl linker. Master's Thesis, Department of Chemistry, Graduate School, Chulalongkorn University, 2004.
- [74] Boontha, B., Development of DNA sequence analysis using PNA probe and MALDI-TOF mass spectrometry. Doctoral dissertation, Department of Chemistry, Graduate School, Chulalongkorn University.
- [75] Boontha, B.; Nakkuntod, J.; Hirankarn, N.; Chaumpluk, P.; and Vilaivan, T. Multiplex mass spectrometric genotyping of single nucleotide polymorphisms employing pyrrolidiny peptide nucleic acid in combination with ion-exchange capture. Anal Chem. 80 (2008): 817-8186.
- [76] Walsh, A.G.; Matewish, M. J.; Burrows, L. L.; Monteiro, M. A.; Perry, M. B.; and Lam, J. S. Lipopolysaccharide core phosphates are required for viability and intrinsic drug resistance in *Pseudomonas aeruginosa*. Mol. Microbiol. 35 (2000): 718-727.
- [77] Available from: <http://www.pseudomonas.com/> [2009, February 11]
- [78] Lilley, D. M. J. Methods in Enzymology, DNA structures part A: synthesis and physical analysis of DNA, pp 389-405. New York: Academic press, 1992.
- [79] Koppelhus, U.; and Nielsen, P.E. Cellular delivery of peptide nucleic acid (PNA). Adv. Drug Deliv. Rev. 10 (2003): 267-280.
- [80] Rasmussen, L. C. V.; Sperling-Petersen, H. U.; and Mortensen, K. K. Hitting bacteria at the heart of the central dogma: sequence-specific inhibition. Microb. Cell Fact. 6 (2007): 24.
- [81] Wolf, Y.; Pritz, S.; Abes, S.; Bienert, M.; Lebleu, B.; and Oehlke, J. Structural requirements for cellular uptake and antisense activity of peptide nucleic acids conjugated with various peptides. Biochemistry. 45 (2006): 14944-14954.
- [82] Demidov, V. V.; Potaman, V. N.; Frank-Kamenetskii, M. D.; Egholm, M.; Buchard, O.; Sönnichsen, S. H.; and Nielsen, P. E. Stability of peptide

nucleic acids in human serum and cellular extracts. Biochem. pharmacol. 48 (1994): 1310-1313.

[83] Available from: http://en.wikipedia.org/wiki/Enzyme_unit [2009, February 11]



ศูนย์วิทยทรัพยากร
จุฬาลงกรณ์มหาวิทยาลัย



APPENDICES

ศูนย์วิทยทรัพยากร
จุฬาลงกรณ์มหาวิทยาลัย

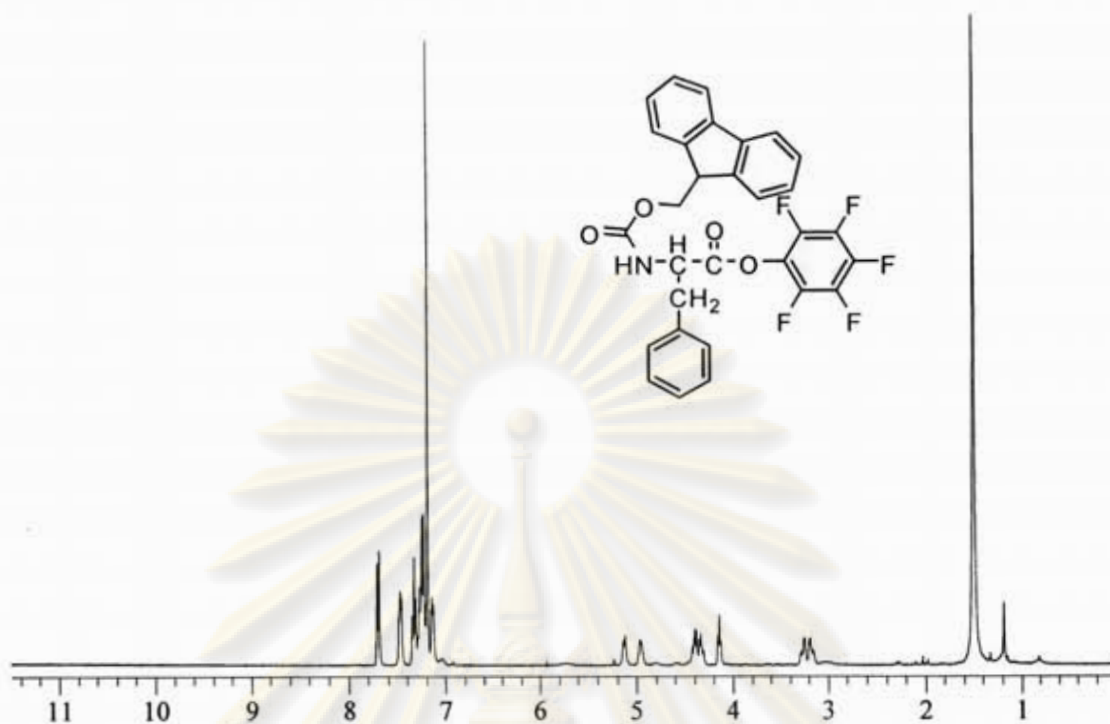


Figure A-1: ¹H NMR spectrum of (N-Fluoren-9-ylmethoxycarbonyl)-L-phenylalanine pentafluorophenyl ester (1)

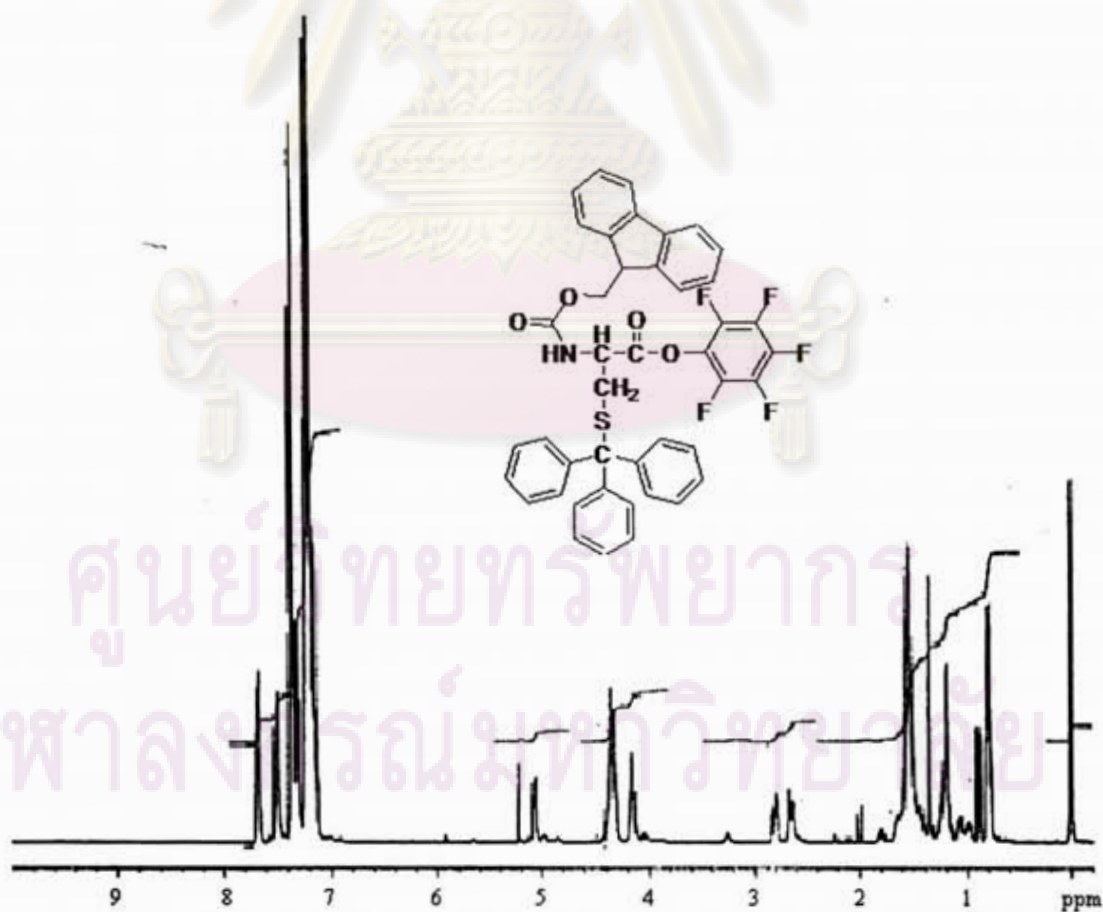


Figure A-2: ¹H NMR spectrum of (N-Fluoren-9-ylmethoxycarbonyl)-S-trityl-L-cysteine pentafluorophenyl ester (2)

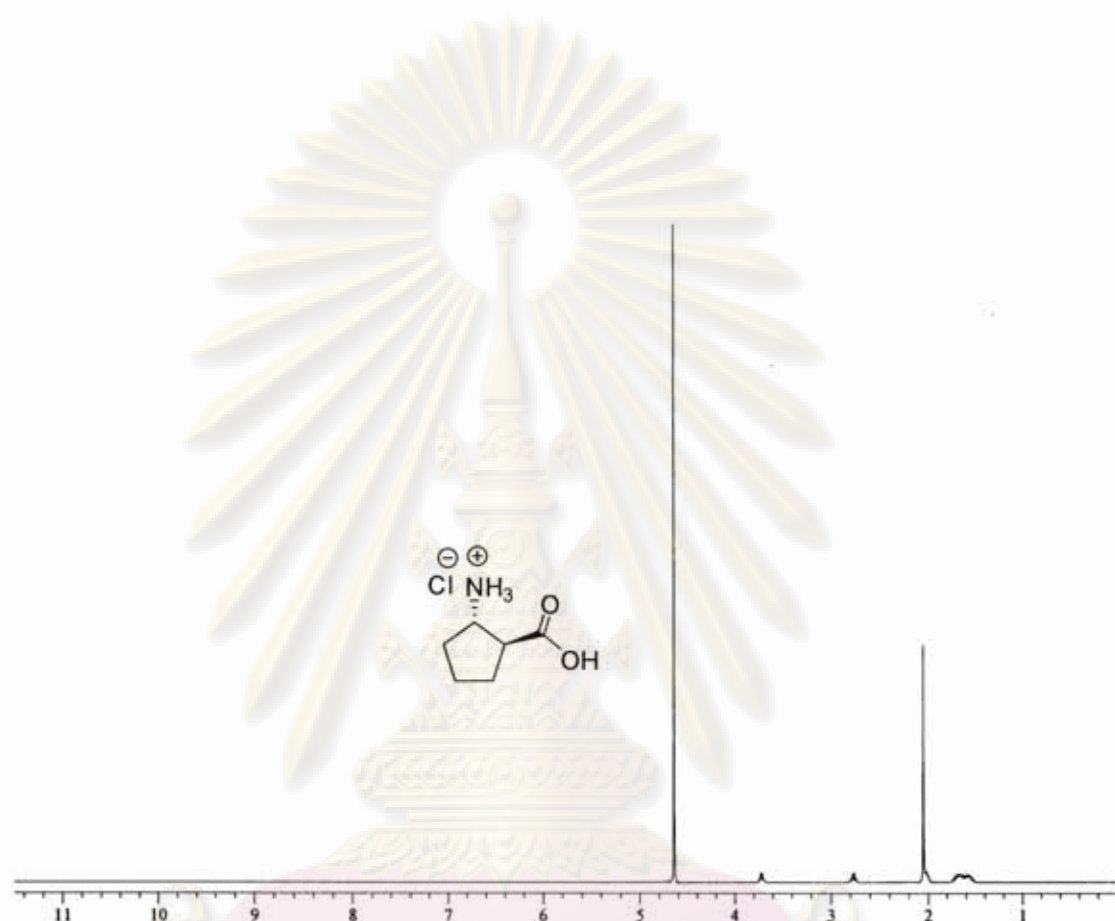


Figure A-3: ^1H NMR spectrum of Ethyl (1*S*, 2*S*)-2-amino-cyclopentanecarboxylate hydrochloride (5)

ศูนย์วิทยทรัพยากร
จุฬาลงกรณ์มหาวิทยาลัย

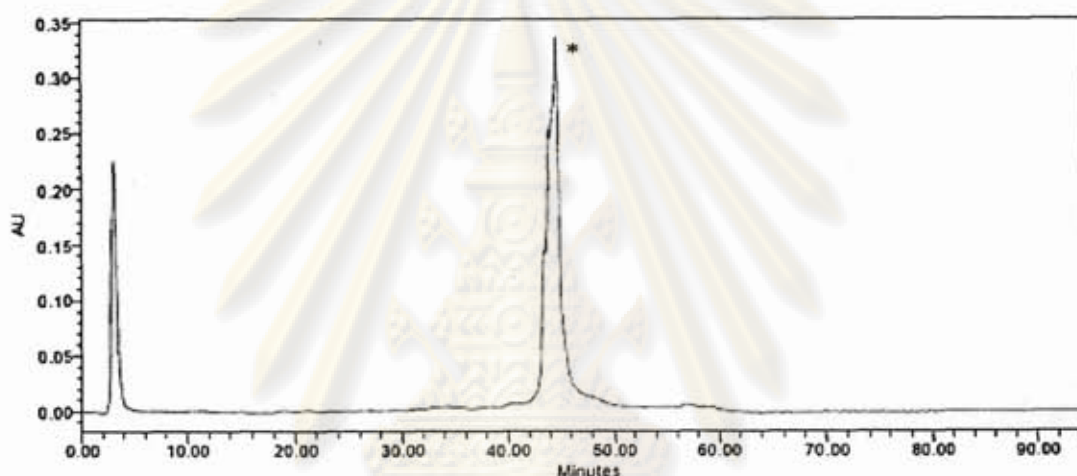


Figure B-1: HPLC chromatogram of Flu-O-TTT-RRRRRRRRRR-NH₂ (Flu-T₃-R₁₀: P5): 260 nm Conditions for reverse-phase HPLC: C-18 column 3 μ m particle size 4.6 \times 50 mm; gradient system of 0.01% TFA in MeOH/water 20:80 to 80:20 in 60 min; hold time 5 min.

* indicated the desired product. (for all graphs)

ศูนย์วิทยทรัพยากร
จุฬาลงกรณ์มหาวิทยาลัย

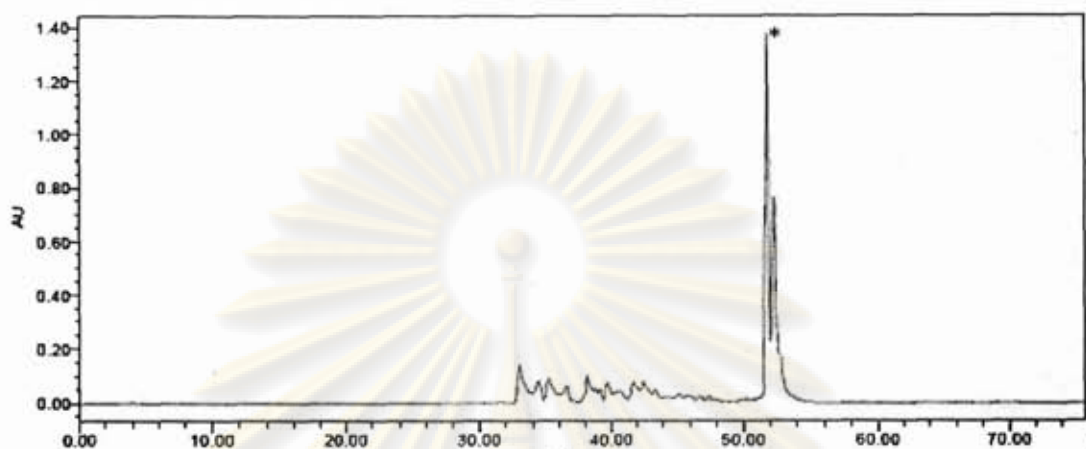


Figure B-2: HPLC chromatogram of H-KFFKFFKFFK-O-TTT-Lys(Flu)-NH₂ (KFF-T₃-Flu: P8): 260 nm. Conditions for reverse-phase HPLC: C-18 column 3 μ m particle size 4.6 \times 50 mm; gradient system of 0.01% TFA in MeOH/water 20:80 to 80:20 in 60 min; hold time 5 min.

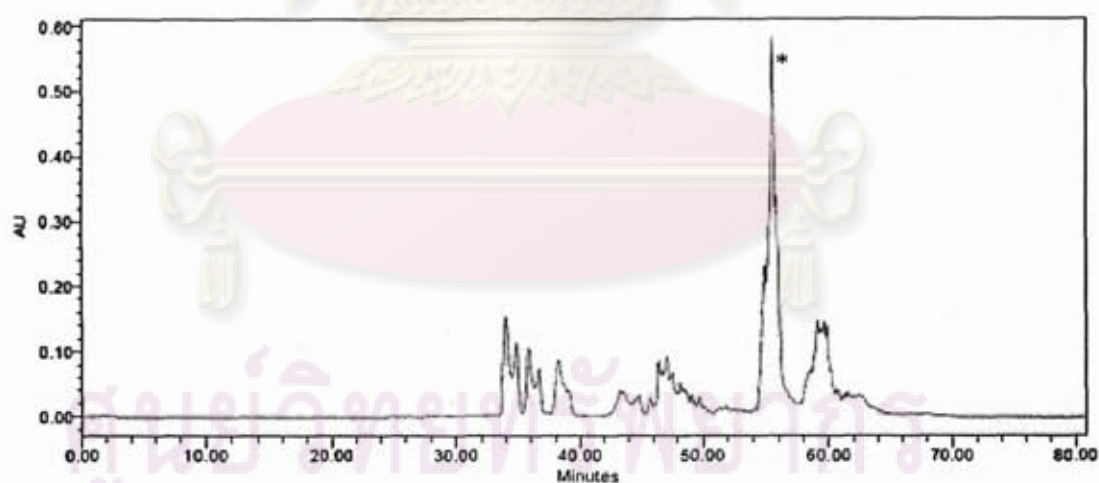


Figure B-3: HPLC chromatogram of H-KFFKFFKFFK-O-TTT-Lys(Flu)-NH₂ (KFF-T₃-Flu: P8): 440 nm. Conditions for reverse-phase HPLC: C-18 column 3 μ m particle size 4.6 \times 50 mm; gradient system of 0.01% TFA in MeOH/water 20:80 to 80:20 in 60 min; hold time 5 min.

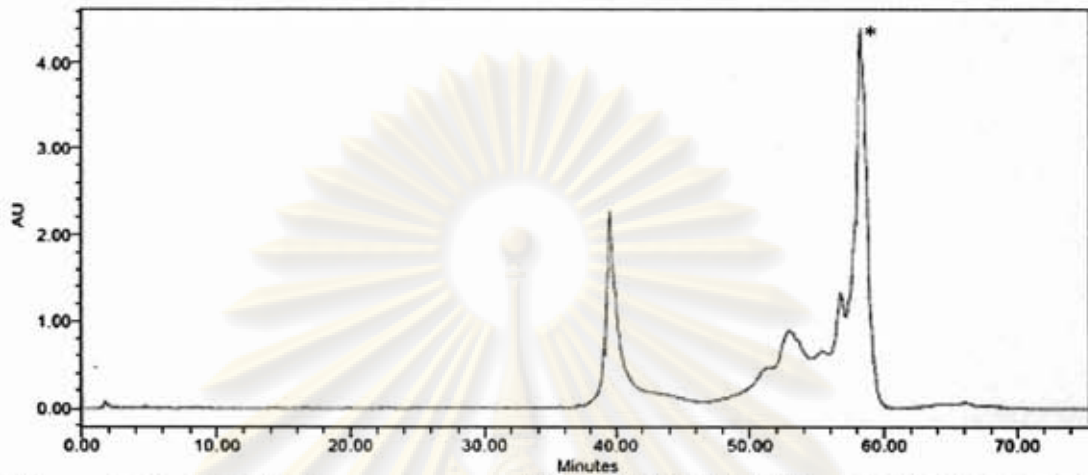


Figure B-4: HPLC chromatogram of Flu-O-TTTTTTTT-O-KFFKFFKFFK-NH₂ (Flu-T₉-KFF: P9): 260 nm. Conditions for reverse-phase HPLC: C-18 column 3 μm particle size 4.6 × 50 mm; gradient system of 0.01% TFA in MeOH/water 20:80 to 80:20 in 60 min; hold time 5 min.

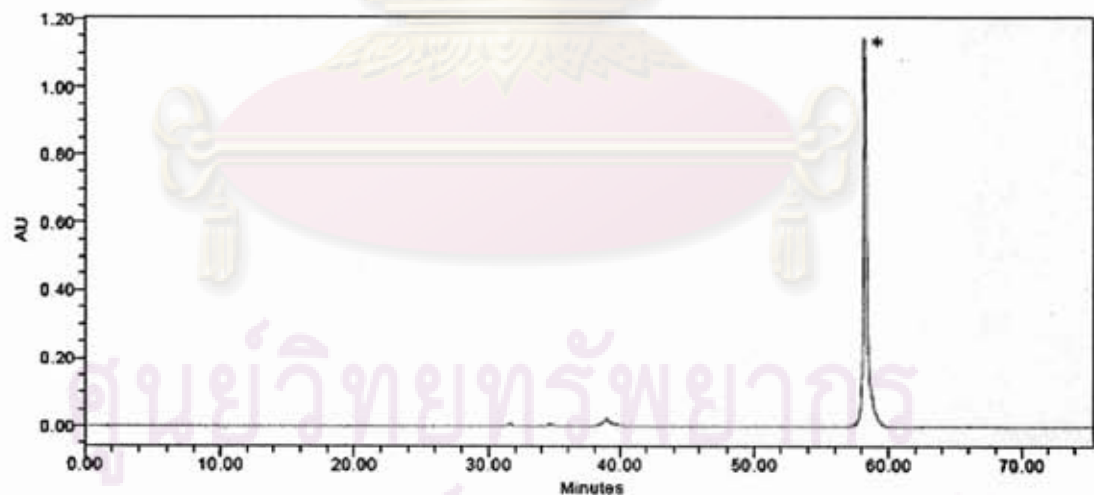


Figure B-5: HPLC chromatogram of Flu-O-TTTTTTTT-O-KFFKFFKFFK-NH₂ (Flu-T₉-KFF: P9): 440 nm. Conditions for reverse-phase HPLC: C-18 column 3 μm particle size 4.6 × 50 mm; gradient system of 0.01% TFA in MeOH/water 20:80 to 80:20 in 60 min; hold time 5 min.

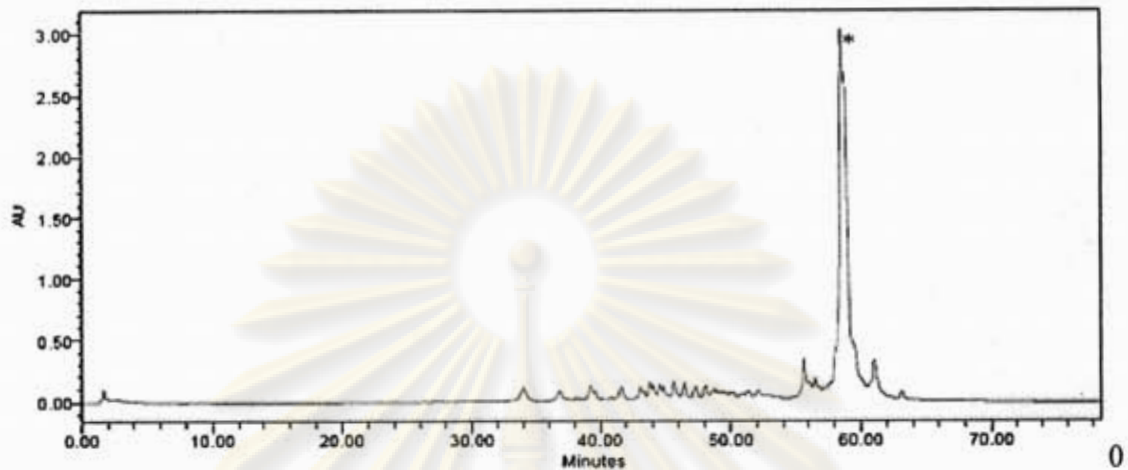


Figure B-6: HPLC chromatogram of H-KFFKFFKFFK-O-TTTTTTTT-Lys(Flu)-NH₂ (KFF-T₉-Flu: P10): 260 nm. Conditions for reverse-phase HPLC: C-18 column 3 μ m particle size 4.6 \times 50 mm; gradient system of 0.01% TFA in MeOH/water 20:80 to 80:20 in 60 min; hold time 5 min.

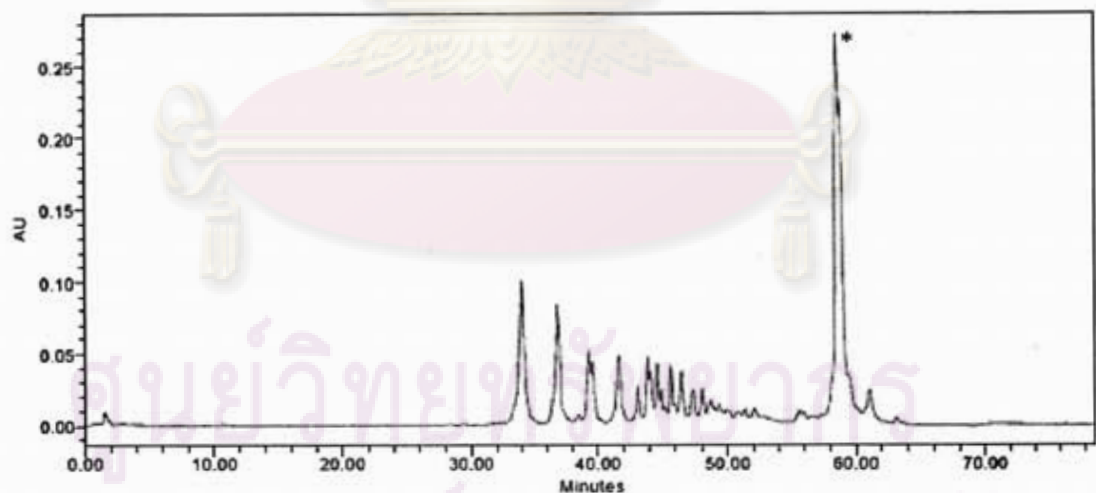


Figure B-7: HPLC chromatogram of H-KFFKFFKFFK-O-TTTTTTTT-Lys(Flu)-NH₂ (KFF-T₉-Flu: P10): 440 nm. Conditions for reverse-phase HPLC: C-18 column 3 μ m particle size 4.6 \times 50 mm; gradient system of 0.01% TFA in MeOH/water 20:80 to 80:20 in 60 min; hold time 5 min.

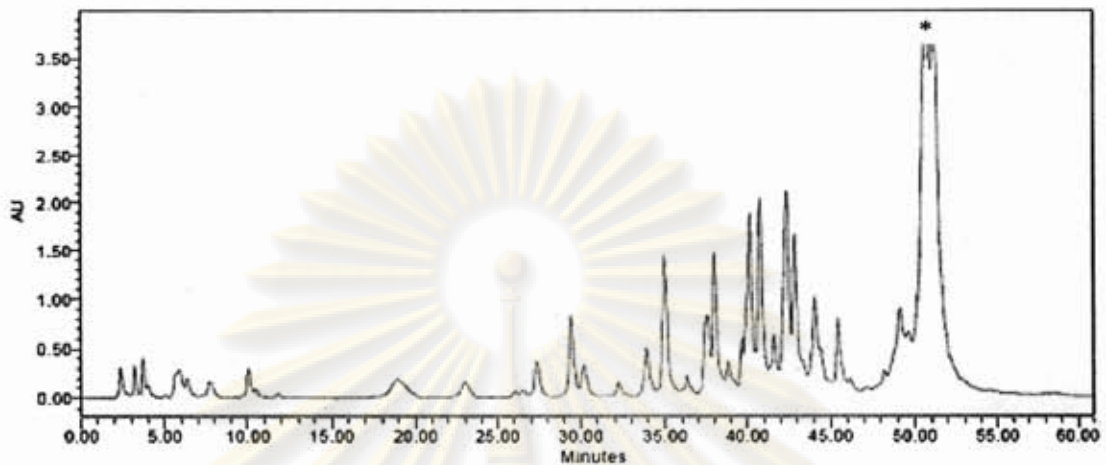


Figure B-8: HPLC chromatogram of Flu-O-TTTTTTTTT-Lys-NH₂ (Flu-T₉-K: P11): 260 nm. Conditions for reverse-phase HPLC: C-18 column 3 μ m particle size 4.6 \times 50 mm; gradient system of 0.01% TFA in MeOH/water 20:80 to 80:20 in 60 min; hold time 5 min.

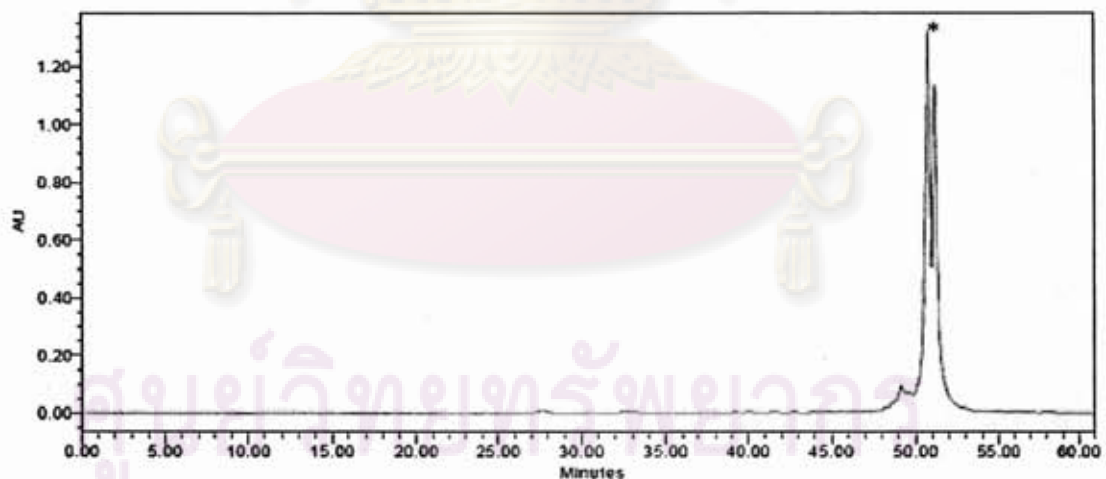


Figure B-9: HPLC chromatogram of Flu-O-TTTTTTTTT-Lys-NH₂ (Flu-T₉-K: P11): 440 nm. Conditions for reverse-phase HPLC: C-18 column 3 μ m particle size 4.6 \times 50 mm; gradient system of 0.01% TFA in MeOH/water 20:80 to 80:20 in 60 min; hold time 5 min.

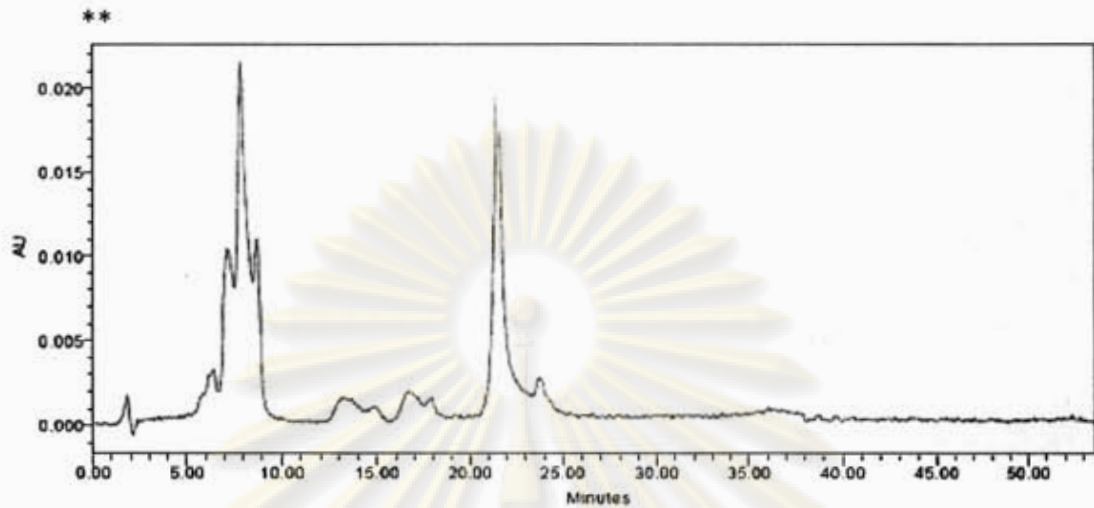


Figure B-10: HPLC chromatogram of Flu-O-TCATGAGGCCT-O-KFFKFFKFFK-NH₂ (Flu-anti-KFF: P12): 260 nm. Conditions for reverse-phase HPLC: C-18 column column 3 μ m particle size 4.6 \times 50 mm; gradient system of 0.01% TFA in MeOH/water 20:80 to 80:20 in 60 min; hold time 5 min.

** No purified product could be obtained.

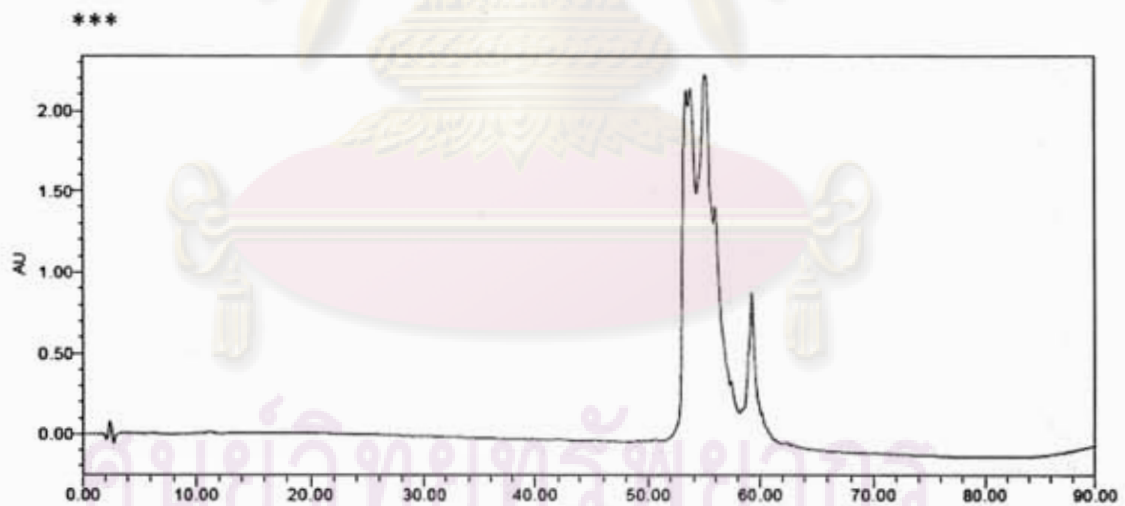


Figure B-11: HPLC chromatogram of Bz-O-TCATGAGGCCT-O-KFFKFFKFFK-NH₂ (Bz-anti-KFF: P13): 260 nm. Conditions for reverse-phase HPLC: C-18 column column 3 μ m particle size 4.6 \times 50 mm; gradient system of 0.01% TFA in MeOH/water 20:80 to 80:20 in 60 min; hold time 5 min.

*** No purified product could be obtained.

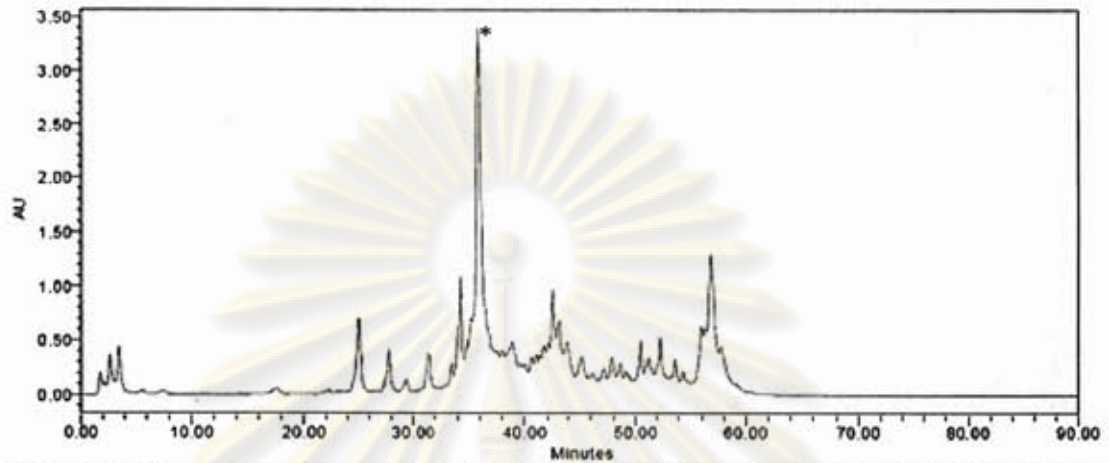


Figure B-12: HPLC chromatogram of Bz-O-KFFKFFKFFK-O-TCATGAGGCCT-NH₂ (Bz-KFF-anti: P16): 260 nm. Conditions for reverse-phase HPLC: C-18 column column 3 μ m particle size 4.6 \times 50 mm; gradient system of 0.01% TFA in MeOH/water 20:80 to 80:20 in 60 min; hold time 5 min.

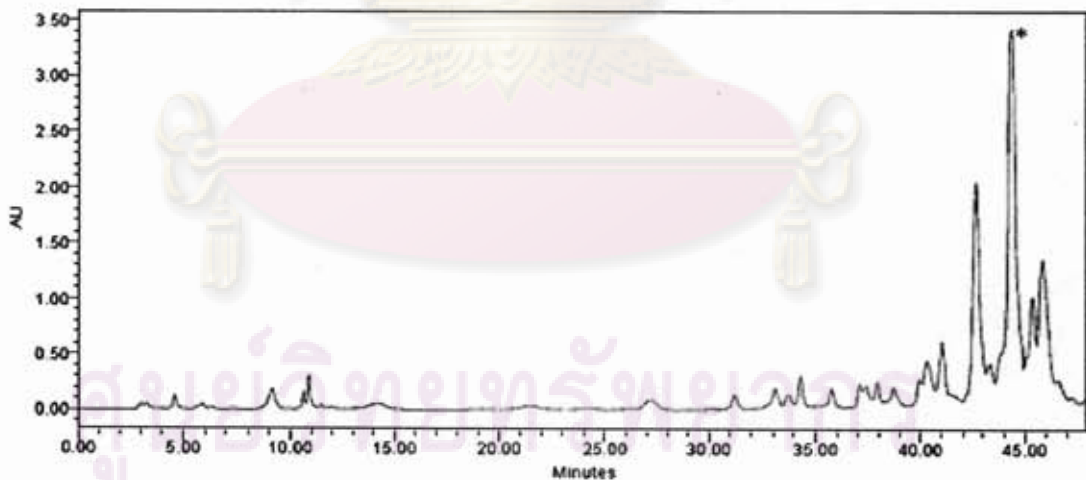


Figure B-13: HPLC chromatogram of Ac-TTTTTTTT-Lys-NH₂ (Ac-T₉-K: P17): 260 nm. Conditions for reverse-phase HPLC: C-18 column column 3 μ m particle size 4.6 \times 50 mm; gradient system of 0.01% TFA in MeOH/water 20:80 to 80:20 in 60 min; hold time 5 min.

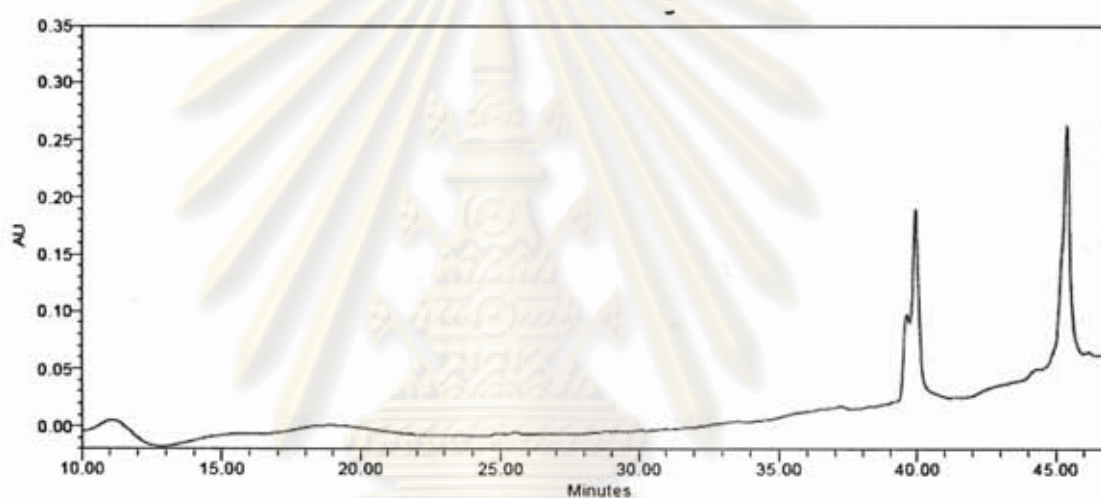


Figure B-14: HPLC chromatogram (215 nm) of the PNA-peptide mixture without proteinase K treatment. Conditions: P17 30 μ M and ACTH 4-10 100 μ M in 100 mM Tris-HCl pH 7.5 at 37° C for 1 h. Conditions for reverse-phase HPLC: C-18 column 3 μ m particle size 4.6 \times 50 mm; gradient system of 0.01% TFA in MeOH/water 10:90 to 90:10 in 60 min; hold time 5 min.

ศูนย์วิทยทรัพยากร
จุฬาลงกรณ์มหาวิทยาลัย

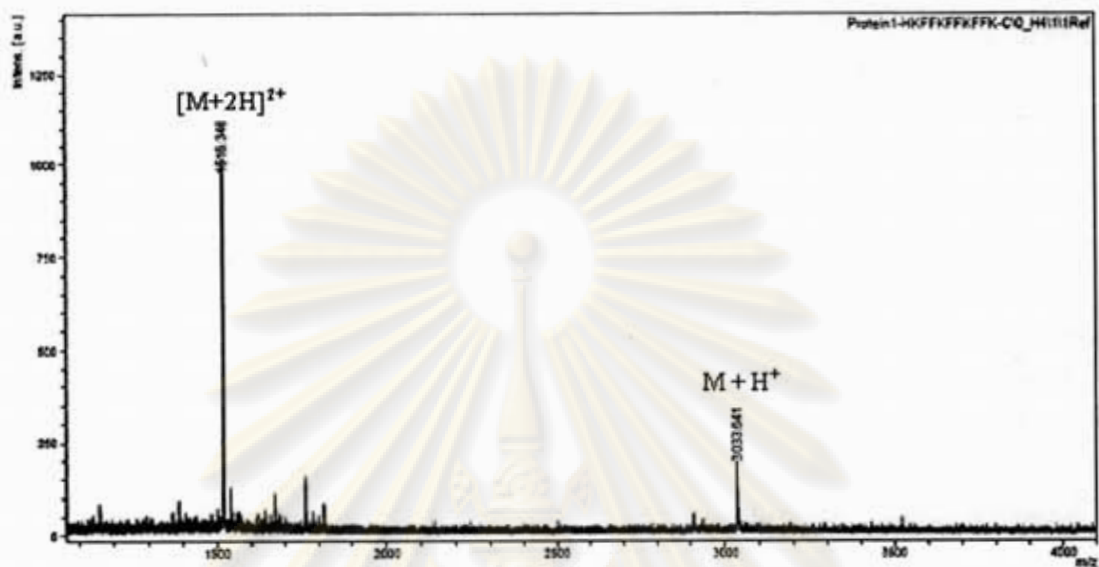


Figure C-1: MALDI-TOF mass spectrum of H-KFFKFFKFFC-NH₂ (KFF-C: P1)

$M \cdot H^+$ calcd (monomer) = 1515.8, $M \cdot H^+$ calcd (dimer) = 3031.6

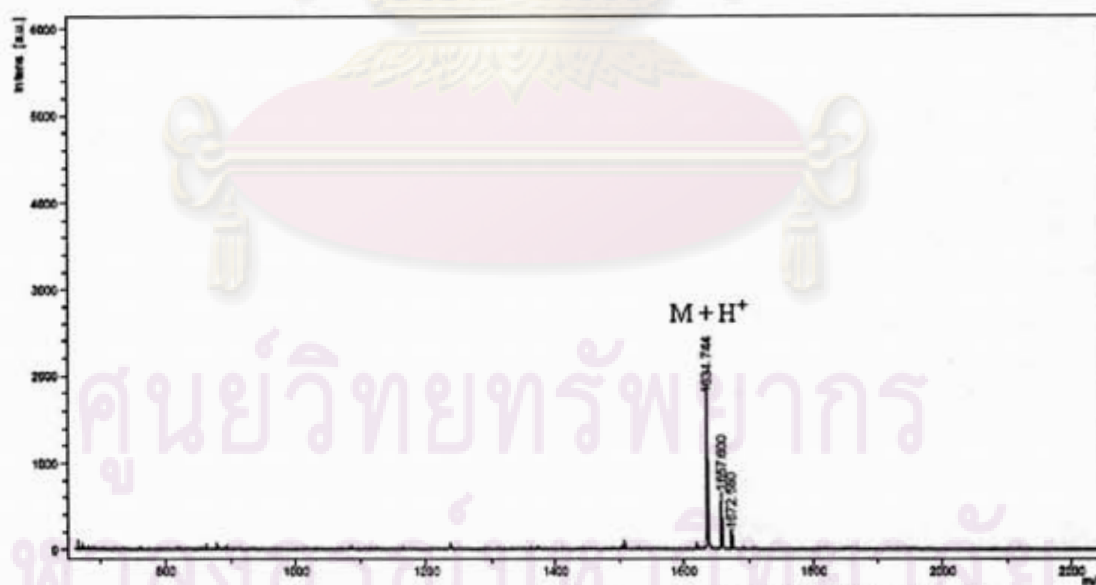


Figure C-2: MALDI-TOF mass spectrum of Fmoc-KFFKFFKFFC-NH₂ (Fmoc-KFF: P2)

$M \cdot H^+$ calcd = 1635.9

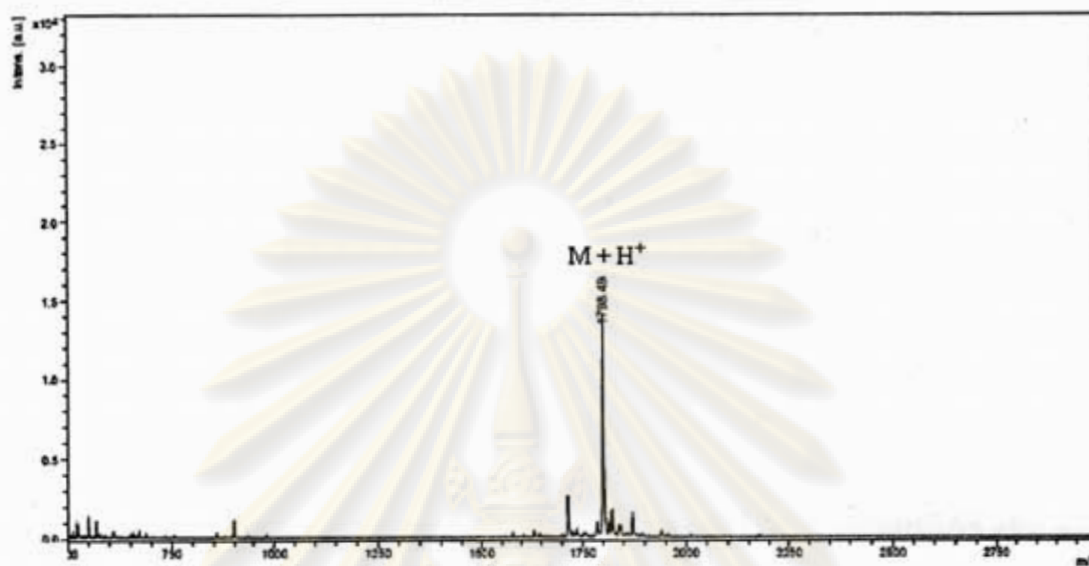


Figure C-3: MALDI-TOF mass spectrum of Fmoc-RRRRRRRRRR-NH₂ (Fmoc-R₁₀: P3) $M \cdot H^+_{\text{calcd}} = 1802.1$

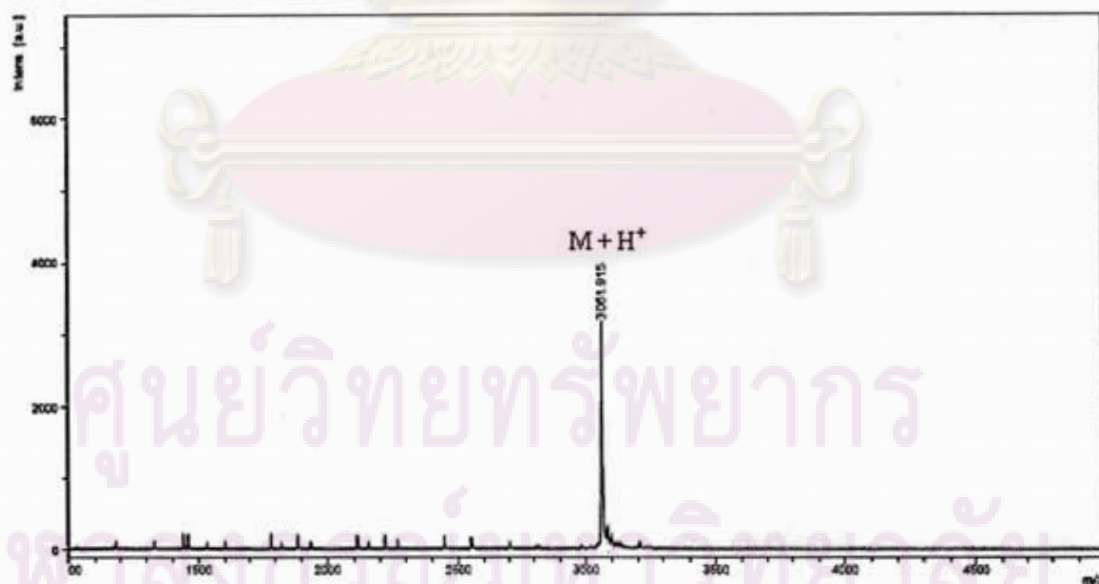


Figure C-4: MALDI-TOF mass spectrum of Flu-O-TTT-KFFKFFKFFK-NH₂ (Flu-T₃-KFF: P4) $M \cdot H^+_{\text{calcd}} = 3059.4$

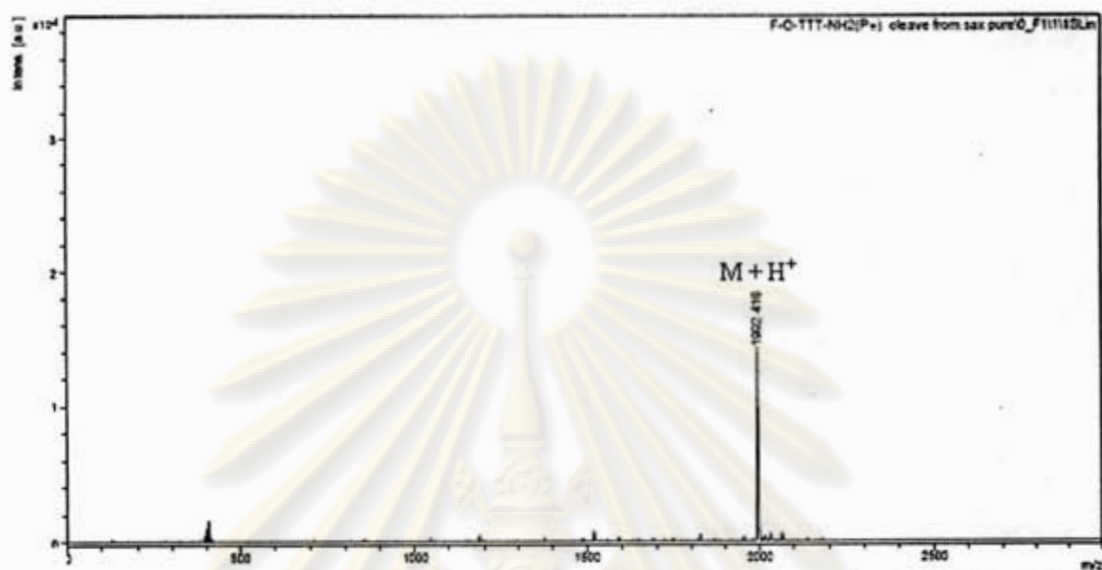


Figure C-5: MALDI-TOF mass spectrum of Flu-O-TTT-Lys(P⁺)-NH₂ (Flu-T₃-Phos: P6) $M \cdot H^+_{\text{calcd}} = 1996.7$

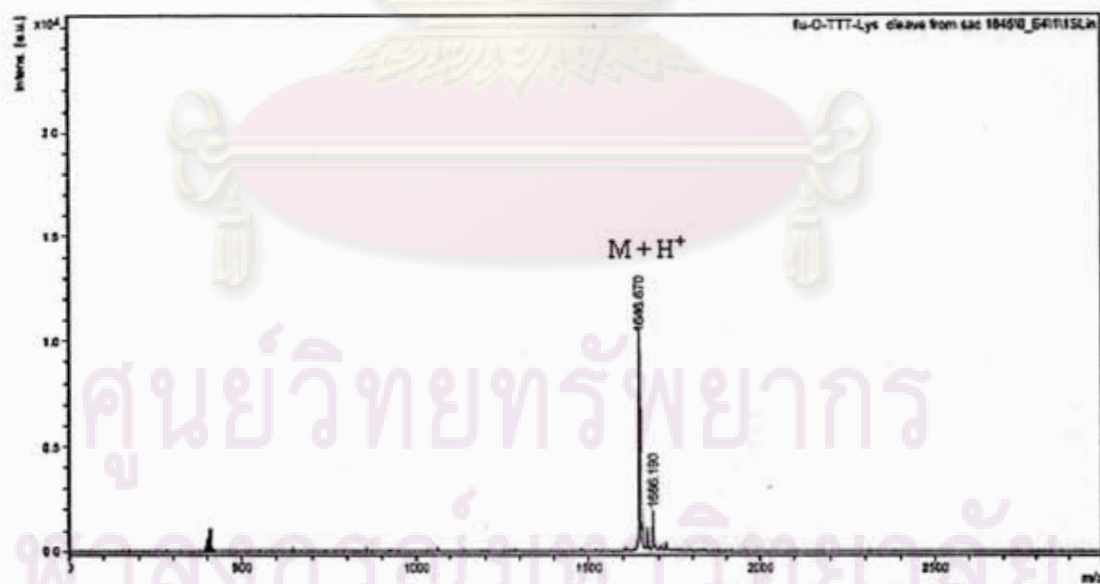


Figure C-6: MALDI-TOF mass spectrum of Flu-O-TTT-Lys-NH₂ (Flu-T₃-K: P7) $M \cdot H^+_{\text{calcd}} = 1646.7$

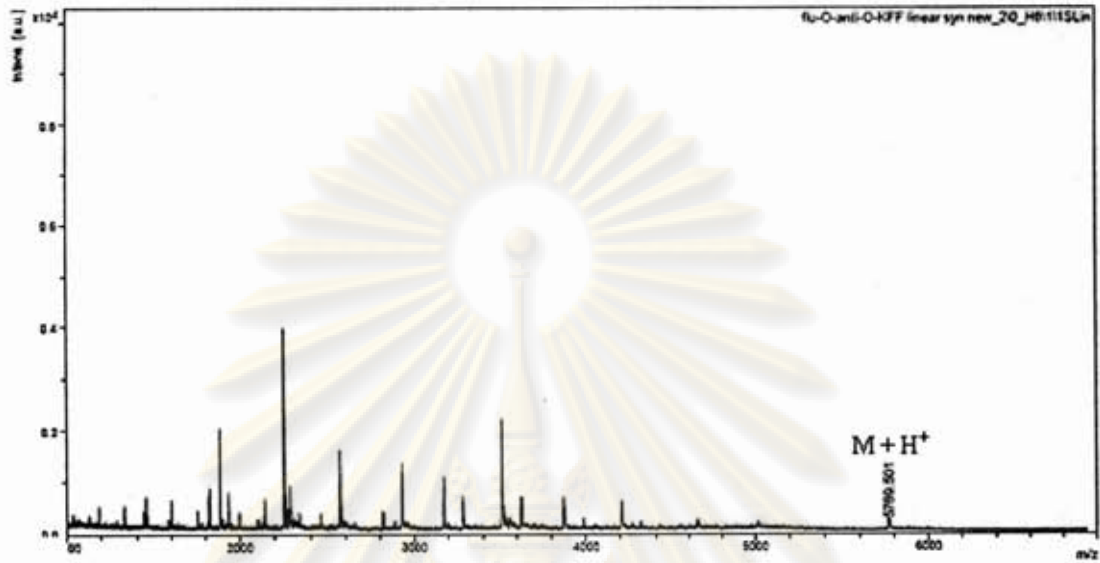


Figure C-7: MALDI-TOF mass spectrum of Flu-O-TCATGAGGCCT-O-KFFKFFKFFK-NH₂ (Flu-anti-KFF: P12) $M \cdot H^+_{\text{calcd}} = 5763.7$

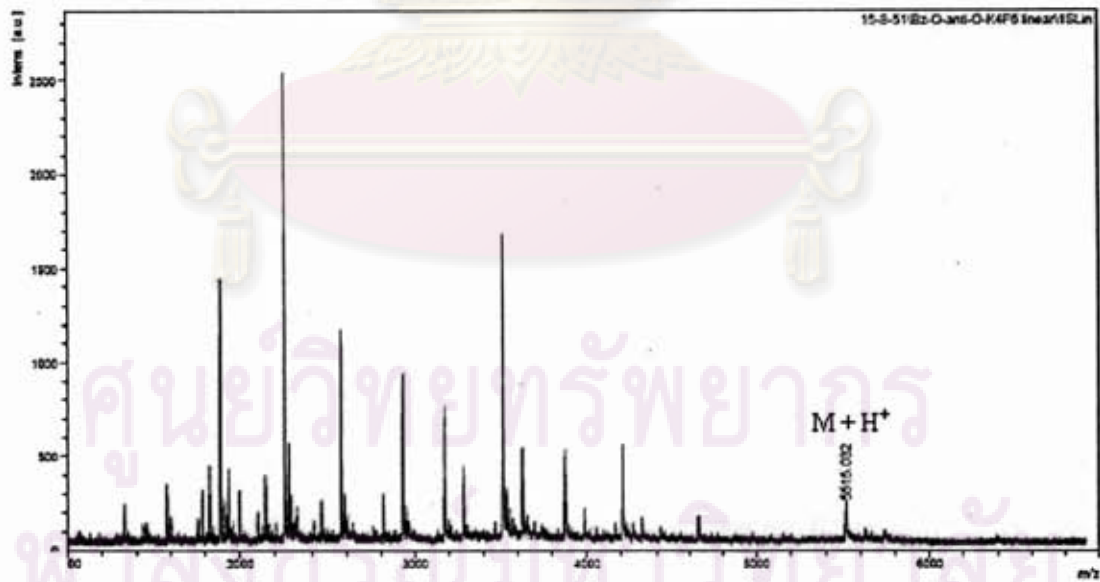


Figure C-8: MALDI-TOF mass spectrum of Bz-O-TCATGAGGCCT-O-KFFKFFKFFK-NH₂ (Bz-anti-KFF: P13) $M \cdot H^+_{\text{calcd}} = 5509.7$

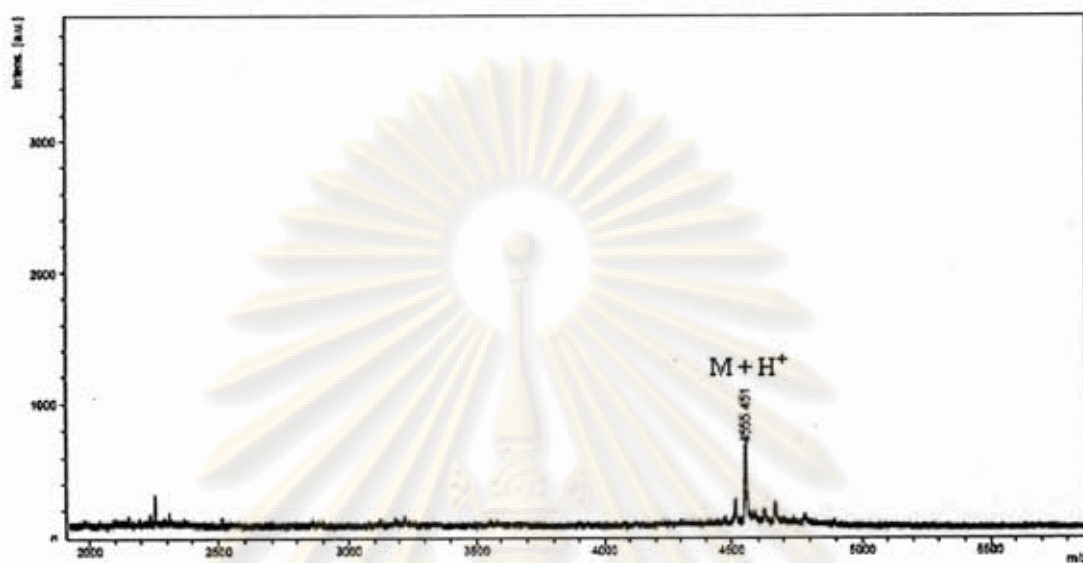


Figure C-9: MALDI-TOF mass spectrum of Flu-O-TCATGAGGCCT-Lys(P⁺)-NH₂
(Flu-anti-Phos: 14) $M \cdot H^+_{\text{calcd}} = 4556.0$

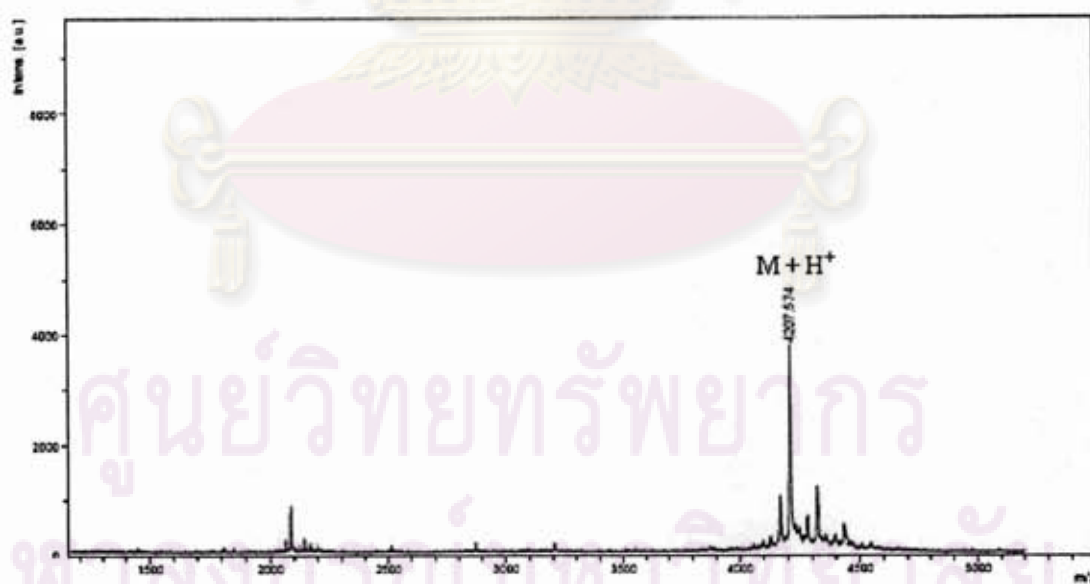


Figure C-10: MALDI-TOF mass spectrum of Flu-O-TCATGAGGCCT-Lys-NH₂
(Flu-anti-K: P15) $M \cdot H^+_{\text{calcd}} = 4207.6$

Selected example of T_m experimental data using UV analysis

Table A-1: Data from UV analysis of Flu-O-TTTTTTTTTT-O-KFFKFFKFFK- NH₂ (P9) & dA₉ at 20.0-90.0 °C

Entry	Temperature (°C)	Absorbance	Correct Temp.* (°C)	Normalized Abs.
1	20.02	0.3797	18.6	1.0000
2	21.02	0.3803	19.5	1.0016
3	22.02	0.3799	20.5	1.0005
4	23.02	0.3788	21.5	0.9975
5	24.02	0.3787	22.5	0.9973
6	25.02	0.3805	23.4	1.0019
7	26.02	0.3808	24.4	1.0027
8	27.02	0.3808	25.4	1.0028
9	28.02	0.3818	26.3	1.0054
10	29.02	0.3819	27.3	1.0057
11	30.02	0.3825	28.3	1.0072
12	31.02	0.3831	29.2	1.0088
13	32.02	0.3834	30.2	1.0095
14	33.02	0.3840	31.2	1.0113
15	34.02	0.3842	32.1	1.0118
16	35.02	0.3843	33.1	1.0120
17	36.02	0.3853	34.1	1.0145
18	37.02	0.3854	35.1	1.0148
19	38.02	0.3858	36.0	1.0159
20	39.02	0.3862	37.0	1.0171
21	40.02	0.3869	38.0	1.0189
22	41.02	0.3873	38.9	1.0199
23	42.02	0.3878	39.9	1.0213
24	43.02	0.3886	40.9	1.0234
25	44.02	0.3889	41.8	1.0242
26	45.02	0.3895	42.8	1.0258
27	46.02	0.3901	43.8	1.0272
28	47.02	0.3907	44.8	1.0288

Entry	Temperature (°C)	Absorbance	Correct Temp.* (°C)	Normalized Abs.
29	48.02	0.3913	45.7	1.0304
30	49.02	0.3918	46.7	1.0319
31	50.02	0.3925	47.7	1.0335
32	51.02	0.3930	48.6	1.0349
33	52.02	0.3935	49.6	1.0362
34	53.02	0.3945	50.6	1.0387
35	54.02	0.3951	51.5	1.0404
36	55.02	0.3957	52.5	1.0419
37	56.02	0.3965	53.5	1.0441
38	57.02	0.3969	54.4	1.0452
39	58.02	0.3974	55.4	1.0464
40	59.02	0.3980	56.4	1.0481
41	60.02	0.3987	57.4	1.0499
42	61.02	0.3994	58.3	1.0517
43	62.02	0.4001	59.3	1.0535
44	63.02	0.4006	60.3	1.0549
45	64.02	0.4013	61.2	1.0568
46	65.02	0.4021	62.2	1.0589
47	66.02	0.4028	63.2	1.0608
48	67.02	0.4037	64.1	1.0632
49	68.02	0.4044	65.1	1.0650
50	69.02	0.4054	66.1	1.0676
51	70.02	0.4064	67.1	1.0703
52	71.02	0.4074	68.0	1.0730
53	72.02	0.4087	69.0	1.0762
54	73.02	0.4099	70.0	1.0793
55	74.02	0.4112	70.9	1.0829
56	75.02	0.4126	71.9	1.0865
57	76.02	0.4142	72.9	1.0907
58	77.02	0.4157	73.8	1.0948
59	78.02	0.4175	74.8	1.0996

Entry	Temperature (°C)	Absorbance	Correct Temp.* (°C)	Normalized Abs.
60	79.02	0.4193	75.8	1.1040
61	80.02	0.4210	76.7	1.1086
62	81.02	0.4226	77.7	1.1130
63	82.02	0.4243	78.7	1.1174
64	83.02	0.4258	79.7	1.1214
65	84.02	0.4272	80.6	1.1249
66	85.02	0.4284	81.6	1.1282
67	86.02	0.4293	82.6	1.1304
68	87.02	0.4303	83.5	1.1331
69	88.02	0.4308	84.5	1.1344
70	89.02	0.4315	85.5	1.1364
71	90.02	0.4317	86.4	1.1369

* The corrected temp. equation was obtained by measuring the actual temp. in the cuvette using a temperature probe and plotting against the set temperature (T_{block}) from 20-90 °C. A linear relationship was gained by $T_{\text{actual}} = 0.9696T_{\text{block}} - 0.8396$ and $r^2 > 0.99$. (T_{actual} = Actual temperature as measured by the built-in temperature probe, T_{block} = Temperature of the heating block)

Correct temperature and normalized absorbance were defined as follows.

$$\text{Correct Temp.} = (0.9696 \times T_{\text{block}}) - 0.8396$$

$$\text{Normalized Abs.} = \text{Abs}_{\text{obs}} / \text{Abs}_{\text{init}}$$

In entry 1; $T_{\text{obs}} = 20.02$ °C, $\text{Abs}_{\text{init}} = 0.3797$, $\text{Abs}_{\text{obs}} = 0.3797$;

$$\text{Correct Temp.} = (0.9696 \times T_{\text{obs}}) - 0.8396$$

$$\text{Correct Temp.} = (0.9696 \times 20.02) - 0.8396$$

$$= 18.6$$
 °C

$$\text{Normalized Abs.} = \text{Abs}_{\text{obs}} / \text{Abs}_{\text{init}}$$

$$= 0.3797 / 0.3797$$

$$= 1.0000$$

In entry 35; $T_{\text{obs}} = 54.02$ °C, $\text{Abs}_{\text{init}} = 0.3797$, $\text{Abs}_{\text{obs}} = 0.3951$;

$$\text{Correct Temp.} = (0.9696 \times T_{\text{obs}}) - 0.8396$$

$$\text{Correct Temp.} = (0.9696 \times 54.02) - 0.8396$$

$$= 51.5$$
 °C

$$\begin{aligned} \text{Normalized Abs.} &= \text{Abs}_{\text{obs}}/\text{Abs}_{\text{init}} \\ &= 0.3951/0.3797 \\ &= 1.0404 \end{aligned}$$

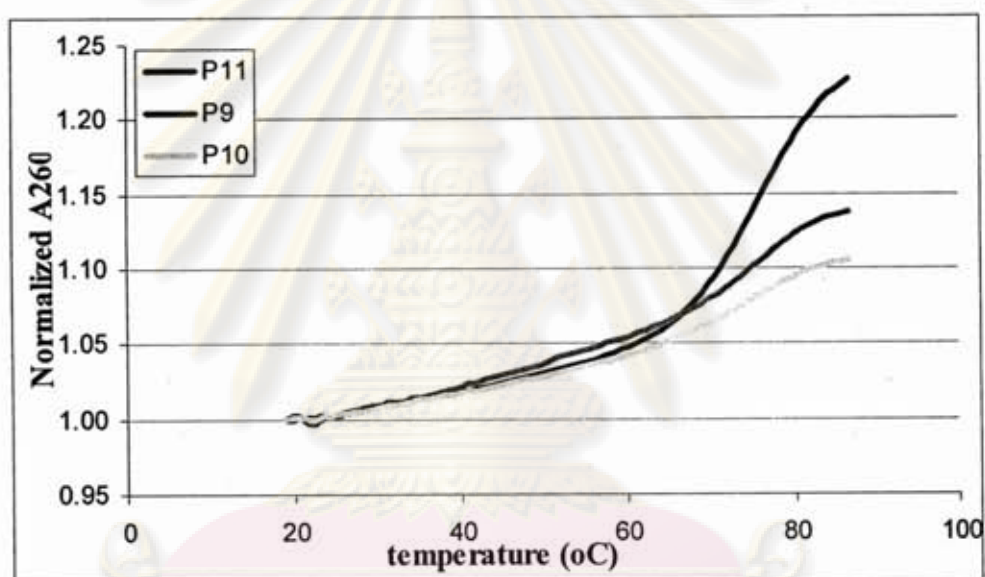


Figure D-1: T_m curves of Flu-O-T₉-Lys-NH₂ (Flu-T₉-K: **P11**), Flu-O-T₉-O-(KFF)₃K-NH₂ (Flu-T₉-KFF: **P9**), H-(KFF)₃K-T₉-Lys(Flu)-NH₂ (KFF-T₉-Flu: **P10**) with d(AAAAAAAAA) (perfect match): Conditions PNA:DNA = 1:1, [PNA] = 1.0 μ M, 10 mM sodium phosphate buffer, pH 7.0, heating rate 1.0 $^{\circ}$ C/min

ศูนย์วิจัยทางการแพทย์
จุฬาลงกรณ์มหาวิทยาลัย

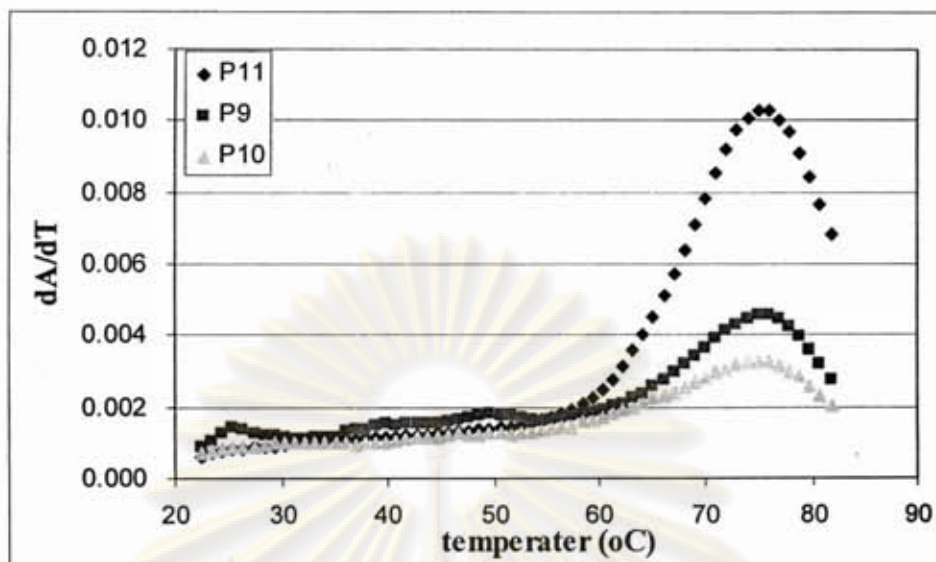


Figure D-2: First-derivative normalized UV- T_m plots of Flu-O-T₉-Lys-NH₂ (Flu-T₉-K: **P11**), Flu-O-T₉-O-(KFF)₃K-NH₂ (Flu-T₉-KFF: **P9**), H-(KFF)₃K-T₉-Lys(Flu)-NH₂ (KFF-T₉-Flu: **P10**) with d(AAAAAAAAAA) (perfect match): Conditions PNA:DNA = 1:1, [PNA] = 1.0 μ M, 10 mM sodium phosphate buffer, pH 7.0, heating rate 1.0 $^{\circ}$ C/min

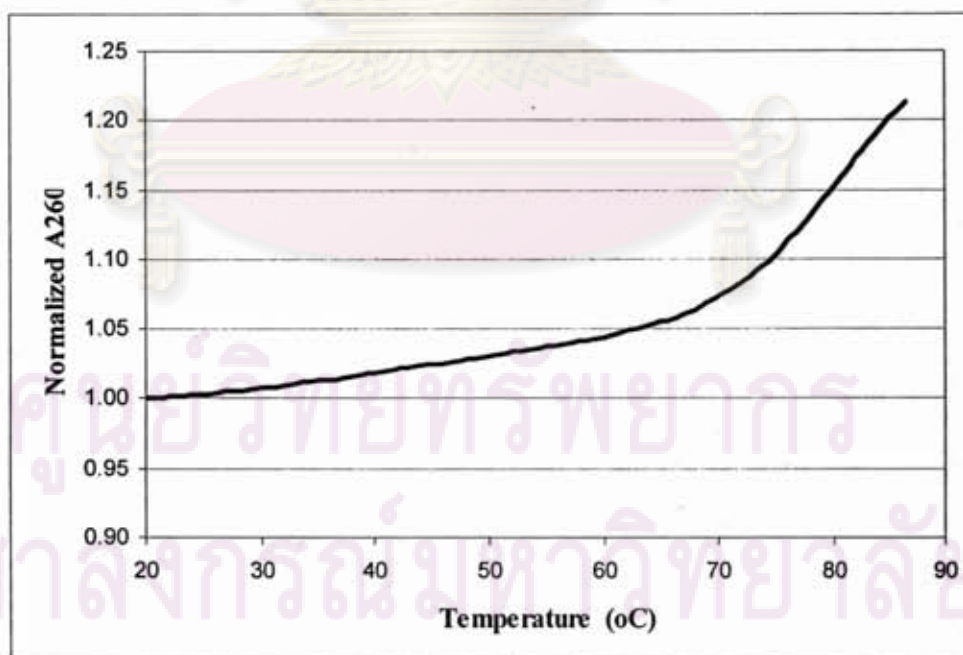


Figure D-3: T_m curves of Ac-TTTTTTTT-Lys-NH₂ (Ac-T₉-K: **P17**) with d(AAAAAAAAAA) (perfect match) Conditions PNA:DNA = 1:1, [PNA] = 1.0 μ M, 10 mM sodium phosphate buffer, pH 7.0, heating rate 1.0 $^{\circ}$ C/min

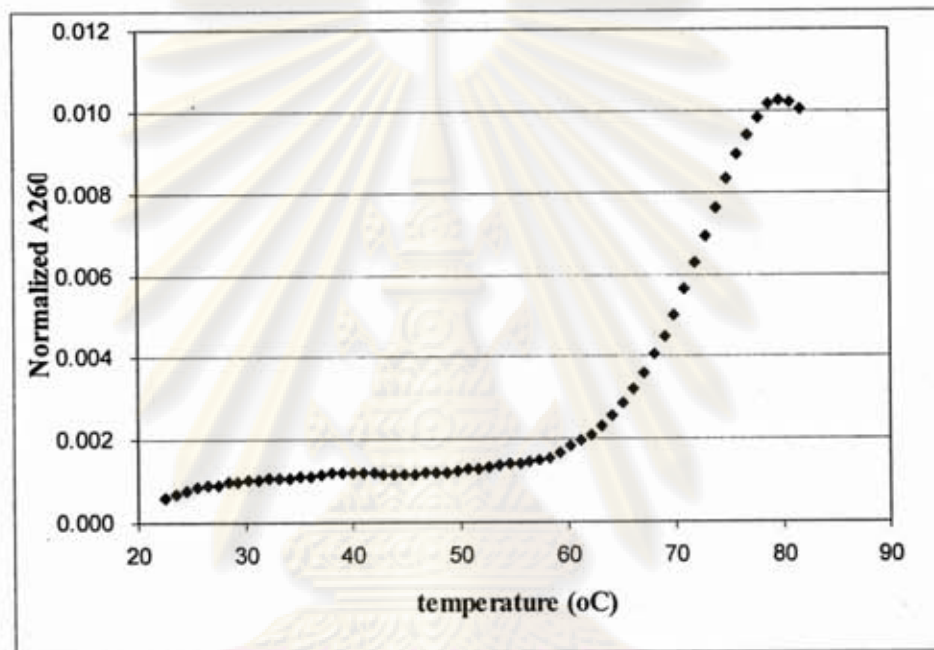


Figure D-4: First-derivative normalized UV- T_m plots of Ac-TTTTTTTT-Lys-NH₂ (Ac-T₉-K: P17) and d(AAAAAAAAAA) (perfect match): Conditions PNA:DNA = 1:1, [PNA] = 1.0 μ M 10 mM sodium phosphate buffer, pH 7.0, heating rate 1.0 $^{\circ}$ C/min

ศูนย์วิทยทรัพยากร
จุฬาลงกรณ์มหาวิทยาลัย

Table B-1: Fluorescence intensities of the solutions obtained from cell culture at 0 h, cell culture at 4 h, supernatant, and lysis (method I) of 0.1× dilution of the *E. coli* ATCC 25922 cells after treatment with PNA conjugates (5 μM, 37 °C for 4 h)

PNA	Solution	Flu of Soln ^a	Flu of BG ^a	Adjust Flu ^c	% of Flu ^d
Flu-O-T ₃ -O-(KFF) ₃ K-NH ₂ (Flu-T ₃ -KFF: P4)	cell culture 0 h	6188.6	248.8	5939.8	100.0
	cell culture 4 h	5181.5	246.2	4935.4	83.1
	supernatant	2592.9	247.0	2345.8	39.5
	lysis	1076.8	146.0	930.8	15.7
Flu-O-T ₃ -O-Lys(P ⁺)-NH ₂ (Flu-T ₃ -Phos: P6)	cell culture 0 h	3161.9	248.8	2913.1	100.0
	cell culture 4 h	3963.7	246.2	3717.5	127.6
	supernatant	4497.8	247.0	4250.8	145.9
	lysis	125.3	146.0	-20.7	-0.7
Flu-O-T ₃ -Lys-NH ₂ (Flu-T ₃ -K: P7)	cell culture 0 h	11943.8	248.8	11695.1	100.0
	cell culture 4 h	11945.0	246.2	11698.8	100.0
	supernatant	12192.0	247.0	11945.0	102.1
	lysis	123.5	146.0	-22.5	-0.2

^a Fluorescence intensity of the solution (excitation 480 nm, emission 510 nm)

^b Fluorescence intensity of background (water)

^c Adjusted fluorescence = Fluorescence of lysis solution – Fluorescence of background

^d % Fluorescence =
$$\frac{(\text{Adjusted fluorescence} \times 100\%)}{\text{Adjusted fluorescence of cell culture at 0 h}}$$

ศูนย์วิทยทรัพยากร
จุฬาลงกรณ์มหาวิทยาลัย

Table B-2: Fluorescence intensities of the solutions obtained from cell culture at 0 h, cell culture at 8 h, supernatant, and lysis (method I) of 0.1× dilution of the *E. coli* ATCC 25922 cells after treatment with PNA conjugates (5 μM, 37 °C for 8 h)

PNA	Solution	Flu of soln	Flu of BG	Adjust Flu	% of Flu
Flu-O-T ₃ -O-(KFF) ₃ K-NH ₂ (Flu-T ₃ -KFF: P4)	cell culture 0 h	6040.8	292.4	5748.5	100.0
	cell culture 8 h	5583.5	244.6	5338.9	92.9
	supernatant	3916.1	268.6	3647.5	63.5
	lysis	582.5	157.4	425.1	7.4
Flu-O-T ₃ -O-Lys(P ⁺)-NH ₂ (Flu-T ₃ -Phos: P6)	cell culture 0 h	3222.9	292.4	2930.5	100.0
	cell culture 8 h	4579.0	244.6	4334.4	147.9
	supernatant	5141.3	268.6	4872.7	166.3
	lysis	136.9	157.4	-20.5	-0.7
Flu-O-T ₃ -Lys-NH ₂ (Flu-T ₃ -K: P7)	cell culture 0 h	11016.0	292.4	10723.7	100.0
	cell culture 8 h	12727.3	244.6	12482.7	116.4
	supernatant	12683.8	268.6	12415.3	115.8
	lysis	134.6	157.4	-22.8	-0.2

Table B-3: Fluorescence intensities of the solutions obtained from cell culture at 0 h, cell culture at 4 h, supernatant, and lysis (method I) of 0.01× dilution of the *E. coli* ATCC 25922 cells after treatment with PNA conjugates (5 μM, 37 °C for 4 h)

PNA	Solution	Flu of soln	Flu of BG	Adjust Flu	% of Flu
Flu-O-T ₃ -O-(KFF) ₃ K-NH ₂ (Flu-T ₃ -KFF: P4)	cell culture 0 h	6841.7	265.6	6576.1	100.0
	cell culture 4 h	5953.2	258.2	5695.0	86.6
	supernatant	3505.2	248.7	3256.5	49.5
	lysis	693.8	46.7	647.1	9.8
Flu-O-T ₃ -O-R ₁₀ -NH ₂ (Flu-T ₃ -R ₁₀ : P5)	cell culture 0 h	5899.0	265.6	5633.4	100.0
	cell culture 4 h	5309.5	258.2	5051.3	89.7
	supernatant	4260.4	248.7	4011.7	71.2
	lysis	80.2	46.7	33.5	0.6
Flu-O-T ₃ -Lys-NH ₂ (Flu-T ₃ -K: P7)	cell culture 0 h	13544.5	265.6	13278.9	100.0
	cell culture 4 h	12644.3	258.2	12386.1	93.3
	supernatant	12755.5	248.7	12506.8	94.2
	lysis	67.2	46.7	20.5	0.2

Table B-4: Fluorescence intensities of the solutions obtained from cell culture at 0 h, cell culture at 8 h, supernatant, and lysis (method I) of 0.01× dilution of the *E. coli* ATCC 25922 cells after treatment with PNA conjugates (5 μM, 37 °C for 8 h)

PNA	Solution	Flu of soln	Flu of BG	Adjust Flu	% of Flu
Flu-O-T ₃ -O-(KFF) ₃ K-NH ₂ (Flu-T ₃ -KFF: P4)	cell culture 0 h	6853.5	321.9	6531.6	100.0
	cell culture 8 h	5771.2	281.0	5490.2	84.1
	supernatant	3695.7	286.8	3408.9	52.2
	lysis	495.9	106.9	389.0	6.0
Flu-O-T ₃ -O-R ₁₀ -NH ₂ (Flu-T ₃ -R ₁₀ : P5)	cell culture 0 h	5867.0	321.9	5545.1	100.0
	cell culture 8 h	4133.7	281.0	3852.7	69.5
	supernatant	3398.5	286.8	3111.8	56.1
	lysis	160.6	106.9	53.7	1.0
Flu-O-T ₃ -Lys-NH ₂ (Flu-T ₃ -K: P7)	cell culture 0 h	13544.5	13649.0	13327.1	100.0
	cell culture 8 h	12644.3	12795.0	12514.0	93.9
	supernatant	12755.5	13269.5	12982.7	97.4
	lysis	67.2	87.8	-19.1	-0.1
		6853.5	321.9	6531.6	100.0

ศูนย์วิทยทรัพยากร
จุฬาลงกรณ์มหาวิทยาลัย

Table B-5: Fluorescence intensities of the solutions obtained from cell culture at 0 h, cell culture at 4 h, supernatant, and lysis (method II) of 0.01× dilution of the *E. coli* ATCC 25922 cells after treatment with PNA conjugates (5 μM, 37 °C for 4 h)

PNA	Solution	Flu of soln	Flu of BG	Adjust Flu	% of Flu
Flu-O-T ₃ -O-(KFF) ₃ K-NH ₂ (Flu-T ₃ -KFF: P4)	cell culture 0 h	6484.4	252.6	6231.8	100.0
	cell culture 4 h	6642.9	276.6	6366.3	102.2
	supernatant	4077.0	229.6	3847.4	61.7
	lysis	1979.0	142.7	1836.2	29.5
Flu-O-T ₃ -Lys-NH ₂ (Flu-T ₃ -K: P7)	cell culture 0 h	13096.3	252.6	12843.8	100.0
	cell culture 4 h	13032.7	276.6	12756.1	99.3
	supernatant	12458.5	229.6	12228.9	95.2
	lysis	149.5	142.7	6.8	0.1
Flu-O-T ₉ -O-(KFF) ₃ K-NH ₂ (Flu-T ₉ -KFF: P9)	cell culture 0 h	1954.3	252.6	1701.8	100.0
	cell culture 4 h	2095.3	276.6	1818.7	106.9
	supernatant	685.2	229.6	455.6	26.8
	lysis	1635.1	142.7	1492.4	87.7
H-(KFF) ₃ K-O-T ₉ -Lys(Flu)-NH ₂ (KFF-T ₉ -Flu: P10)	cell culture 0 h	1235.5	252.6	1139.2	100.0
	cell culture 4 h	1137.8	276.6	1088.9	91.6
	supernatant	567.6	229.6	517.1	32.4
	lysis	4137.1	142.7	3344.6	361.1
Flu-O-T ₉ -Lys-NH ₂ (Flu-T ₃ -K: P11)	cell culture 0 h	7472.3	252.6	7290.2	100.0
	cell culture 4 h	7467.1	276.6	7353.1	100.6
	supernatant	6645.8	229.6	6584.6	90.3
	lysis	85.3	142.7	105.9	-0.5

ศูนย์วิทยทรัพยากร
จุฬาลงกรณ์มหาวิทยาลัย

Table B-6: Fluorescence intensities of the solutions obtained from cell culture at 0 h, cell culture at 2 h, supernatant, and lysis (method II) of 0.1× dilution of the *E. coli* ATCC 25922 cells after treatment with PNA conjugates (5 μM, 37 °C for 2 h)

PNA	Solution	Flu of soln	Flu of BG	Adjust Flu	% of Flu
Flu-O-T ₉ -O-(KFF) ₃ K-NH ₂ (Flu-T ₉ -KFF: P9)	cell culture 0 h	2536.4	279.4	2257.0	100.0
	cell culture 2 h	1940.0	292.5	1647.5	73.0
	supernatant	659.1	310.4	348.7	15.5
	lysis	1522.8	185.5	1337.3	59.3
H-(KFF) ₃ K-O-T ₉ -Lys(Flu)-NH ₂ (KFF-T ₉ -Flu: P10)	cell culture 0 h	1420.0	279.4	1140.6	100.0
	cell culture 2 h	1394.9	292.5	1102.4	96.7
	supernatant	581.0	310.4	270.6	23.7
	lysis	3013.0	185.5	2827.5	247.9
Flu-O-T ₉ -Lys-NH ₂ (Flu-T ₃ -K: P11)	cell culture 0 h	7347.9	279.4	7068.5	100.0
	cell culture 2 h	6945.8	292.5	6653.3	94.1
	supernatant	6347.5	310.4	6037.1	85.4
	lysis	341.0	185.5	155.5	2.2

Table B-7: Fluorescence intensities of the solutions obtained from cell culture at 0 h, cell culture at 2 h, cell culture at 4 h, supernatant, and lysis (method II) of 0.1× dilution of the *E. coli* ATCC 25922 cells after treatment with PNA conjugates (5 μM, 37 °C for 4 h)

PNA	Solution	Flu of soln	Flu of BG	Adjust Flu	% of Flu
Flu-O-T ₉ -O-(KFF) ₃ K-NH ₂ (Flu-T ₉ -KFF: P9)	cell culture 0 h	2593.9	283.6	2310.3	100.0
	cell culture 2 h	2026.4	281.8	1744.6	75.5
	cell culture 4 h	2007.8	283.9	1723.8	74.6
	supernatant	760.4	305.1	455.3	19.7
	lysis	1424.2	225.8	1198.5	51.9
H-(KFF) ₃ K-O-T ₉ -Lys(Flu)-NH ₂ (KFF-T ₉ -Flu: P10)	cell culture 0 h	1461.6	283.6	1178.0	100.0
	cell culture 2 h	1395.2	281.8	1113.4	94.5
	cell culture 4 h	1268.8	283.9	984.9	83.6
	supernatant	575.4	305.1	270.4	23.0
	lysis	1958.3	225.8	1732.5	147.1
Flu-O-T ₉ -Lys-NH ₂ (Flu-T ₃ -K: P11)	cell culture 0 h	7409.9	283.6	7126.2	100.0
	cell culture 2 h	7013.2	281.8	6731.4	94.5
	cell culture 4 h	2593.9	283.6	2310.3	100.0
	supernatant	2026.4	281.8	1744.6	75.5
	lysis	2007.8	283.9	1723.8	74.6

Table B-8: Optical densities at 590 nm of cell growth at 0 h, 4 h and 8 h of 0.1× dilution of the *E. coli* ATCC 25922 cells after treatment with PNA conjugates (5 μM, 37 °C for 8 h)

PNA	Time (h)	Optical density
Flu-O-T ₃ -O-(KFF) ₃ K-NH ₂ (Flu-T ₃ -KFF: P4)	0	0.048
	4	0.117
	8	0.233
Flu-O-T ₃ -O-Lys(P ⁺)-NH ₂ (Flu-T ₃ -Phos: P6)	0	0.050
	4	0.123
	8	0.240
Flu-O-T ₃ -Lys-NH ₂ (Flu-T ₃ -K: P7)	0	0.049
	4	0.117
	8	0.235
Background (water)	0	0.048
	4	0.114
	8	0.238

Table B-9: Optical densities at 590 nm of cell growth at 0 h, 4 h and 8 h of 0.01× dilution of the *E. coli* ATCC 25922 cells after treatment with PNA conjugates (5 μM, 37 °C for 8 h)

PNA	Time (h)	Optical density
Flu-O-T ₃ -O-(KFF) ₃ K-NH ₂ (Flu-T ₃ -KFF: P4)	0	0.040
	4	0.069
	8	0.159
Flu-O-T ₃ -O-R ₁₀ -NH ₂ (Flu-T ₃ -R ₁₀ : P5)	0	0.039
	4	0.050
	8	0.117
Flu-O-T ₃ -Lys-NH ₂ (Flu-T ₃ -K: P7)	0	0.038
	4	0.062
	8	0.146
Background (water)	0	0.038
	4	0.062
	8	0.145

Table B-10: optical densities at 590 nm of cell growth at 0 h, 4 h and 8 h of 0.1× dilution of the *E. coli* ATCC 25922 cells after treatment with PNA conjugates (5 μM, 37 °C for 4 h)

PNA	Time (h)	Optical density
Flu-O-T ₉ -O-(KFF) ₃ K-NH ₂ (Flu-T ₉ -KFF: P9)	0	0.0490
	2	0.0598
	4	0.0938
H-(KFF) ₃ K-O-T ₉ -Lys(Flu)-NH ₂ (KFF-T ₉ -Flu: P10)	0	0.0578
	2	0.0630
	4	0.0925
Flu-O-T ₉ -Lys-NH ₂ (Flu-T ₉ -K: P11)	0	0.0475
	2	0.0630
	4	0.0962
Background (water)	0	0.0487
	2	0.0640
	4	0.1008

ศูนย์วิทยทรัพยากร
จุฬาลงกรณ์มหาวิทยาลัย

VITAE

Miss Benjawan Boonkaew was born on December 27th, 1982 in Songkhla, Thailand. She received Bachelor Degree of Science in Chemistry (First class Honored) from Prince of Songkla University in 2006. In the same year, she was admitted to the Master's degree of Science, majoring in Chemistry, at Chulalongkorn University and graduated in the academic year of 2008.



ศูนย์วิทยทรัพยากร
จุฬาลงกรณ์มหาวิทยาลัย